UNIVERSITY OF TUSCIA, ITALY

DEPARTMENT OF ECOLOGICAL AND BIOLOGICAL SCIENCES (DEB)

PhD Course in
Ecology and Sustainable Management of
Environmental Resources
Curriculum: Environment, Adaptation and Healthy
XXXI Course

"Omics analysis of microgravity effects on osteoblastic cells: mitochondrial alterations and cellular regression of the mature phenotype"

(s.s.d. BIO/11)

PhD student
Anna Michaletti

Coordinator of PhD course
Prof.ssa Roberta Cimmaruta

Tutor
Prof.ssa Sara Rinalducci
Prof. Lello Zolla

A.Y. 2018/2019

AIM

The absence of gravity is one of the most extreme conditions that humans can undergo. The astronauts in spaceflights, especially long-term, undergo to numerous physiological changes. Astronauts are subjected to extreme temperature, oxidative stress, radiation exposure, and other environmental stresses. In addition, microgravity (Sμg) influences the structure, development, function, evolution and behaviour of all living organisms. So, weightlessness can impact various aspects of the astronaut health, including effects on the immune system, cardiac cells, muscles and bones. Despite the numerous studies that have been conducted to date, the knowledge of spaceflight effects on the human body are still too limiting. These changes are allowed by modifications of several biological pathways due to alterations of gene expression and signal transduction pathways. So, the body adapts to the condition of microgravity, reaching a new equilibrium. This causes different levels of hormones and alterations in the functionality of the cardiovascular system, dysfunctions in the endothelial, bone and muscular cells caused by variations in severity.

In order to better explain the consequences of gravity absence, we carried out a study on human primary osteoblasts (hpOBs) from healthy donors with the aim of revealing the effects of Sμg on cellular response. The investigation has been undertaken by ultra-structural, immune-cytochemistry, cell biochemistry and quantitative mass spectrometry (MS) for proteomic and metabolomic analyses.

By using proteomic thecniques, it was performed a comparative analysis between proteins present in osteoblasts placed under normogravity conditions and samples that were previously placed in simulated microgravity. By differential proteomics it was thus possible to establish which proteins are expressed in normo and in microgravity and evaluate their trend. To understand which biological processes, cellular components and molecular functions were most affected by the absence of gravity, it was carried out a functional annotation through appropriate bioinformatics tools.

Furthermore, this work also aimed to carry out a metabolomic analysis of the cellular samples, in order to highlight the alterations induced by microgravity by comparing the metabolites extracted from the osteoblastic cells. The identified metabolites allowed us to trace the most influenced metabolic pathways by evaluating the impact of each metabolite on the entire metabolic process. By combining information derived by omics studies with histochemical and ultrastructural approaches, it was possible to obtain a complete picture of

the interactions between different molecular pathways. Our data could be useful to understand the alterations induced by spaceflights and to study different osteo-degenerative diseases developping on Earth, through basic research and the application of technological tests.

Summary

1 INTRODUCTION

1.1 THE MICROGRAVITY

Space represents a hostile environment for humans, because it is characterized by high vacuum, temperature extremes, meteoroids, space debris, ionospheric plasma, microgravity (μg), so that spatial flights represent risks for human health (Rea et al., 2015).

All life on Earth has evolved in the presence of gravity, but only we are beginning to understand the fundamental role of gravity in terrestrial biological processes (Feger et al, 2016).

As defined by NASA in 2009, "Gravity is a force that governs movement throughout the universe. The force of gravity keeps all of the planets in orbit around the sun".

Gravity is one of the four fundamental physical forces, together with electromagnetic force, weak nuclear interaction force and nuclear interaction force. The Earth creates a gravitational field such that all objects are attracted towards it, according to the Newton's Law. This is the law of universal gravitation and is valid for all bodies of the Universe. Gravity affects many of the processes that have some impacts on life sciences, such as capillarity, laminar flows, osmosis, interface phenomenan and crystal growth. The dynamics of fluids on the Earth is strongly conditioned by gravity. For a better understanding of certain physical, chemical or biological phenomena or for the study of the complex interactions of forces of a different nature involved in certain processes in liquids and gases, sometimes it is useful to eliminate the effect of gravity.

Microgravity is expressed as a fraction of g (from 10^{-2} g to 10^{-6} g). The microgravity condition arises whenever an object is in free fall, that is, it falls faster and faster, with an acceleration exactly equal to that due at gravity (1g) (Amaldi, 1998).

It will be important knowing the limits of life in microgravity conditions for designing long term manned missions in space. Thus, it will be give useful information also to improve life even on Earth. In fact, conducting experiments in real and simulated microgravity conditions allows the scientists to study phenomena and mechanisms in different fields such as biology, physiology and chemistry by removing the effects of gravity. Currently, astronauts live and work on board the International Space Station (ISS), and in the near future, space missions will be directed to the Moon and Mars and will require long stays for members of the crew (Kononikhin et al, 2017).

Because spaceflights are one of the most extreme conditions to which humans are subjected, exposure to Microgravity has been associated with various physiological changes, expacially in astronauts. More than 500 men today have participated in long-term space missions, but the human body is extremely affected by spatial flight. In particular, it decrease immune function, there is a loss of bone density (similar to osteoporosis), and muscular atrophy. The effects on cardiac physiology of the astronauts indicate that microgravity cause cellular stress and it has the ability to negatively affect human health.

Astronauts, in their journey beyond the orbit of the Earth, are subjected to extreme temperatures, oxidative stress, radiation and other environmental stresses in addition to microgravity. So, understanding the impact of microgravity on biological systems requires fundamental knowledge of how it influences molecular processes within various cellular compartments.

Studies mainly focused on the bones, the immune and nervous systems and skeletal muscle cells these researches revealed pleiotrophic effects due to microgravity that direct cells to apoptosis or early senescence, altering cell division and differentiation and influencing the protein turnover (Feger et al, 2016). Furthemore, the development of orthostatic hypotension (sharp decline of the blood pressure) and instability after the return from spaceflight, was a significant problem for astronauts (Figure 1.1) for more than four decades (Convertino, 2002).

The body adapts to the flight relatively quickly and reaches a new equilibrium. This is characterized by different levels of hormones and impaired functionality of cardiovascular system, due to dysfunctions in the endothelial cells caused by gravity changes (Heppener, 2008; Grosse et al, 2012).

Among the main changes that occur during the adaptation to microgravity are included also (Kononikhin et al, 2017):

- loss of muscle and bone mass. This loss amounts to about 1-2% every month, 10-15 times faster than severe osteoporosis (Heppener, 2008);
- changes in renal function;
- changes in gene expression and protein synthesis levels.
- reduction of the vestibular function of the ear, causing the so-called " spatial nausea ", very similar to seasickness;
- alterations of the immune system

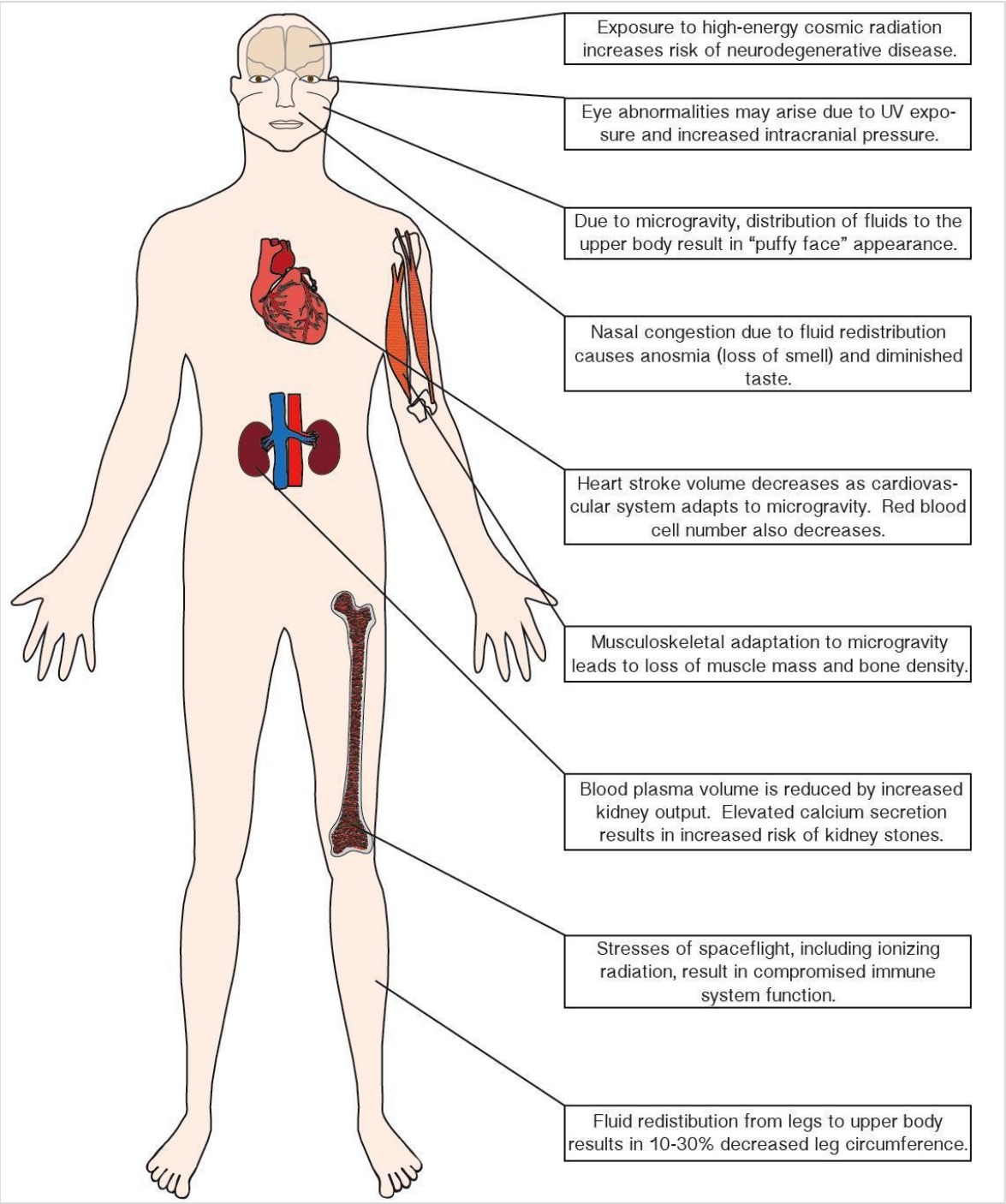

Figure 1.1. Several physiological changes in human body, associated with the exposure of microgravity

Cells can adapt to the microgravity condition, reorganizing its cytoskeleton. Under microgravity, the cytoskeleton is destined to become less "important", because it does not need to support the load due to hydrostatic pressure (Arfat et al, 2014).

1.1.1 THE MICROGRAVITY AND CENTRAL NERVOUS SYSTEM

Sometimes, for astronauts it is difficult to adapt to the microgravity environment, because during a spaceflight mission, they do not receive the same stimuli from the surrounding environment as on Earth. The central nervous system processes involved in the development of the astronaut's sense of direction are perturbated. The vestibular apparatus inside the inner ear is mainly affected: this condition usually altered orientation perception and leads to a loss of balance, due to a deconditioning of motion sensors as well as of the somatosensory system. This disorientation is the main symptom of a temporary disease: Space Adaptation Syndrome (SAS), that causes the Space Motion Sickness (SMS). SAS is caracterizated by sensory conflict between inputs from visual and tactile senses and inputs from the vestibular organs (Lackner & Dizio, 2006). Thus, it is necessary to reorganize the orientation apparatus with adaptive changes in the neural system to perceive different spatial information. Visual cues and references become fundamental to astronauts.
Microgravity exposure altered other tissues and organs such kidney, with formation of renal stones, after spaceflight (Pietrzyk et al., 2007).

1.1.2 THE MICROGRAVITY AND KIDNEY

The kidney stone formation during spaceflight could also be due to an increase in nanobacteria (NB) growth under microgravity conditions. Indeed, it has been hypothesized that nanobacteria play a crucial role in the deposition of calcium phosphates and carbonates in the kidney. In 2005 Çiftçioğlu et al. conducted an experiment on effects of microgravity on the multiplication and calcification, analyzing nanobacteria cultures placed in HARV (High Aspect Rotating Vessels) a NASA instrument. It is a rotating cell culture system in which stress and cell damage are maximally reduced or absent. Nanobacteria have been proposed to be infectious agents capable of invading and damaging the epithelium of the collecting duct of the urinary system, causing formation of calcium phosphate. It was also observed that in microgravity many microorganisms increase the multiplication, growth and virulence rates. In particular, the nanobacteria multiply five times faster when placed in 0g (Çiftçioğlu et al, 2005).

1.1.3 THE MICROGRAVITY AND IMMUNE SYSTEM

Alterations in immune system causes serious problems, because it is induced a considerable reduction of the astronauts' immune defenses, compromising the process of healing of lesions and functions of monocytes and granulocytes. In particular, an important issue in spaceflight consequences is the observed deterioration of the immune system resulting in a secondary immunodeficiency that can lead to increase infections or autoimmunity (Meshkov et al., 1995). Studies on the immune system performed by Gridley et al., showed that microgravity has a significant effect on T cell distribution, function, and gene expression after a short-term spaceflight. Moreover, the potential for astronauts to develop cancer could be enhanced by the expression of cancer related genes (Gridley et al., 2009) and alterations in natural killer cell function, due to the reducted number and cytotoxic activity of natural killer cells (Meshkov et al., 1995).

1.1.4 *THE MICROGRAVITY AND BLOOD CIRCULATION*

The space environment has numerous effects on blood circulation. On Earth, the heart distributes blood throughout the body and gravity helps draw blood to the lower limbs (Norsk, 2010). In space the force to pull body fluids down is missing. (Kononikhin et al, 2017). A visible effect is in fact the "swollen face" of the astronauts during the first days after the launch, which is caused precisely by the redistribution of body fluids from the lower extremities to the head (Heppener, 2008). Sometimes, changes that currently occurr in the physiological systems of the body during a spaceflight, are considered as short-term effects, and generally deemed reversible, while the time necessary to recover from the effects of microgravity for some systems is quite long (Kononikhin et al, 2017). Recent evidence has also shown that 20-25% of astronauts on the International Space Station (ISS) developed persistent ocular problems, in particular, when the fligh has a duration of more than 4 months (Kononikhin et al, 2017).

1.1.5 *THE MICROGRAVITY, ENDOPLASMATIC RETICULUM AND MITOCHONDRIA*

Microgravity exposure is a stress factor that strongly influences the physiology of mammals (Thiel et al., 2012; Battista et al., 2012; Chang et al., 2012; Mangala et al., 2011; Singh et al., 2010; Paulsen et al., 2010). At the proteomic level, there are three types of cellular responses to this element of stress: the so-called "heat shock" response at the

cytoplasmic level and the protein unfolding (UPR) at the endoplasmic reticulum and at the mitochondrial level. Cells increase the expression of chaperone proteins that help in the refolding of misfolded proteins and alleviate protein aggregation. So, heat shock proteins (Hsps) can be activated or induced by a number of stresses and they protect the cells promoving the cell survival (Morimoto et al., 1996). Exposure of cells to stress, such as microgravity, causes accumulation of unfolded proteins in the ER, activating a phenomenon known as the "Unfolded protein response" (UPR), that generally promotes cell survival (Hori et al., 2006).

Cells capable of cell division respond to stress by entering the cell cycle, rather than by global protein synthesis, thus increasing the possibility of daughter cell to survive. On the contrary, specialized non-dividing cells that are able to re-enter the cellular cycle, respond to stressful conditions through different mechanisms, so they keep own functionality. An example is rapresented by cardiomyocytes, the fundamental cellular type of heart. Under favorable conditions, cardiomyocytes spend energy to preserve the contractile function and the mitochondria. This is achieved through protein regulation, for esample maintaining the balance between synthesis and degradation of proteins of the contractile apparatus and mitochondria. Feger et al., (2016) conducted a proteomic study on cardiomiocites under microgravity. They found several proteins differentially modulated after 120 hours in microgravity conditions. In particular, it was seen that in microgravity cardiomyocytes spend energy to maintain mitochondrial homeostasis and that they have decreased protein tournover.

In fact, by analyzing the effects of microgravity on these cells it was demonstrated that the mitochondria are the organelles more influenced by this stress. The pathways that undergo major changes are the citric acid cycle (TCA), the synthesis of ATP, carbohydrate and amino acid metabolisms.

For these reasons, we supposed that these changes in the mitochondrial homeostasis also occur in different kind of cells, in particular, in osteoblasts, grown under microgravity conditions.

1.1.6 THE MICROGRAVITY IN MUSCLE CELLS

On Earth, we must constantly use certain muscles to support ourselves against the force of gravity. These muscles are called antigravity muscles and include the gastrocnemius (calf muscles), the quadriceps, and the muscles of the back and neck. Muscle contraction, physical effort, exercise, the movement against resistance, continuous contractions to maintain the standing station are the means that allow the muscle to remain efficient (Son et al., 2013). An increase in physical activity, represents the stimulus to increase its volume (hypertrophy muscle) (Lee & Kang, 2013). In space, the absence of gravity does not require maintenance of the upright position and muscle contraction occurs, except under particular conditions and in rare moments, with minimal effort. Because astronauts work in a weightless environment, they need a very little muscle contraction to support their bodies. Studies have shown that astronauts lose up to 20-30% of muscle mass in spaceflights lasting for 270 days (Di Prampero & Narici, 2003). This loss corresponds to a loss of strength that can be potentially dangerous if an astronaut has to perform an emergency procedure on returning to the Earth's gravitational field. Although muscle mass and strength can re-establish once the astronauts have returned to Earth, keeping muscles in space is a concern, especially for long-duration space missions.

Spatial flights have been shown to cause muscle atrophy as well as a loss of strength and power. The atrophy derives mainly from a reduced protein synthesis probably due to the removal of the "antigravity load". Contractile proteins are less than other cellular proteins and actin filaments are less than myosin. The decrease in contractile proteins explains the decrease in strength per section transverse, while the loss of thin filaments may be the reason for the increase of the maximum speed of shortening in type I and IIa fibers.

Leivo et al., already in 1998 (Leivo et al., 1998), showed that in rabbits, immobilization of anti-gravity muscle for more than 3 days induced muscle atrophy and appearance of abnormal mitochondria and sarcoplasmic changes.

Skeletal muscles showed significant changes during spaceflight (Ohira e al., 1992). In particular, information regarding atrophy shows a distinction between selective effects on slow or fast fibers (Caiozzo et al.,1996; Campione et al., 1993). The greatest level of atrophy has been observed in the soleo muscle, a sort of slow-twitch antigravity skeletal muscle (Sandonà et al., 2017), and many slow-twitch muscle fibers presented a conversion from slow to fast muscle fibers (Caiozzo et al.,1996). In contrast, the fast-twitch muscle received

less effects (Campione et al., 1993). So, the fast type II fibers were more susceptible to atrophy induced by microgravity than fibers of type I (Fitts et al, 2000; Fitts et al, 2001). Curiously, muscle loss seems to happen most radically in the upper body; the contrary, bone loss tends to cause the most serious effects in the lower body.

Microgravity can also induce changes at the metabolic level. From studies performed both during spacelights and on models in the absence of gravity, it emerges that microgravity reduces the ability of the skeletal muscles of the limbs to oxidize free fatty acids. So, the use of carbohydrates increased, but this does not seem to depend on a reduction in the function of the enzymes of the β-oxidation pathways and the Krebs cycle. The use of carbohydrates seems to derive from the inhibition of carnitine palmitoyltransferase (CPTI), the enzyme that limits the rate of oxidation of long chain fatty acids (Fitts et al, 2001).

Thus, the space environment alters the body and complex physiological and psychological changes depend on mission length, especially in the muscle and bone system. These tissues result to be the most altered ones after the microgravity exposure.

1.2 THE MICROGRAVITY AND BONE TISSUE

Several scientists (Smith & Heer 2002; LeBlanc et al., 2000; McCarthy 2005; Di et al., 2011; Hammond et al., 2001; Qian et al., 2009; Van Loon, 2007) suggested that, in microgravity conditions, normal physiological processes, such as the functional integrity of muscles and bone mass, result to be affected. So, microgravity is an ideal physical stimulus to evaluate bone cell responses in stress conditions. Studies in vitro showed modifications in bone cell attachment structures and cytoskeletal reorganization (Aleshacheva et al., 2015; Grimm et al., 2011; Grosse et al., 2012; Ma et al., 2014; Ulbrich et al., 2011). These changes may be involved in bone mineral loss, that is considerated one of the most serious problems induced by long-term weightlessness (Arfat et al., 2014).

1.2.1 BONE TISSUE

Bone is a specialized form of connective tissue that serves as both a tissue and an organ system within higher vertebrates. As such, its basic functions include locomotion, protection, and mineral homeostasis (Downey & Siegel, 2006). The biomechanical properties of the skeletal system play a crucial role in structural support, load-bearing for movement and physical protection of the inner organs (McGovern et al., 2018). Despite these characteristics, the bone is very light, and the resistance-weight association is due to the highly organized structure of the bone itself. Furthermore, in addition to mineral storage and calcium homeostasis roles, the bone organ has important haematopoietic and immunological functions as the site of blood cell generation and immune cell differentiation. (Bauer & Muschler, 2000; Hollinger and Kleinschmidt, 1990).

Bone exhibits four types of cells: osteoblasts, bone lining cells, osteocytes, and osteoclasts (Figure 1.2) (Buckwalter et al., 1996; Downey & Siegel, 2006) and its matrix contains an organic and an inorganic component. Bone consists of 70% of inorganic component, 20% of organic component, and 10% of water. Approximately 90% of organic content is type I collagen.

Morphologically, it is characterized either as cancellous (spongy, trabecular) or as cortical (compact). Functionally, cancellous bone is more closely associated with metabolic capabilities than cortical bone, whereas cortical bone generally provides greater mechanical strength. Although bone exhibits significant mechanical strength at a minimum weight, its biomechanical properties allow for significant flexibility without compromising this

mechanical strength. Despite its inert appearance, bone is a highly dynamic organ (Downey & Siegel, 2006). Throughout human life, bone tissue is subjected to a continuous turnover process whereby old bone is removed and replaced by new bone by the coupled processes of bone resorption and bone formation. Bone remodelling is a highly complex process due to coordinated actions of osteoclasts, osteoblasts, osteocytes, and bone lining cells which together form the temporary anatomical structure called basic multicellular unit (Dallas et al., 2013). Old bone is replaced by new bone, in a cycle comprised of three phases: (1) initiation of bone resorption by osteoclasts, (2) the transition (or reversal period) from resorption to new bone formation, and (3) the bone formation by osteoblasts (Sims & Gooi, 2008; Matsuo & Irie, 2008).

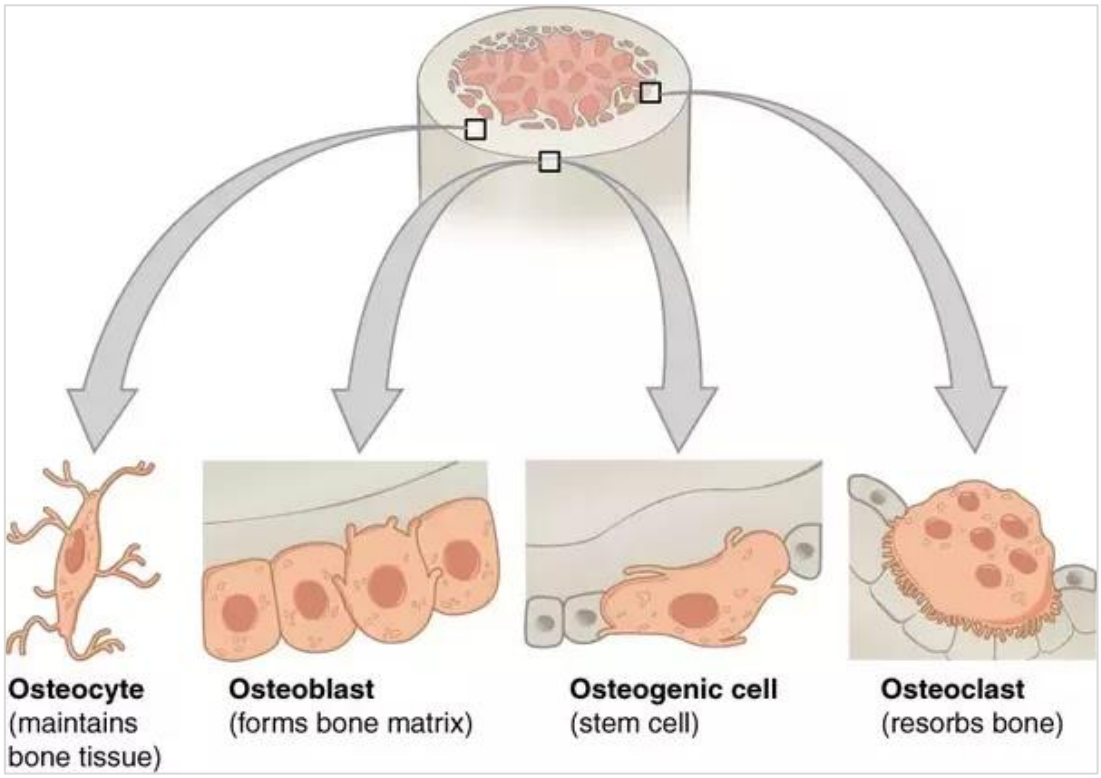

Figure 1.2. Bone is a mineralized connective tissue that exhibits four types of cells: osteoblasts, bone lining cells, osteocytes, and osteoclasts.

Normal bone remodeling is necessary for fracture healing and skeleton adaptation to mechanical use, as well as for calcium homeostasis (Dallas et al., 2013). On the other hand, an imbalance of bone resorption and formation results in several bone diseases such as osteoporosis (Khosla et al., 2013), whereas the contrary may result in osteopetrosis (Sobacchi et al., 2013). Resorption is much faster than formation: bone can be resorbed in

2-3 weeks, but it takes at least three months to rebuild it (Fonseca, 2008). Bone resorption is probably the first event that occurs in response to a mechanical stress signal (Robling & Turner, 2009). In fact, resorption and formation are tightly coupled, so that after resorption a formation phase occurs and, normally, the amount of bone resorbed will be formed in the succeeding phase. This coordination arises from the linkage between osteoblasts and osteoclasts, which is mediated by the release of growth factors from bone during resorption. The equilibrium between bone formation and resorption is necessary and depends on the action of several local and systemic factors including hormones, cytokines, chemokines, and biomechanical stimulation (Phan et al., 2004; Crockett et al., 2011). Osteoblasts are responsible for the production of collagen and non-collagenous proteins including osteocalcin, bone sialoprotein, osteopontin, and osteonectin (Tsao et al., 2017; Nakamura, 2007).

1.2.2 BONE CELLS

The 4 cellular elements of bone are differentiated by their origin. Osteoblasts, osteocytes, and bone lining cells originate from mesenchymal stem cells (MSC) known as osteoprogenitor cells. By these cells originate chondrocytes, myoblasts, adipocytes and tendon cells, depending on the transcription factors that regulate the pathway (Harada & Rodan, 2007; Krane, 2005; Stains & Civitelli, 2003). Osteoblasts are either incorporated into the new bone as osteocytes or remain on the surface as lining cells whereas osteoclasts originate from hemopoietic stem cells. The location of these cells also varies. Bone cells found along the surface of bone include osteoblasts, osteoclasts, and bone lining cells, whereas osteocytes are in the interior of bone (Figure 1.3) (Buckwalter et al., 1996; Marks & Hermey, 1996; Florencio-Silva et al., 2015).

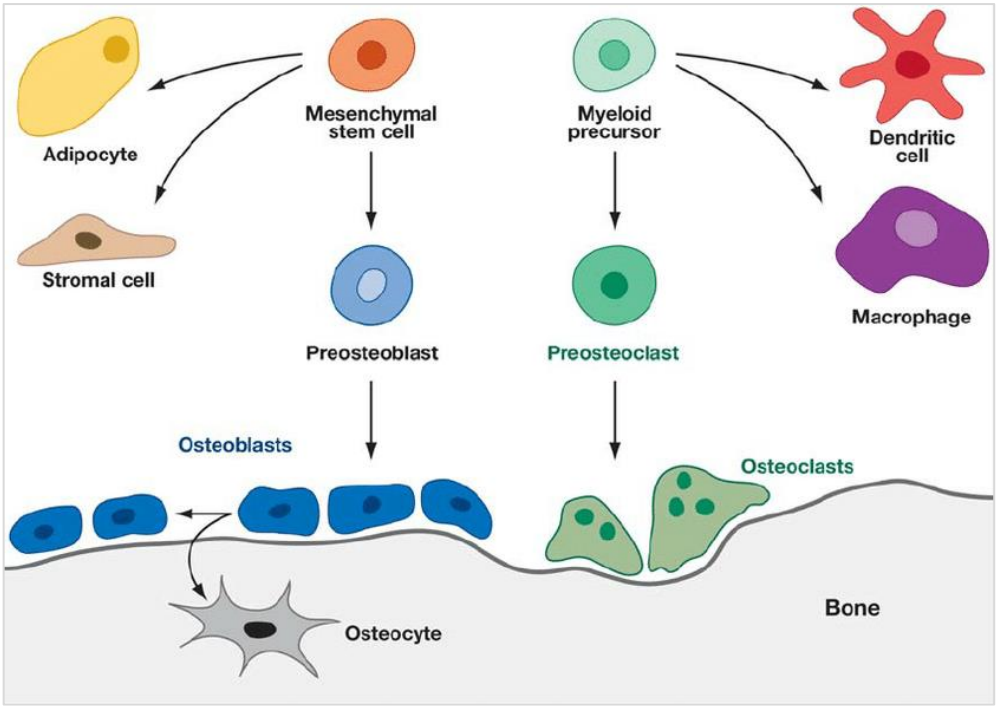

Figure 1.3. Osteoblasts are specialised fibroblast-like cells of primitive mesenchymal origin called osteoprogenitor cells that originate from pluripotent mesenchymal stem cells of the bone marrow. Osteocytes are cells lying within the bone itself and are 'entrapped' osteoblasts. Osteoclasts are large multinucleated phagocytic cells derived from the macrophage-monocyte cell lineage.

1.2.2.1 Osteoclast

The maturation of macrophages in osteoclasts requires the presence of osteoblasts or bone marrow stromal cells that secrete the M-CSF (macrophage colony stimulating factor) that is bound to the c-fms receptor present on osteoclast precursors. Furthermore, contact between osteoblasts / stromal cells and macrophages is required, through the link between the RANK receptor and its RANKL ligand, belonging to the TNF (Tumor Necrosis Factor) and TNF-R family. Another protein involved in osteoclastogenesis is osteoprotegerine (OPG), which competes with the RANK receptor (Figure 1.4). Osteoclasts are multinucleated cells that are found on the surface of bone trabeculae in resorption, in the form of giant polynuclear cells ranging from 20 to 100 μm of diameter (Nakayama et al., 2014). They are much less basophilous than osteoblasts and are provided with numerous mitochondria and poor endoplasmic reticulum. They are polarized cells whose surface has a characteristic streaky border consisting of cytoplasmic extensions among which are apatite crystals, derived from bone lysis, and often microfibrils of collagen.

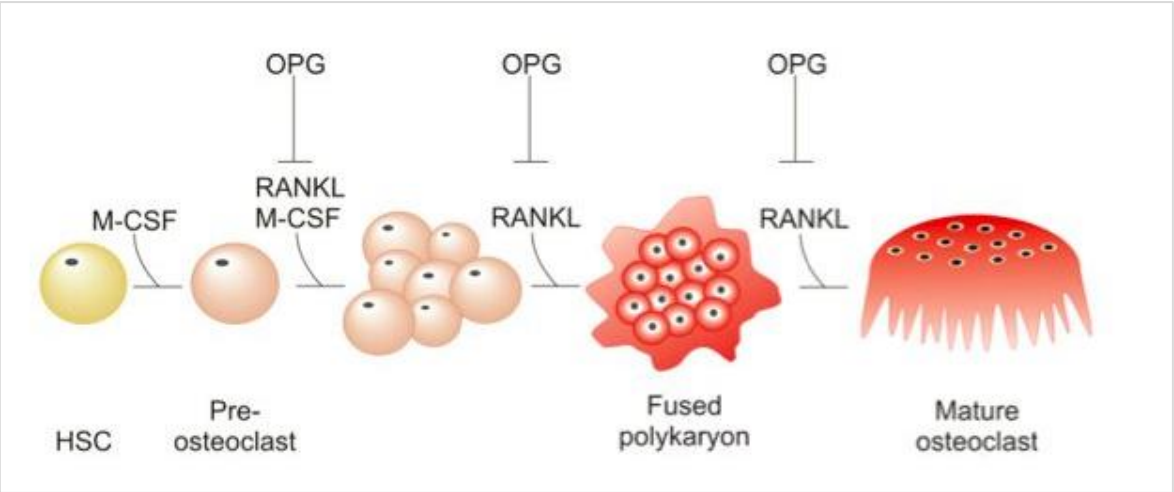

Figure 1.4. Differentiation of osteoclasts. Osteoclast precursors express RANK receptors and c-Fms and differentiate into osteoclasts in the presence of RANKL and M-CSF. Osteoblastic cells secrete OPG, which inhibits the RANKL–RANK interaction between osteoblastic cells and osteoclast precursors. Multinucleated osteoclasts also express RANK, and RANKL induces the bone-resorbing activity of osteoclasts via the interaction with RANK.

The main function of osteoclasts is the erosion of the organic and inorganic matrix, exerted by acidification of the extracellular space at the level of the border and secretion of hydrolytic enzymes of lysosomal origin; in fact, it is present an ATPase that helps the acidification of the gaps allowing the dissolution of hydroxyapatite crystals. In this region, proteins and enzymes, such as TRAP (tartrate-resistant acid phosphatase), cathepsin K and MMP-9 (matrix metalloproteinase-9) are transported in the Howship lacunae, inducing bone degradation (Florencio-Silva et al., 2015).

MSC can instead differentiate, in adipocytes and chondrocytes as well as in osteoblasts and osteocytes (Arfat et al., 2014).

1.2.2.2 Osteoblast

Osteoblasts have a very important role in creating and maintaining skeletal architecture; these cells are responsible for the deposition of bone matrix and for osteoclast regulation (Mohamad, 2008). Morphologically, they are cuboidal cells that are located along the bone surface comprising 4–6% of the total resident bone cells (Capulli et al., 2014). These cells show morphological characteristics of protein synthesizing cells, including abundant rough endoplasmic reticulum and prominent Golgi apparatus, as well as various secretory vesicles (Capulli et al., 2014; Marks & Popoff, 1988). Osteoblasts are present

throughout life, but their activity is highest during embryonic skeletal formation and growth. In an adult organism, osteoblasts are activated when there is need to regenerate a defect or when the bone matrix has been depleted (Jensen et al., 2010). Only a fraction of the mature osteoblasts will be incorporated into newly formed bone matrix and remains settled as an osteocyte. The remaining mature osteoblasts will die or become relatively inactive and form bone lining cells (Matic et al., 2016).

Bone lining cells are thin, elongated cells that cover most bone surfaces in the mature skeleton. Cytoplasmic extensions or gap junctions often link them to each other or to osteocytes. Because they are metabolically inactive, bone lining cells contain fewer organelles and less cytoplasm than osteoblasts (Buckwalter et al., 1996; Marks & Popoff, 1988; Marks & Hermey, 1996; Holtrop, 1990). Cell-cell interaction among osteoblast-lineage cells is important for their differentiation and function (Nakamura, 2007). Arana-Chavez et al. (1995) reported three types of cell adhesion in osteoblasts at early developmental stage by electron microscopy: focal tight junctions, adherens junctions, and gap junctions. Tight junctions are thought to be involved in maintaining cell polarity and preventing macromolecules to enter the intercellular spaces, but, in osteoblasts, they may not play a role in segregation of bone matrix from extracellular fluid. Osteoblasts, bone lining cells, and osteocytes are connected by their cell processes through gap junctions. These junctions are involved in transport of ions and micromolecules among osteoblast-lineage cells. Adherens junctions are thought to be involved in signal transduction via cell-cell interaction. These junctions are composed by cadherins. Major adherens expressed in osteoblasts are N-cadherin and cadherin-11 (Ob-cadherin) (Tsukita et al., 1991; Di Benedetto et al., 2010). Moreover, Kawaguchi et al. (Kawaguchi et al., 2001) suggested that cell-cell adhesion via cadherins could contribute to regulation of differentiation, function and survival of osteoblasts.

MSCs could differentiate into chondrocytes, osteoblasts, myoblasts, and adipocytes (Aubin et al., 2006). Commitment of MSCs to tissue-specific cell types is orchestrated by morphogens, developmental signalling pathways and transcriptional regulators that serve as key factors.

The process of osteoblast differentiation, starting from MSCs, can be subdivided in to three stages, characterized by expression of certain molecular markers (Stein et al., 2004): 1) proliferation; 2) extracellular matrix synthesis and maturation; and 3) mineralization (figure 1.5).

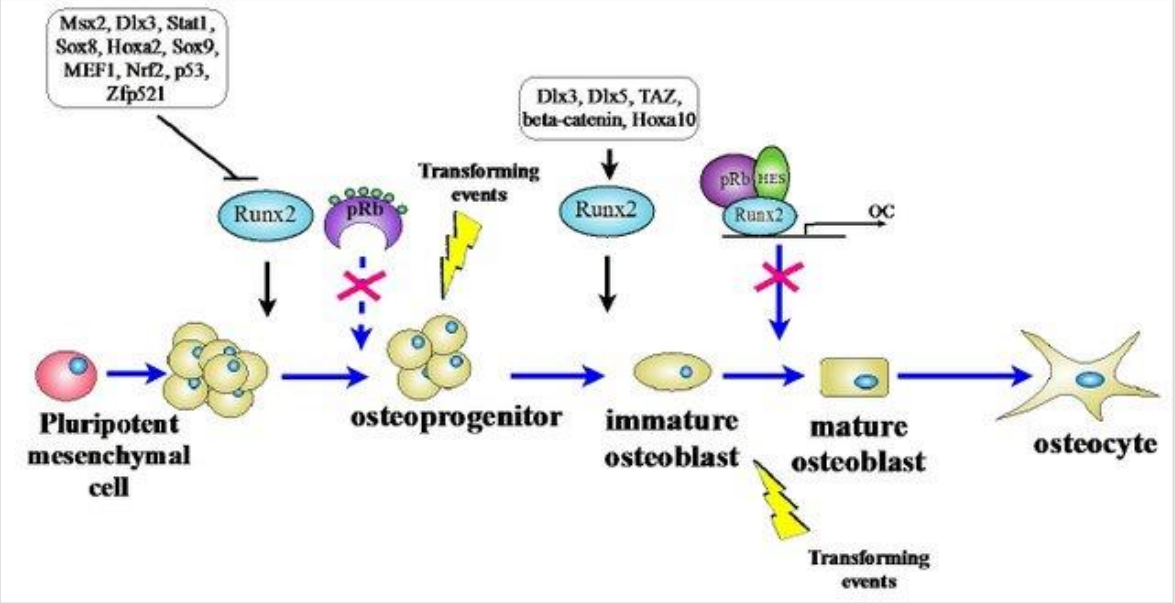

Figure 1.5. Molecular pathways involved in osteoblast differentiation.

First at all, the cells continue to proliferate and express fibronectin, collagen, TGFb receptor 1, and osteopontin. In the second step they exit the cell cycle and start differentiating, while maturating the extracellular matrix with Alp and collagen. In Stage 3 matrix mineralization occurs when the organic scaffold is enriched with osteocalcin, the second most abundant protein in bone after collagen, which promotes deposition of mineral substance (Komori et al., 1997; Raghavendran et al., 2014). At this stage the osteoblast become cuboidal cells (Long, 2012).

The most important transcription factors are Cbfa1(also known as Run trelated transcription factors 2, Runx2), Osx (Osterix) and ATF4 (Holtrp, 1990; Poole, 1991). In the absence of Runx2 and Osx, no osteoblasts are formed, so these factors are crucial for osteoblast differentaition (Capulli et al., 2014; Ducy et al., 197). Additionally, *Runx2* is the master gene of osteoblast differentiation (Ducy et al., 1997; Komori et al., 1997; Stein et al., 2014). During embryonic development, *Runx2* is expressed just before osteoblast differentiation and only in mesenchymal cells committed to become either chondrocytes or osteoblasts. Subsequently, the expression of this transcription factor becomes limited to osteoblasts (Ducy et al., 2000) and is required for the expression of osteoblast-specific proteins, such as osteocalcin (Mackie, 2003). So, Runx2 is important during the exit of preosteoblasts from the cell cycle (end of growth – start of matrix maturation) and during late maturation stages of osteoblasts (Stein et al., 2004).

In general, ALP (alkaline phosphatase), BSP (bone sialoproteins) and ColI (collagen matrix I protein) are early markers for osteoblast differentiation, while PTHR and OCN appears late, simultaneously with mineralization. Osteoblasts also produce cytokines including insulin-like growth factor I, II and transforming growth factor β (TGF-β) (Lian et al., 1999). These growth factors are stored in calcified bone matrix and play an important role in differentiation and function of osteoblasts. Thus, bone matrix acts as a storage site of growth factors in addition to calcium and phosphates (Nakamura et al., 2007).

Other factor synthetized including the bone morphogenetic proteins (BMP members of the transforming growth factor β family) and members of the Wingless (Wnt) pathways (Baron & Kneissel, 2013). Wnt activates three distinct intracellular signalling cascades: the Wnt/b-catenin pathway, the Wnt/Ca2+ pathway and the Wnt/planar polarity pathway. The Wnt/b-catenin pathway is frequently referred to as the canonical pathway. The canonical Wnt/ β catenin pathway has multiple roles in osteoblastogenesis; provides early development cues that indirectly mediate the initial cascade of gene expression for skeletal development, bone formation and osteoblast differentiation (Yavropoulou & Yovos, 2007; Saidak et al., 2015; Hill et al.,2005). Binding of Wnt to Frizzled and LRP5/6 receptors (low-density lipoprotein receptor related protein 5/6) induces a signalling cascade that allows the accumulation of β-catenin in the citosol. Beta-catenin then enters the nucleus where it promotes the transcription of target genes. It results in expression of an early osteoblast marker, the alkaline phosphatase (ALP) (Lopes et al., 2007).

BMP play important roles in directing fate decisions for MCSs. BMPs are members of the TGFb superfamily, and the ligand binds to a receptor on cell surface, which activates SMAD proteins. Throught a signalling cascade they regulate transcription of target genes. Osteogenic BMPs are BMP2, 4 and 7 (Chen et al., 1997; Florencio-Silva et al., 2015). The microenvironment, in particular the mechanical stresses, affects the expression of BMP2, which under physiological conditions is the main osteogenetic factor in that it promotes osteoblast differentiation by increasing the expression of the matrix proteins (Dai et al, 2013). TGFβ can provide competence for early stages of chondroblastic and osteoblastic differentiation, but it inhibits myogenesis, adipogenesis and late stage osteoblast differentiation (Pittenger et al., 1999; Binaco et al., 2001; Friedman et al., 2006; Aubin et al., 2006). BMPs promote differentiation of osteoblasts by preventing MyoD expression (Katagiri et al., 1996) and inducing *Runx2* expression. (Nishimura et al., 2012). *Runx2* is the fundamental gene in this differentiation process, so the absence of osteoblasts in knockout mice for this gene, causes a cartilaginous skeleton (Florencio-Silva et al, 2015). During

differentiation, osteoblasts express a characteristic genetic pattern that distinguishes them from other types of cells. During the transition from preosteoblast to mature osteoblast an increase in the expression of Osx and of sialoproteins I / II (BSP) is also observed. Mature osteoblasts form a single layer of cuboidal cells, containing abundant endoplasmic reticulum and a large Golgi complex. At the end of the phase of bone formation, osteoblasts can be incorporated into the bone as osteocytes, which are interconnected stellar cells that regulate the turnover of bone material (Long, 2012). Osteoblasts that remain on the surface of bone facing the periosteum have an option of becoming inert bone-lining cells nor undergo apoptosis. Bone-lining cells are flat quiescent cells that cover the bone surface, where neither the processes of formation or bone resorption occur. The cells of lining have secretory activity that derives / depends on the physiological bone state, so they can reacquire their secretory activity, becoming larger and cuboidal (Florencio-Silva et al., 2015).

Numerous factors influence the number of osteoblasts that choose each of these pathways, including the type of bone (Parfitt, 1990), age, species, hormonal status and health status. (Franz-Odendaal et al, 2006). In the last few years it has been argued that in the osteocytogenesis process a subpopulation of osteoblasts on the bone surface slows down the production of matrix compared to adjacent cells and remains under the matrix produced by neighboring osteoblasts (Dallas & Bonewald, 2010). Initially it was considered a passive mechanism, as some osteoblasts remained "trapped" in osteoids, which then they passively mineralize. However, there are structural and morphology changes that suggests that it is rather an active process: among these, the formation of dendritic processes as well as the reduction of cytoplasmic volume. It has been proposed that it is the osteoid i.e. the cell that is becoming osteocyte, to control and regulate the mineralization and not the osteoblasts on the bone surface (Dallas & Bonewald, 2010).

The process of differentiation is characterized by important morphological and ultrastructural changes (Adamo et al, 2006), like a reduction of cell size (cell volume reduction of about 70% from preosteoblast to osteocyte), an extension of the endoplasmic reticulum and Golgi, an increase of the cellular processes as well as intracellular organelles changes (decrease in number) (Franz-Odendaal et al, 2006). At the end of the osteocyte maturation process, downregulation is observed of osteoblast genes / markers such as OCN, BSP II, collagen I and ALP, while osteocyte-specific markers such as DMP1 (dentine matrix protein 1) are more expressed (Florencio-Silva et al, 2015). Among the main functions of the osteocytes are its ability to act as mechanosensors. These cells can be affected by pressure variations and to facilitate the adaptation of the bone to the mechanical forces to which are

daily subjected. Furthermore, the apoptosis of the osteocytes constitutes a resorption signal bone (Florencio-Silva et al, 2015).

1.2.3 MICROGRAVITY EFFECT IN BONE TISSUE

Several scientists (Smith & Heer M 2002; LeBlanc et al., 2000; McCarthy 2005; Di et al., 2011; Hammond et al., 2001; Qian et al., 2009; Van Loon, 2007) have suggested that, in microgravity conditions, normal physiological processes, such as the functional integrity of muscles and bone mass, result to be affected. So, microgravity is an ideal physical stimulus to evaluate bone cell responses in stress conditions. Studies in vitro showed modifications in bone cell attachment structures and cytoskeletal reorganization (Aleshacheva et al., 2015; Grimm et al., 2011; Grosse et al., 2012; Ma et al., 2014; Ulbrich et al., 2011). These changes may be involved in bone mineral loss, that is considerated one of the most serious problems induced by long-term weightlessness (Arfat et al., 2014).

The exposition on microgravity has been associated with several physiological changes observable in astronauts, including loss of bone mass as in the case of osteoporosis (Nabavi et al, 2011). It is known that the microgravity disturbs the relationship between osteoclast and osteoblast activity. Bone pathologies derive precisely from the imbalance between the reabsorption processes and bone formation. The first study examining osteoclasts and osteoblasts placed simultaneously in the condition of microgravity, was performed by Nabavi (2011). He observed a significant increase in bone resorption, or osteoclastic activity. There are several bone diseases in which osteoblast inhibition and osteoclast activation play a crucial role, for example multiple myeloma (Terpos & Dimopoulos, 2005), osteoporosis, periarticular osteopenia in patients with rheumatoid arthritis (Yudoh et al, 2000; Gravallese, 2002), osteomyelitis, osteopetrosis (Manolagas, 1998) and metastatic cancer (Roodman, 2001).

Tamma et al. in 2009 conducted an in vivo study under microgravity conditions. It's emerged that a prolonged exposure to microgravity resulted in a loss of 1-2% by mass bone for each month in flight, in the regions of the legs and the lumbar vertebral column (Tamma et al., 2009). For example, the femur showed reduced mineralization and a increased reabsorption after 4 days under microgravity conditions (Nabavi et al, 2011). Microgravity, real or induced, inhibits cell differentiation osteoprogenitors in mature osteoblasts, by hindering the responsiveness of Cbfa1 to BMP2, then the responsiveness of osteoblasts to the cytokines that promote their proliferation and differentiation (Dai et al, 2013). Astronauts and

cosmonauts did show a distinct loss of bone mineral density in the lumbar spine, the pelvis, and the proximal femur (Grigoriev et al., 1998), and the extent of bone loss varied up to 20% (Vico et al., 2000).

A significant increase in the osteoblast cell area was also observed in microgravity conditions, compared to control cells grown in normogravity conditions (Hughes-Fulford., 2002). This increase in cell size can be attributed to the alteration of the F-actin or to the decrease of the mechanical stiffness that normally leads to cell expansion (Saxena et al., 2007). These evidence led to hypothesize that MSCs are sensitive to microgravity (Merg et al., 2011). Several cellular components such as nucleotides and microtubules (MTs), are varied in cells grown under microgravity conditions. The cytoskeleton is involved in fundamental cell processes, including form (Fletcher & Mullins, 2010), proliferation (Provenzano & Keely, 2015), motility and migration (Tang & Gerlach, 2017), protein synthesis, transport, signal transduction (Forgacs et al., 2004) and apoptosis (Atencia et al., 2000). The cytoskeleton is connected to the extracellular environment through adhesion complexes in membrane, known as "focal adhesions" (FAs). The complexes of focal adhesions include integrins and specific proteins, such as vinculin, talina, paxillin and zixin that physically connect the extracellular membrane to intracellular actin microfilaments (Kuo, 2013).

Cytoskeletal variations are strictly related to morphology and nuclear function (Starr, 2007) and the magnified nuclei observable in osteoblasts may derive from this cytoskeletal dysfunction (Nabavi et al., 2011). Nabavi et al., also observed a significant increase in abnormal nuclei in osteoblasts, therefore apoptotic death of osteoblasts in microgravity may occur, a salso observed later by Ndozangue-Touriguine et al. (2008). This could be connected to the so-called anoikis phenomenon, which involves nuclear fragmentation (Valentijn et al, 2004), induced when anchor-dependent cells detach themselves from their extracellular matrix (Grossmann et al, 2001). This is often related to the decrease in focal adhesions (Nabavi et al, 2011).

Other studies demonstrated that F-actin cytoskeletal disturbance is correlated to inhibition of osteogenic differentiation of MSCs and osteogenic precursor cells (Huang et al., 2009; Zayzafoon et al., 2004). Furthermor, some authors suggested that these changes to F-actin cause disturbances and alterations of Rho GTPase activity (Zayzafoon et al., 2004).

The rupture of interactions between collagen I and integrins and the signal reduction mediated by the integrins themselves are both mechanisms for the reduction of osteoblast differentiation (Meyers et al, 2004). Integrins are transmembrane heterodimeric receptors

which bind proteins of the extracellular matrix and produce signals for cell survival and differentiation.

Studies conducted on the expression of integrins and their function in differentiation showed that, after 7 days under microgravity conditions, the MSC, had a reduced expression of the ColI and a considerable increase in the expression of the α2 and β1 integrins specific for ColI (Ebnerasuly et al., 2017) Furthermore ColI is also hyperexpressed in the mesenchymal stem cells of subjects affected by osteoporosis (Pino et al., 2012). Despite the overexpression such integrins, the PYK2 (proline-rich tyrosine kinase 2) was significantly reduced. In addition it was observed a reduction of the MAPK cascade following the decrease Ras (induction of MAP kinase cascade) and ERK expression. ERK is essential in the regulation of osteoblast differentiation, because it activate Runxβ, an essential osteoblastic transcription factor. So, the microgravity negatively regulates the integrin / MAPK signaling and, consequently, osteoblastogenesis, while promoting the differentiation of MSC in adipocytes, increasing the expression of PPARγ (proliferator-activator range receptor) (Zhang et al., 2018).

Moreover, osteoblasts after exposure to microgravity show defects in cell surface adhesion complexes and in the cytoskeleton. In particulrar, it was observed a depolymerization of F-actin, correleted with cytoskeletal reorganization involved in bone loss (Arfat et al, 2014).

To understand the metabolic changes in microgravity conditions, several studies wer carried out.

1.3 OMICS SCIENCES

The word omics refers to a field of study in biological sciences including genomics, transcriptomics, proteomics, or metabolomics, that study genome, proteome, transcriptome, or metabolome, respectively. More specifically genomics is the science that studies the structure, function, evolution, and mapping of genomes and aims at the characterization and quantification of genes; Transcriptome represents the set of all messenger RNA molecules in one cell, tissue, or organism; Proteomics is the science that studies those proteins as related to their biochemical properties and functional roles, and how their quantities, modifications, and structures change during growth and in response to internal and external stimuli. Finally, metabolomics is the science that studies all chemical processes involving metabolites, that are the end products of cellular processes, in a biological cell, tissue, organ, or organism. More specifically, metabolomics is the study of chemical fingerprints that specific cellular processes establish during their activity (Prakash et al., 2010). Transcriptomics, proteomics and metabolomics reveal the biological function of a gene. The methods of measuring cellular molecules, such as RNA, proteins, and metabolites are now knon as "-omic-" technologies, based on their ability to characterize most members of a family of molecules in a single analysis by substantially increasing the number of proteins/genes that can be detected simultaneously (Prakash et al., 2010). The primary aim of omics sciences is to identify, characterize, and quantify all biological molecules that are involved in the structure, function, and dynamics of a cell, tissue, or organism. (Prakash et al., 2010) (Figure 1.6).

The different functional levels analyzed by the Omics sciences are integrated in the context of the systems biology, a new field of science, which offers an innovative approach to the study of biological systems. Until a few years ago, in fact, traditional biology has focused on identifying individual cellular components and on the study of their functions in a separate way, with an approach that is called "reductionist". However, in recent years, awareness has arisen that a biological system is the sum of several parts, and its functioning can not be mirrored by the function of a single component. Thus, in contrast to reductionism, systems biology promotes a "holistic" approach: a biological system is seen as a complex network of dynamic interactions among its components, such as genes, mRNAs, proteins and metabolites, studying the entire "omica cascade" (Prakash et al., 2010; Bremer, 1983).

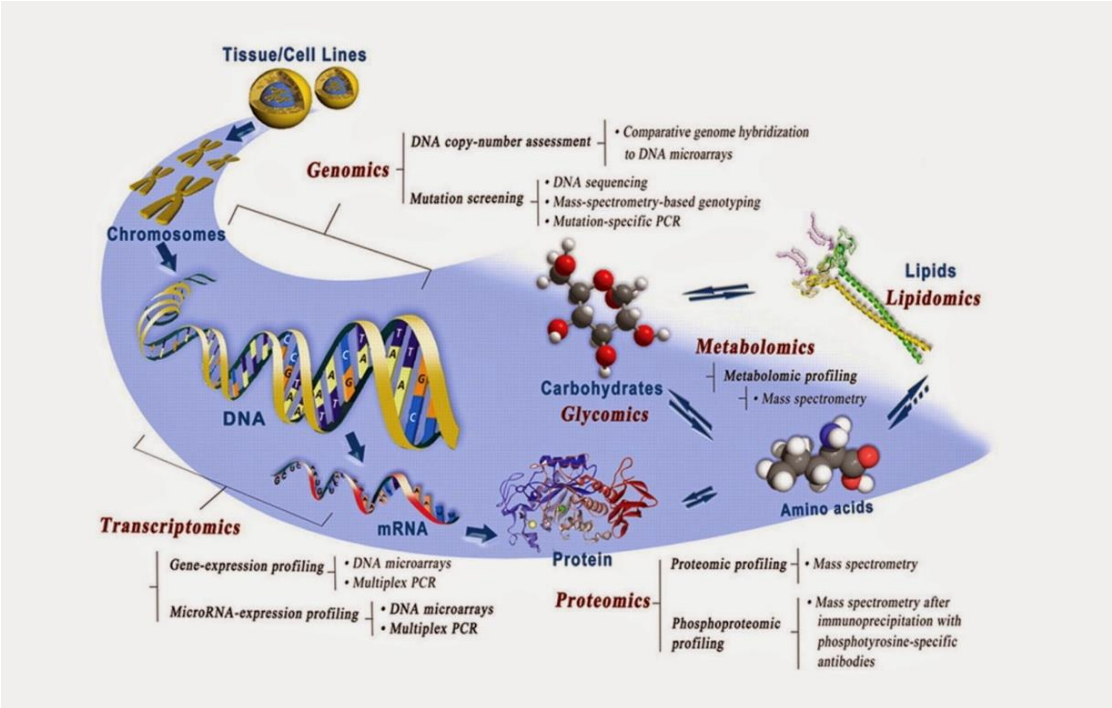

Figure 1.6. Omics technologies and their corresponding analysis targets.

In this thesis the important role of proteomics and metabolics, in the science world related to new reserches, as dealing with the impact of microgravity of on the human health will be elucidated, with particular attention to osteoporosis development in microgravity conditions. Information obtained by proteomics and metabolomics studies will enable short-term studies with highly sensitive endpoints to test new therapeutic strategies.

1.3.1 PROTEOMICS

The term "proteomics" was first used by Marc Wilkins in 1996 to denote the "PROTein complement of a genOME" (Wilkins et al., 1996). Proteomics is the characterization of proteome, including expression, structure, functions, interactions and modifications of proteins at any stage (Domon et al., 2006). The proteome also fluctuates from time to time, cell to cell and in response to external stimuli. Proteomics in eukaryotic cells is complex and exhibits extensive dynamic range due to post-translational modifications, which arise at different sites by numerous ways (Krishna et al., 1993). The proteomics would be considered as the most relevant data set to characterize a biological system (Cox et al., 2007), because it is one of the most significant methodology to

comprehend the gene function. In particular, fluctuations in gene expression level can be determined by the analysis of transcriptome or proteome to discriminate between two biological states of the cell (Aslam et al., 2016). Thanks to the information obtained through genomic information and to improvements in analytical technologies proteomics is becoming increasingly important for the study of many different aspects. Protein studies are essential to reveal molecular mechanisms, since proteins are components of major signaling and biochemical pathways. Especially proteome could be use to underline cell growth, cell development, and its interactions with the environment, in order to identify protein expression profiles, protein modifications and protein networks in relation to cell function and biological processes (Westermarck et al., 2013). The aim of proteomics is also to do an integrated study of proteins and their biological functions and processes, protein structure and protein –protein interactions.

The human body may contain more than 2 million proteins with different functions. This protein diversity is due to alternative splicing and post-translational modifications of proteins. In fact, many types of information cannot be obtained from the study of genes alone, because the exon-intron structure of most genes cannot be accurately predicted by bioinformatics (Dunham et al., 1999). So, proteomics results more useful for characterizing cells and tissues (Prakash et al., 2010).

Studying the proteomic is a rather difficult undertaking because we are dealing not only with an unspecified number of elements, many of them unknown, but also with a molecular system extremely dynamic. Morover, the different proteins can be present in very different concentrations and then request a very fine calibration of the experimental protocols in order to allow all of them can be resolved and highlighted simultaneously. So, in the last years researchers developed increasingly sensitive and suitable systems to manage a large number of elements at the same time. Among the new technologies most widely used in the laboratory, there is mass spectrometry, a known technique that allows identification, characterization and partial sequencing of proteins (Reinders et al., 2004). Proteomics uses various technologies such as one-and two-dimensional gel electrophoresisis, identifying the relative mass of a protein and its isoelettric point (Prakash et al., 2010; Wittmann-Liebold et al., 2006; Görg et al., 2004), and high resolution liquid chromatography (HPLC) (Nagele et al., 2004). A typical proteomics experiment needs three steps: (i) the separation and isolation of proteins from a cell line, tissue, or organism; (ii) the acquisition of protein structural information for the purposes of protein identification and characterization; and (iii) database utilization (Figure 1.7) (Wilke et al., 2003; Nagele et al., 2004).

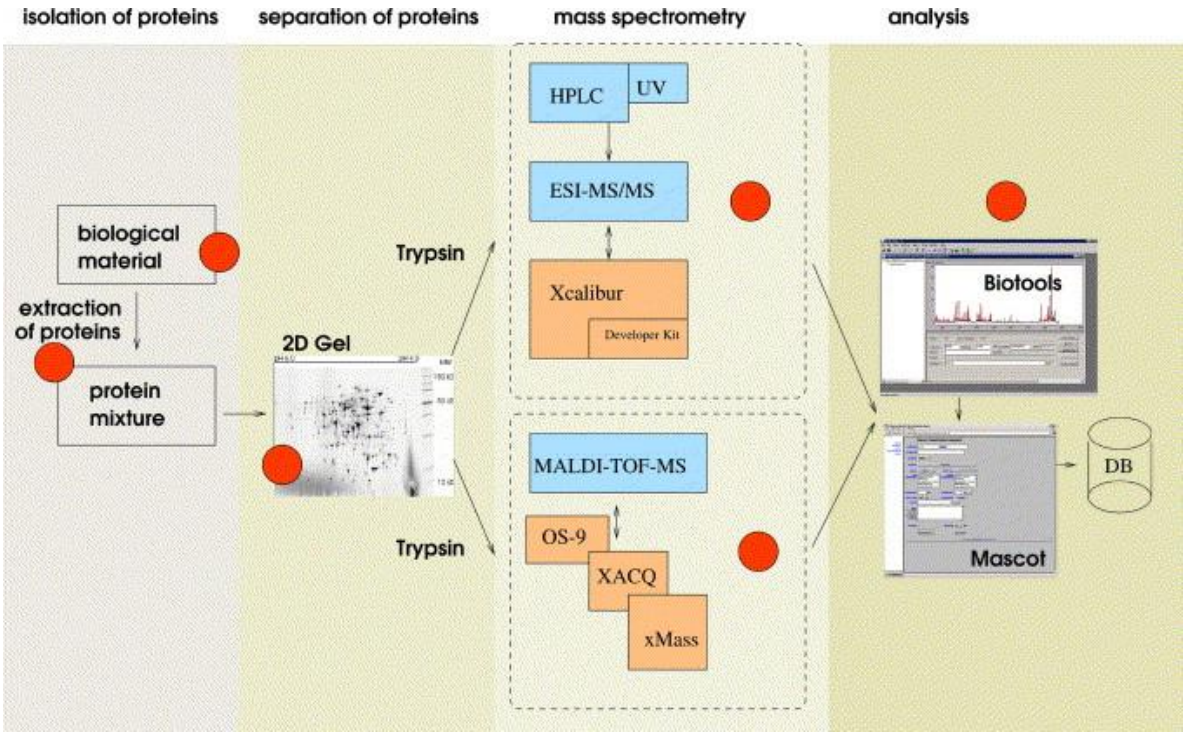

Figure 1.7. Different steps of a proteome experiment. Firstly, there is the preparation of the biological material where parameters like media composition, temperature or stress conditions need to be documented. Then the protein sample is extracted, separated and digested. Additionally, it needs that gel images/chromatograms ans machine parameters are archived during these steps. Finally, mass spectra are obtained and analyzed with different software tools (e.g. Mascot) (Wilke et al., 2003). Different color identify the need of bioinformatic tool (red circle), the use of hardware (blu square) and the use of sofware (pink square).

Knowing all the proteins of a cell is essential to compare diseases from the diagnostic capacity of recognizing the presence of a patology with the greatest speed and efficiency and therapeutic point of view, to develop specific approaches. In particular, by the proteomics approach it is possible to distinguish cellular responses to molecular damage and detect possible new biomarkers based on molecular responses to functional perturbations and cellular damage. Moreover, biomarkers could be used for diagnosis and to find a therapeutical approach to different patologies. Despite proteomics can also be applied to determine a several of tasks within the cell, no single omics science is sufficient to facilitate a comprehensive understanding of the complex human biology and physiology (Boja et al., 2014). So, the integration of several omics sciences is fundamental, expecially in clinical use.

1.3.2 *METABOLOMICS*

Metabolomics is the newest of these Omics and is defined as the set of metabolites (small molecules with molecular weight <1.5 kDa) produced or present in a biological system (Carraro et al., 2009). This science complements the more traditional omical sciences through the investigation of properties that can not be directly evaluated by proteomics and genomics.

Epigenetic modifications (Ellis et al., 2007), or even changes in the expression of DNA that can not be assessed by knowledge of the DNA sequence itself, can also indirectly influence the metabolome (Hollywood et al., 2006).

It is obvious that a complex biological system is affected and continuously modified in relation to the physiological state and to the interactions with the external environment, generating new metabolic pathways. Metabolomics, studying and quantifying the metabolites present in biological fluids, offers a vision of the instantaneous system, providing useful information for the understanding of the processes underway in the organism analyzed (Figure 1.8).

It is considered the "omic" science closest to phenotypic expression because it reflects both the information contained in the genetic code and the influences derived from interaction with the environment. In fact, the metabolites can be seen as the final product of gene expression and protein activity, thus defining the biochemical phenotype of a biological organism.

Another characteristic of the metabolome is its highly dynamic nature: this allows the metabolome to be a very rapid indicator of perturbations of a system (Bremer et al., 1983). Thanks to the close correlations of the metabolome with the genotype, the physiology and the environment, this science offers the unique opportunity to define the correlations between genotype and phenotype and the relationships between phenotype and environment (Gomase et al., 2008; Griffin et al., 2004; Eden et al., 2010).

The metabolomic analysis can be applied in the medical field. The metabolome is characterized by a great variety of chemically different molecules, such as amino acids, organic acids, carbohydrates, lipids. These compounds are present in different concentrations and not all of them are present in all tissues and biofluids. We must also consider the presence and role of exogenous metabolites deriving from diet, drugs, microbial flora or other. Metabolomics allows the identification of either metabolic patterns or individual metabolites, useful for understanding the etiology of a pathology and for

following its progression over time, especially in the context of multifactorial diseases. Furthermore, the identification of unexpected and unknown metabolites may allow to formulate new pathogenic hypotheses (Nicholson et al., 2008; Mamas et al., 2009; Van der Greef et al., 2004). Thus, metabolomics play a fundamental role in determining moment by moment the metabolic response resulting from external stimuli, unlike genomics which only provides a static prediction of how a system can evolve.

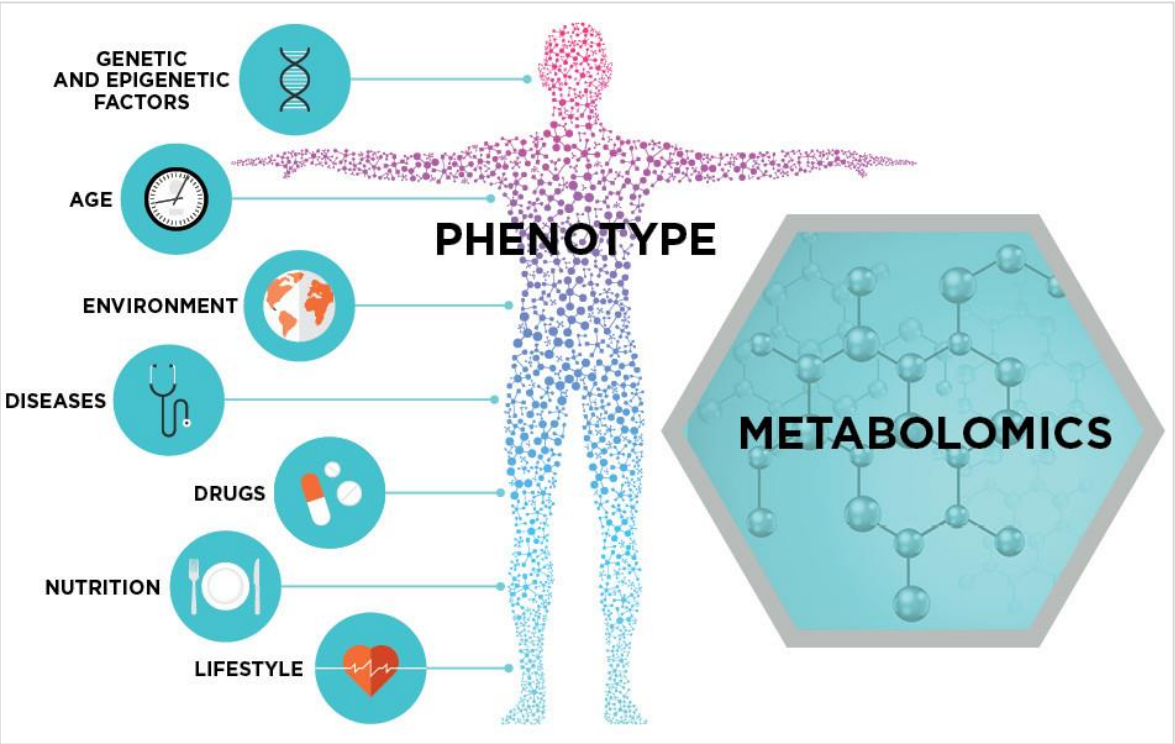

Figure 1.8. More than 40,000 metabolites are known to be in the human body. Metabolites that appear in biological fluids provide very useful information about a patient's current health.

In order to obtain a complete metabolomic analysis, it is necessary to obtain the determination and quantification of the metabolites that provide the image of the biochemical state of the biological system examined (Wang et al., 2010). For the study of metabolites, different complementary methodologies are used, for each level of information. The first is a highly specific approach that focuses on the qualitative and quantitative analysis of a single analyte, such as a disease marker or the substrate of an enzymatic reaction (Dettmer et al., 2007). This is indicated as a "target analysis". On the contrary, the "metabolite profiling" is instead an approach focused on the analysis of a group of metabolites belonging to a specific metabolic pathway or a certain class of compounds.

Target analysis and metabolic profiling are generally hypothesis-guided approaches, therefore based on previous knowledge, as well as selective, since they focus on a small number of metabolites; they are therefore not considered as a true type of metabolomic approach (Carraro et al., 2009; Dettmer et al., 2007). The “metabolite fingerprinting” is instead an approach that starts from the evaluation of the greatest number of possible metabolites, for the definition of metabolic patterns or "fingerprinting" associated to a given condition. The primary purpose is not the identification of the individual metabolite, but rather the definition of the metabolic characteristics that are able to discriminate between the groups under examination. The metabolite fingerprinting is a real omic approach, because it guarantees a global study of the metabolites, not guided by a priori hypotheses. This type of analysis provides a numerical representation of the data obtained which constitutes a digital metabolic fingerprint.

Once the specific pattern of a certain condition is identified, the structural identification of the relevant metabolites is proceeded: this allows to identify significant biomarkers in the distinction between different pathophysiological conditions. First of all, it is left open the possibility of identifying unexpected or even unknown biomarkers, which can pave the way for a better understanding of not fully clarified pathophysiological mechanisms and become the target of new therapies (Nicholson et al., 2002; Madsen et al., 2010).

1.3.3 PROTEOMICS AND METABOLOMICS IN MICROGRAVITY

Because many serious physiological changes occur during spaceflight, many experimental tools and methods have been developed to study microgravity. Recently proteomic and metabolomic approaches are widely accepted and used to understand biological processes. Both have been used to find effective countermeasures to spaceflight-induced alterations. Significant progress has been made in identifying the proteins and metabolites responsible for these changes.

Microgravity might generate an unique stress not achievable with cell culture studies in normogravity conditions. The stressful environment of space causes changes in bacteria and fungi, animals and people. So, it is important to study mammalian cells, animals, bacteria and plants exposed to simulated and real microgravity. Moreover it is necessary to detect the cellular changes that cause the medical problems often observed in astronauts, cosmonauts or animals returning from prolonged space missions for medical and biotechnological reasons. Research on numerous types of human cells exposed to weightlessness has been

conducted in recent years. The astronauts during the Space travelers face health problems such as genetic changes and cancer development (Koop et al., 2018; Pereda-Loth et al., 2018; Sahana et al., 2018). So, the comparison of protein contents of cells grown under normal 1g and of cells exposed to weightlessness could be useful to understand changes that occur during spaceflights (Krüger et al., 2017). These kind of experiments, are often performed using devices as the Rotating Wall Vessel (RWV), the 2D Clinostat or the Random Positioning Machine (RPM), built by Dutch Space (Leiden, NL) which prevent cell sedimentation (Riwaldt et al., 2017).

In order for in vitro tissue engineering under microgravity conditions to succeed, the features of the cell that change need to be known. Many studies suggest that the effects of microgravity on major cell functions depend on the responding cell type.

In the last few years, many protemics studies have been carried out on microorganisms (Rea et al., 2016), on neonatal rat cardiomyocytes (Feger et al., 2016), on mice hippocampus (Sarkar et al., 2006) on crustacean (Trotter et al., 2016), on human neuroblastoma cells (Zhang et al., 2013), and on other kind of cells, tissue and organisms, under microgravity conditions. Moreover, several metabolomics studies have recently been carried out (Feng et al., 2016; Chen et al., 2016; Orsini et al., 2017; Costantini et al., 2017; Blazer et al., 2017), to underline mechanisms of these changes and their molecular consequences, but nobody has yet carried out an integrative approach using these two omics techniques.

Because gravity plays a key role in regulating cell processes, such as proliferation and differentiation and cell functions, here, we discuss on how the proteome and metabolome of osteoblastic cell respond to microgravity, focusing on mithocondrial changes and alteration of differentiation that occurs during micogravity conditions.

2 EFFECTS OF MICROGRAVITY ON OSTEOBLAST MITOCHONDRIA: A PROTEOMIC AND METABOLOMICS PROFILE

2.1 INTRODUCTION

Since space flight began, alterations in gravity (hypergravity and/or microgravity) represent a powerful physical cue for modelling both anatomy and function of living organisms (Ikawa et al., 2011; Xue et al., 2011). Exposure to altered hyper-gravity can cause detrimental effects on muscle mass, composition, and contractility, as well as on bone density, with long-term effects even after return to normal gravity (Lee et al., 2015). Moreover, hypergravity affects myoblast proliferation and differentiation (Ciofani et al., 2012), PC12 neuron-like cell differentiation in vitro (Genchi et al., 2015), cyclooxygenase-2 expression in the heart vessels in vivo (Oshima et al., 2005), and the immune system (Gueguinou et al., 2012). On the other hand, the absence of gravity is also an extreme biological stressor and its impact on biological systems is ill-defined. Microgravity has the capability of inducing decreased immune function, bone density loss, and skeletal muscle atrophy and affects cardiac physiology of astronauts on off-planet missions (Bungo et al., 1987; Williams et al., 2009). In vivo, the most severe effects on astronauts relate to reduction in bone mass and osteopenia, which accompany extended spaceflight (Collet at al., 1997). Predominantly, microgravity induces pleiotropic effects in several tissues; bone, immune and nervous system, and skeletal muscle cells rearrange their cytoskeletal organisation and protein turnover, directing cells toward apoptotic death or premature senescence, altering cellular division and differentiation (Lescale et al., 2015; Nichols et al., 2006). It is well documented that bone mineral density (BMD) of astronauts decreases at specific weight-bearing sites during spaceflight (Chatani et al., 2015), suggesting that osteoclasts and osteoblasts are gravitationally sensitive (Nabavi et al., 2011). Gravitational biology studies report that gravitational force is a key factor in tissue construction (Porazinski et al., 2015) and bone remodelling (Del Signore et al., 2004; Fitts et al., 2001). The response of biological cells to microgravity stressors is not only tissue-specific but also cell histotype-dependent. In vitro, osteoblastic cells are hypo-functional as, upon microgravity exposition, cells undergo alterations of cellular integrity with modified microtubule structure, focal adhesions and increasingly fragmented nuclei (Jee et al., 1983). Conversely, osteoclast cells are hyper-stimulated by microgravity, displaying higher numbers of discrete resorption pits and

increased cellular activity with an enhanced expression of mitochondrion-related genes and reduced roundness of mitochondria (Schatten et al., 2001; Nabavi et al., 2004; Hu et al., 2015). Mitochondria in skeletal muscle tissue can undergo rapid and unusual changes as a result of changes in muscle use and environmental conditions. Endurance exercise training can increase mitochondrial volume by up to 50% in previously untrained subjects (Hoppeler et al., 2003). Although exhaustive physiological and cellular information on the response of osteoblast cells to microgravity has been collected, the gravitational stress-response proteins that are activated and mechanisms of the downstream effects are poorly understood. Thus, with the aim of revealing effects of microgravity on molecular processes beyond the cellular hypo-gravity response, two complementary mass spectrometry-based analytical 'omics' approaches were employed: proteomics and metabolomics. It is generally accepted that proteomics, based on mass spectrometry, allows for the relative quantitation of a large number of proteins concurrently and in a relatively unbiased manner (Feger et al., 2016), while metabolomics information supports and corroborates the effects of the differential proteins found. Thus, a combination of two omics techniques, proteomics and metabolomics, was used to investigate the energy homeostasis of human cells exposed to simulated microgravity. Overall, this investigation drew an exhaustive picture of how mitochondria in human primary osteoblasts are unctionally dysregulated by gravitational unloading. We believe these findings will contribute to a more complete understanding of the cell physio-pathological processes which accompany astronauts' diseases. In our opinion, evaluation of the biological effects of microgravity on energy homeostasis would be of help in space medicine for developing countermeasures to assure safe and effective aerospace missions.

2.2 MATERIAL AND METHOD

2.2.1 SIMULATED MICROGRAVITY

The desktop Random Positioning Machine (RPM) system (Dutchspace, The Netherlands) was used for conducting examinations on the influence of the force of gravity on eukaryotic cells (Borst et al., 2009). All experiments were carefully planned according procedures previously described (Wuest et al., 2015). Briefly, the rotating frame of the desktop RPM was placed inside an ordinary cell culture CO_2 incubator. The software responsible for controlling the motion of RPM employed a tailored algorithm, which rotated with a random speed in such a way that the mean gravity vector reliably converged to zero

over time, and it concurrently reduced fluid motion in the culture flask. In order to avoid artifacts and to minimise centrifugal acceleration, the samples were compactly placed around the center of rotation. Cell samples were carefully processed for *in vitro* cultivation: the culturing media were accurately sealed with a transpiring membrane, which was pressed to completely remove air bubbles from the culture chamber. Control samples were processed in the same manner. Plates were placed beside the RPM machine so that all samples shared identical culture conditions.

2.2.2 PATIENT CHARACTERISTICS

Patients selected for the study were screened to exclude any associations with clinical or pathological variables (carefully grouped on the bases of BMD parameters obtained by dual-energy X-ray absorptiometry (DEXA) T-score greater that -1). No patients showed any signs of bone or joint disease or autoimmune disorder. Informed consent was obtained from all patients. The biopsies were collected from high energy fractures of femoral head of healthy patients during hip replacement surgery. The bioptic samples from selected patients were taken to set up primary cells and human primary cells were cultured *in vitro*. All procedures were approved by the Institutional Review Board of Policlinico Tor Vergata Hospital, Rome, Italy (approval reference number # 85/12). Since no effects of sex on adaptation to space had been previously observed (Ploutz-Snyder et al., 2014), we decided to analyse osteoblasts from both male and female patients in order to determine average effects.
Experiments were performed in accordance with relevant guidelines and regulations. Human primary osteoblasts (hOBs) were isolated from 3 donors (2 male and 1 female; average age 53 years; female 52 years, males 49 and 59 years) undergoing hip arthroplasty surgery and used to perform separate experiments investigating the effects of microgravity *versus* normogravity conditions.

2.2.3 ISOLATION AND CULTURE OF PRIMARY HUMAN OB CELLS

Primary cultures of osteoblasts were isolated from the cancellous bone of healthy patients with high-energy femoral fracture. The bone tissue was minced, thoroughly washed to remove any remaining soft tissue, and placed in 6-well plates to initiate explant cultures. The culture medium consisted of DMEM/F12 (DMEM w/o L- glutamine w/ 25mM Hepes,

Biowest, Nuaillé, FR.) supplemented with 15% FBS, 50 µg/mL gentamicin and 0.08% Fungizone, penicillin streptomycin (Sigma Chemical Co., St Louis, MO, USA), and amphotericin B (biowest) and was changed twice per week. Cells were treated to select and isolate homogeneous populations of osteoblasts according to previously reported methods (Siggelkow et al., 1999). Briefly, after dissection, trabecular bone chips were repeatedly washed with PBS at 37°C for 2 h in shaking conditions. Then, two distinct enzymatic digestions were repeated and performed at 37°C. The first digestion employed 1mg/ml Trypsin from porcine pancreas ≥ 60 U/mg (SERVA Electrophoresis GmbH Heidelberg, DE) resuspended in PBS buffered at pH 7.2. After washing, trypsinized bone chips underwent to repeated digestions with a second type of protease employing 2.5 mg/ml Collagenase NB 4G Proved grade ≥ 0.18 U/mg (SERVA Electrophoresis GmbH, Heidelberg, DE) in PBS buffer with Calcium and Magnesium. The supernatants from the 4th bone-chips digestion was collected and centrifuged at 310 RCF for 5'. The cell pellets were suspended in DMEM with 15% FBS, thus cells were then grown in low calcium media, supplemented with fetal bovine serum (10%; Intergen, Purchase, NY, USA), penicillin (50 U/ml), and streptomycin (50 pg/ml). When the cultures reached confluence in 3-5 weeks, the bone chips were removed, and the cellular outgrowths treated with trypsin (0.05%) and EDTA (0.02%) to prepare single cell suspensions. All cells were incubated at 37°C and 5% CO2. Upon confluence, cells were detached from the plates by trypsinization, counted and subcultured at a density of 5000 cells/cm2 for three passages. Osteoblast proliferation was compared between different tissue sources at passage one. Third passage cells were used in all other experiments.

2.2.4 OSTEOBLAST CHARACTERISATION

Primary osteoblasts were cultured for two weeks in osteogenic medium (OGM) containing 10 mM biglycerol phosphate, 50 µM ascorbic acid, 25 ng/ml bone morphogenetic protein-2 (BMP-2; R&D Systems) in 10% serum containing alpha MEM. After two weeks of incubation, the cells were assessed for alkaline phosphatase activity as an indicator of differentiation. Morphological inspection was carried out to assess HA precipitated crystals. Osteoblast phenotype was characterised by immunohistochemistry as BMP-2, RUNX-2 and RANK-L (paper in preparation).

2.2.5 ASSAYS TO EVALUATE THE EFFECT OF SIMULATED MICROGRAVITY ON CELL NUMBER

Cells were seeded in a monolayer at 18 000 to 40 000 cells/cm^2 and cultured until the confluence was reached. When required, cells were detached by incubating plates with trypsin/versine solution for 10 minutes at 37 °C. The number of viable cells were assessed using the trypan blue dye *exclusion* procedure. Cell solution was mixed 1:1 with trypan blue stain (Invitrogen) and cells with intact membranes (viable cells) were counted using a haemocytometer device under an *o*ptical microscope (Nikon Eclipse TE 2000-5). Counts were performed in twice and repeated for three biological replicates. To determine the number of viable metabolically active cells (i.e. possessing active mitochondria), the cell titer 96 AQ cell colorimetric assay (Promega) was employed, following the manufacturers' instructions. After incubation for four hours, MTS formazan soluble product was measured at absorbance 490 nm with a Tecan Spark 10N spectrophotometer reader. Spectrophotometric determination of cell protein content was evaluated by the biuret colorimetric analysis of peptides and the bicinchoninic acid (BCA) method, with readings at wavelengths of 310 nm and 562 nm, respectively (Biuret reagent kit, Sigma-Aldrich; *BCA* Protein *Assay* Kit, The Thermo Scientific Pierce).

For all three assays, standard curve validated that the absorbance (at 490nm, 310nm or 562nm, respectively) read were directly proportional to the number of living cells in culture. The effect of the treatment on the number of cells was reported in term of percentage, as follows: the percentage calculation was based on the ratio of the mean value of microgravity-treated samples to the mean value of normo-gravity (control) samples. The statistical significance of data was determined using the Student's t-test.

2.2.6 MS SAMPLE PREPARATION

On day 5, microgravity-treated and control cells (3 biological replicates) were washed in phosphate saline buffer. Cellular suspensions were centrifuged at 1500 *g* for 5 min. The supernatant was discarded, and the cell pellet was resuspended in lysis buffer (7 M urea, 2M tiourea, 4% w/v CHAPS, 40 mM Tris-HCl, 0.1 Mm EDTA, 1mM DTT, 50 mM NaF, and 0.25 mM Na_2VO_4).

The 2D-Quant Kit (GE Healthcare) was used for determination of total protein concentration. Aliquots (150 µg) of each sample were loaded per lane and separated through

a 16–8% linear gradient polyacrylamide gel. Each lane was cut into 72 slices, approximately 2-mm thickness; these were subjected to in-gel trypsin-digestion according to the protocol of Schevchenko et al (Schevchenko et al., 1996).

2.2.7 LC-MS/MS ANALYSIS

Peptide extracts were analysed using a split-free, nano-flow liquid chromatography system (EASY-nLC II, Proxeon, Odense, Denmark) coupled with a 3D-ion trap (model AmaZon ETD, Bruker Daltonik, Germany), equipped with an online ESI nanosprayer (fused-silica capillary, 0.090 mm OD, 0.020 mm ID) in positive ion mode. For all experiments, a 15 µL sample volume was loaded by the autosampler onto a homemade 2 cm fused silica precolumn (100 µm I.D.; 375 µm O.D.; Reprosil C18-AQ, 5µm, Dr. Maisch GmbH, Ammerbuch-Entringen, Germany). Sequential elution of peptides was accomplished using a flow rate of 300 nL/min and a linear gradient from Solution A (2% acetonitrile; 0.1% formic acid) to 50% of Solution B (98% acetonitrile; 0.1% formic acid) in 40 min over the precolumn on-line with a homemade 15 cm resolving column (75 µm I.D.; 375 µm O.D.; Reprosil C18-AQ, 3 µm, Dr. Maisch GmbH, Ammerbuch-Entringen, Germany). The acquisition parameters for the mass spectrometer were as follows: dry gas temperature, 220 °C; dry gas, 4.0 L/min; nebulizer gas, 10 psi; electrospray voltage, 4000 V; high voltage end-plate offset, −200 V; capillary exit, 140 V; trap drive: 63.2; funnel 1 in 100 V out of 35 V and funnel 2 in 12 V out of 10 V; ICC target, 200,000 and maximum accumulation time, 50 ms. The sample was measured with the Enhanced Resolution Mode at 8100 m/z per second (which allows monoisotopic resolution up to four charge stages), scan range from m/z 300 to 1500, 5 spectra averaged, and rolling average of 1. The “Smart Decomposition” was set to “auto”.

Label-free quantitative analyses were performed in biological triplicates by using the spectral counting method based on normalized exponentially modified protein abundance index (emPAI) as described by Shinoda et al (Shinoda et al., 2010). In detail, for each protein the following percentage was calculated:

$$\text{Protein content (\%)} = \text{emPAI}/\Sigma\text{emPAI} \times 100.$$

Statistically significant differences were identified by unpaired t-student test.

2.2.8 MS DATA ANALYSIS

Compass DataAnalysis 4.0 software (Bruker Daltonics) was used for data processing. Generated MGF files were then merged per lane and used in a database search (SwissProt, version 20150612), using the Mascot Daemon application included in an in-house MASCOT server (version 2.5, Matrix Science, London, UK) with the following constraints: taxonomy = Homo sapiens (20207 sequences); enzyme = trypsin; missed cleavage = 1; peptide and fragment mass tolerance = ± 0.3 Da; fixed modifications = carbamidomethyl (Cys); variable modifications = oxidation (Met).

Label-free quantitative analyses were performed on three biological triplicates using the spectral counting method based on normalised exponentially modified protein abundance index (emPAI), as described by Shinoda et al (Shinoda et al., 2010).

To obtain a comprehensive description of the over-represented biological processes and functionally-related groups of proteins within our dataset, a Bioinformatic Gene Ontology analysis was performed using the on-line FunRich (Functional Enrichment analysis tool) software 3.0 (www.funrich.org). The default Homo sapiens genome was used as background.

2.2.9 METABOLOMIC EXTRACTION

For each treatment, $1 * 10^6$ cells (3 biological replicates × 3 technical replicates × 2 conditions; n = 18) were first subjected to three freeze-melt cycles (freezing in ice at 4 °C for 5 min, melting at 37 °C for 5 min; for 5 times). Next, 400 µl of freezing methanol and 600 µl of freezing chloroform were added to the cells. Samples were vortexed for 30 min at max speed at 4°C. The next day, samples were centrifuged at 16000 *g* for 15 min at 4 °C. Supernatants were then evaporated to dryness using an SPD2010–230 SpeedVac Concentrator (Thermo Savant, Holbrook, USA). When samples were completely dried, 60 µl of 5% formic acid was added to the dried residue and vigorously vortex-mixed.

2.2.10 UHPLC-HRMS

Twenty microliters of each sample were injected into an Ultra High-Performance Liquid Cromatography (UHPLC) system (Ultimate 3000, Thermo) and run on a Positive mode. Samples were loaded onto a Reprosil C18 column (2.0 mm × 150 mm, 2.5 µm; Dr Maisch, Germany) for metabolite separation. Chromatographic separations were achieved at a

column temperature of 30 °C; and flow rate of 0.2 mL/min. For positive ion mode (+) MS analyses, a 0–100% linear gradient of solvent A (ddH2O, 0.1% formic acid) to B (acetonitrile, 0.1% formic acid) was employed over 20 min, returning to 100% A in 2 min and a 6-min post-time solvent A hold. Acetonitrile, formic acid, and HPLC-grade water and standards (≥98% chemical purity) were purchased from Sigma Aldrich. The UHPLC system was coupled online with a mass spectrometer Q Exactive (Thermo) scanning in full MS mode (2 μscans) at 70,000 resolution in the 67 to 1000 m/z range, target of 1106 ions and a maximum ion injection time (IT) of 35 ms 3.8 kV spray voltage, 40 sheath gas, and 25 auxiliary gas, operated in negative and then positive ion mode. Source ionization parameters were: spray voltage, 3.8 kV; capillary temperature, 300 ° C; and S-Lens level, 45. Calibration was performed before each analysis against positive or negative ion mode calibration mixes (Piercenet, Thermo Fisher, Rockford, IL) to ensure sub ppm error of the intact mass. Metabolite assignments were performed using computer software (Maven,18 Princeton, NJ), upon conversion of raw files into.*mzXML* format through MassMatrix (Cleveland, OH).

2.2.11 DATA ELABORATION AND STATISTICAL ANALYSIS

Replicates were exported as mzXML files and processed using MAVEN 5.2. Mass spectrometry chromatograms were elaborated for peak alignment, matching and comparison of parent and fragment ions, and tentative metabolite identification (within a 2ppm mass-deviation range between observed and expected results against the imported KEGG database). Untargeted metabolomic profiling of cells from two independent cohorts of treated and control cells was conducted to reduce noise in the data analysis. Pre-processing was performed to exclude xenobiotics, carbohydrates, and metabolites with more than a 3-fold difference to the control group (p <0.01).

Metabolites detected across both groups that met acceptability criteria and were further analysed using MetaboAnalyst 3.0 software. Metabolite set enrichment analysis (MSEA) and pathway analysis (MetPA) were used to determine the biological processes involved in the conditions of interest. Both have been developed to identify and to interpret patterns in concentration changes of human osteoblast metabolites under conditions of microgravity.

The metabolic pathways affected the most by the “weightlessness” treatment in human osteoblast cells were screened by MetPa, assessing the differential impact of metabolites

on the overall metabolism (the pathway library was restricted to Homo sapiens and *p*-value <0.05).

The difference between the two groups was compared using the unpaired t-test with GraphPad Prism version 5.0 GraphPad software (La Jolla Ca); $*p < 0.05$ was considered significant.

2.3 RESULTS

The commercialized systems of desktop Random Positioning Machine (RPM) were employed as a ground-based model for simulating microgravity (or near weightlessness) for purified human primary osteoblast cells. Primary cultures of human osteoblasts were obtained from the cancellous bone of healthy donors with high-energy femoral fracture. First of all, we examined the macroscopic effects of simulated microgravity treatment on cellular biology, employing standard cell-biochemical assays. For each sample set, the relative cell viability was determined using three biochemical methods as follows: i) number of intact cells (i.e., number of trypan blue impermeable cells); ii) value of cell protein content (performed according to Biuret and BCA assay); and iii) formazan MTS formation (determined by colorimetric assay which detects the conversion of 3-(4,5-dimethylthiazol-2-yl)-2,5-diph enyltetrazolium bromide; MTT). With all three methods, the effect of gravitational unloading was calculated as the ratio of the mean value of treated group over the mean value of normogravity cells, expressed as a percentage. Figure 1 shows that 110 hours of microgravity treatment did not appear to alter human primary osteoblast (hpOB) proliferation, as the number of intact cells and cell protein content in the sample exposed to microgravity showed a slight decrease with respect to the normogravity cells. Regarding the mitochondrion-cell functionality, results of the formazan MTS assay showed that with microgravity there was a significant decrease in biocellular reduction efficiency ($p < 0.05$) (Fig. 2.1), thereby indicating that the prevalent impact of microgravity treatment affected mitochondrial metabolism rather than cell vitality. This apparent discrepancy was further investigated, focusing on mitochondrial metabolism using two “omics” approaches. Therefore, the hpOBs cells were exposed to simulated microgravity for 110 hours and then examined for proteomic and metabolomic changes.

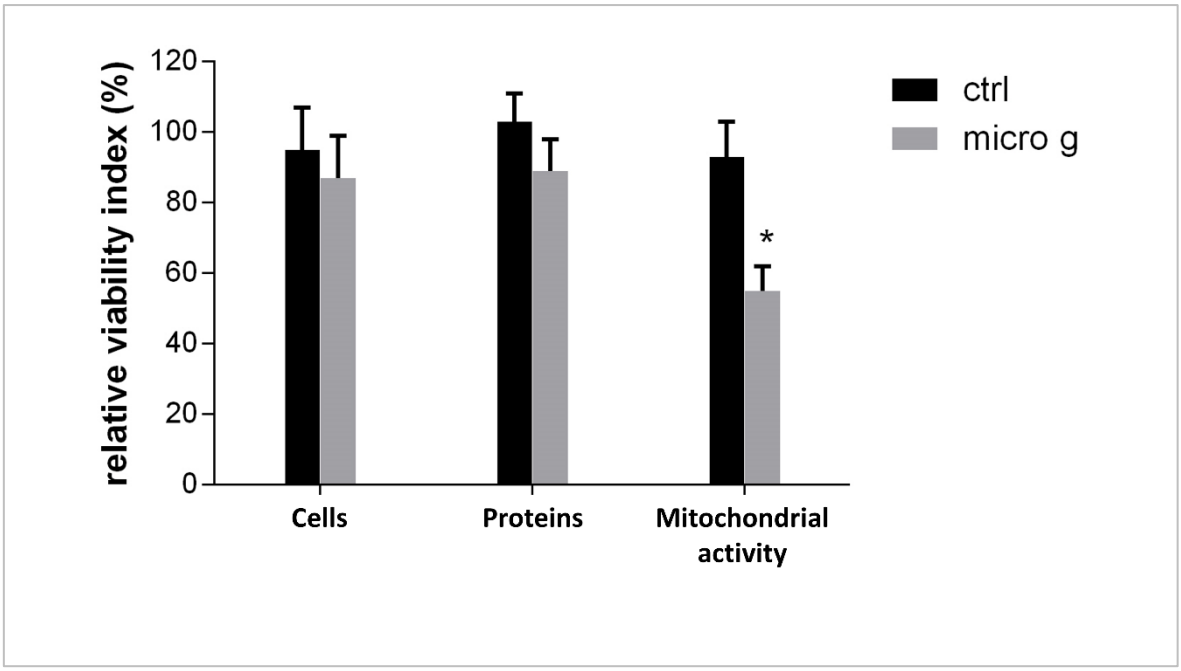

Figure 2.1. Effect of microgravity on viability of hpOB cells. The relative effect of microgravity treatment was expressed as relative cell viability index. The results were expressed as a percentage of: i) number of cells with intact plasma membrane (trypan blue impermeable cells), ii) cell protein content (BCA absorbance), and iii) metabolically active cells (MTS absorbance). Histograms represent mean ± SD (n = 6), black columns refer to control samples, whereas grey columns represent 110 hours-microgravity-exposed cells. Statistical significance was determined busing Student's t-test. Significant decrease relative to respective control values at $p < 0.05$ is denoted as *.

2.3.1 PROTEOMIC PROFILING

Purified protein extracts were eluted and separted through a 16–8% linear gradient polyacrylamide gel 1D SDS-PAGE and analyzed by nano-LC-MS/MS system (Figure 2.2A). Proteome changes associated with microgravity were analysed using FunRich (Platform 3.0). As shown in the Venn diagrams, the identification of peptide sequences from the hpOB proteome generated 813 and 978 proteins from normogravity- and microgravity-exposed samples, respectively (562 proteins were in common between the two conditions) (Figure 2.2B).

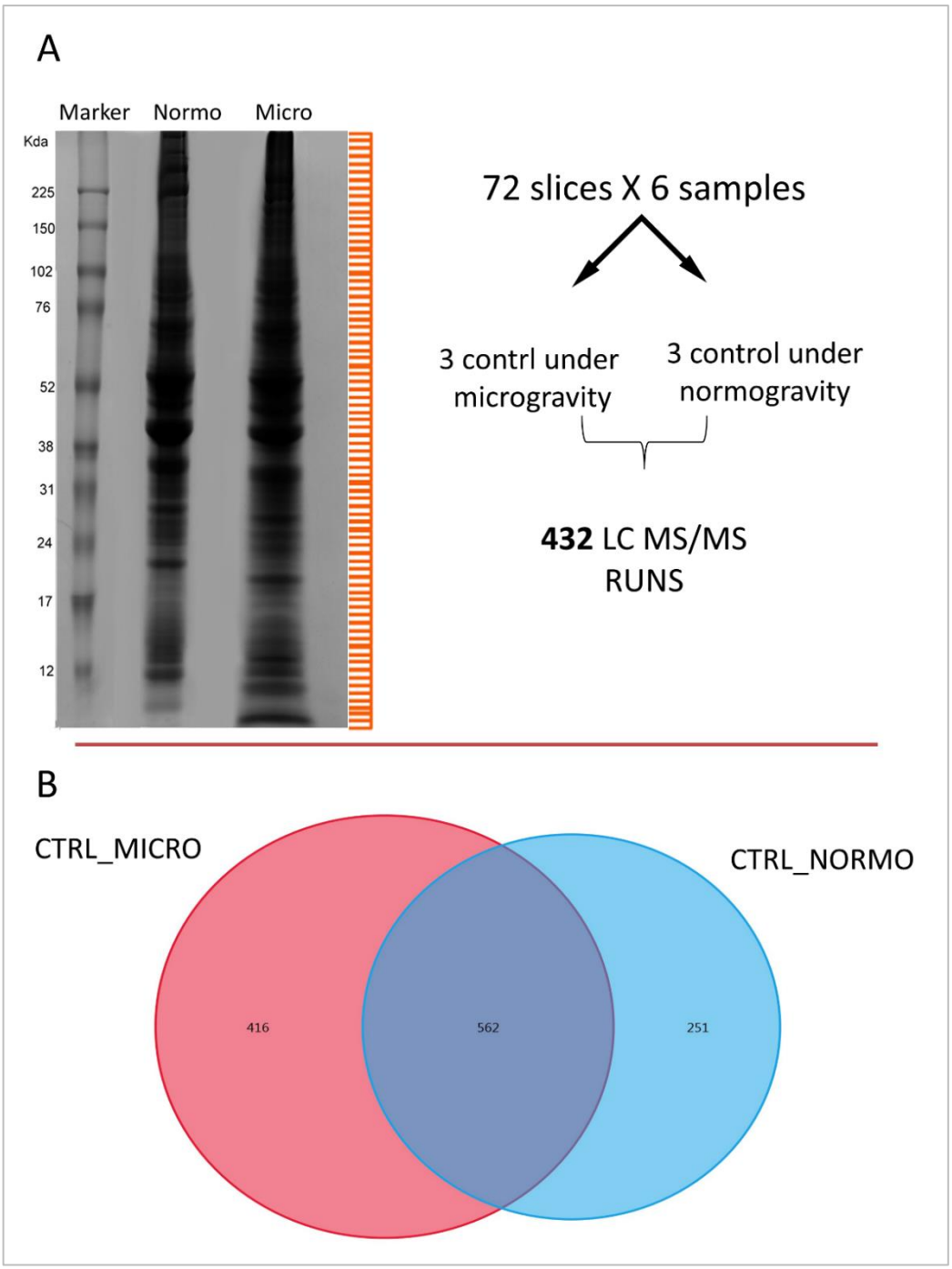

Figure 2.2 In panel (**A**) is shown one dimensional SDS-PAGE (16–8% linear gradient polyacrylamide gel). 150 µg of human osteoblast proteome were loaded into each gel lane. Three technical replicates per condition were used. The gel was stained with Comassie. In panel (**B**) Diagram Venn depicted the comparative protein profiling of human osteoblast under normogtravity and under microgravity. It was reveleted that 251 proteins were detected only in normogravity, 416 were detected only in microgravity and 562 were shared.

The whole identified proteome was analysed first using Gene Ontology (GO) biological process annotations through FunRich and then using a stand-alone software tool which allows functional enrichment analysis of complex protein and gene datasets (Figure 2.3).

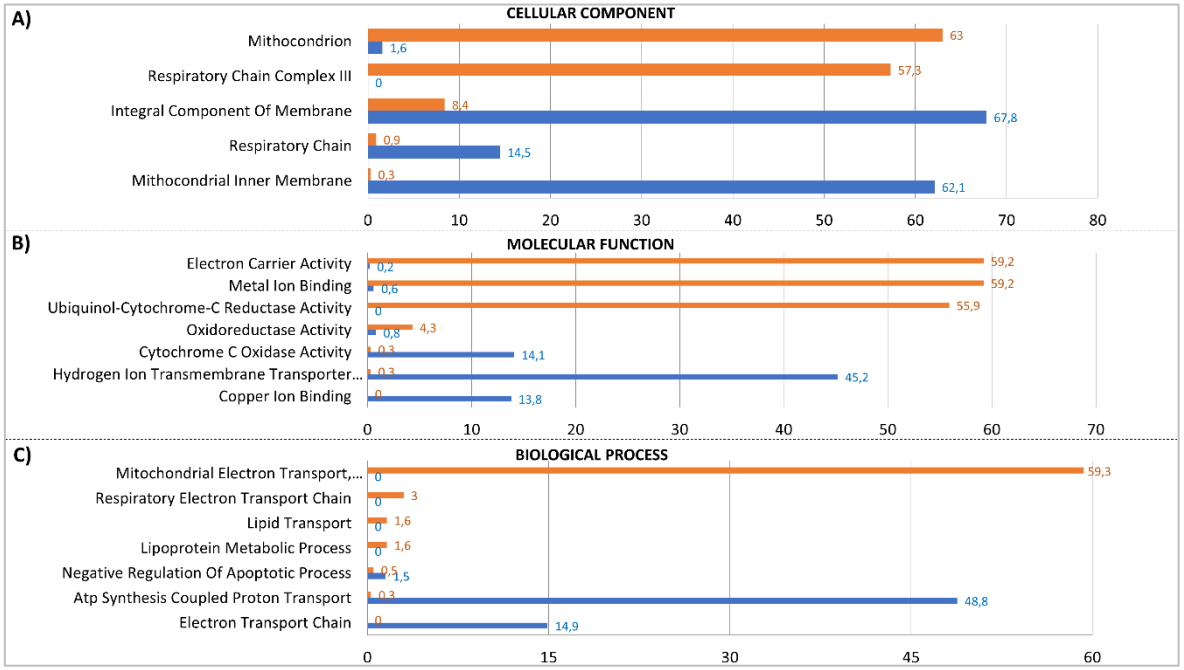

Figure 2.3. Functional enrichment analysis of hpOB under Normogravity and Microgravity using FunRich. Bioinformatics Gene Ontology-based classification of proteomes according to three categories: cellular component (**A**), molecular function (**B**), and biological process (**C**). Numbers next to the bars represent levels of normogravity (blue bars) and microgravity (orange bars), respectively. Only categories with >2-fold change are shown.

According to FunRich Bioinformatics analysis, the whole set of proteins could be classified according to categories based on three annotated biological processes: the cellular component (Figure 2.3A), molecular function (Figure 2.3B) and biological process (Figure 2.3C). Figure 3 displays only those categories showing greater than a two-fold change. Among all cellular components, Figure 3 clearly shows that the mitochondrion was affected the most by microgravity. Over 50% of the hypogravity-sensible proteins are related to mitochondrial processes, including mitochondrial protein homeostasis (mitochondrial protein import) and energy production. In this paper, we focused our attention on those proteins involved in the respiratory chain, glycolytic metabolism and antioxidant enzymes; the remaining protein categories have been investigated in a subsequent study (paper in

preparation). With regard to the mitochondrial proteome, microgravity reduced the integral component of the membrane and, in particular, proteins of the inner membrane, such as the respiratory chain Complex IV (by about 14%), while Complex III increased by 60%. Table 2.1 shows that several mitochondrial enzymes were altered, suggesting that glycolysis, the PPP (pentose phosphate pathways) and Kreb's cycle are sensitive to gravity. Among Kreb's cycle enzymes, of particular note are succinate dehydrogenase (Complex II), fumarase (FUMH) and malate dehydrogenase (MHDM), were reduced by microgravity (50%; 53% and 62% respectively). Moreover, Table 2.1 listed the specific proteins belonging to Complex III and IV which were up or down-regulated. Finally, an additional interesting group concerned with antioxidant enzymes were listed which are involved in mitochondrion perturbation. This group includes glutathione peroxidase (GPX7), peroxiredoxin 4 (PRDX4), 5 (PRDX5) and 6 (PRDX6), superoxide dismutase (SODC) and glutathione peroxidase 8 (GPX8), all of which were over-expressed in the gravitational unloading environment. Interestingly, ROS production increased significantly (data not shown).

2.3.2 METABOLIC PROFILING OF OSTEOBLASTS UNDER MICROGRAVITY

To explore the microgravity-induced perturbations on hpOB cells, a quantitative metabolic comparison was carried out between metabolomes extracted from normogravity- and microgravity-cultured cells. Multivariate statistical analyses were employed for the HPLC-MS data sets. Using this approach, 137 metabolites detected across both groups met acceptability criteria and were further analysed using bioinformatics tools (MetaboAnalyst 3.0 software) (Figure 2.4). Glycolysis, Kreb's cycle, PPP, the glycerol-phosphate shuttle, as well the malate-aspartate shuttle, were all significantly reduced by microgravity (in agreement with proteomic analysis). Microgravity also influenced aspartate metabolism and galactose metabolism, which are apparently connected to mitochondrial dysfunction (see Discussion).

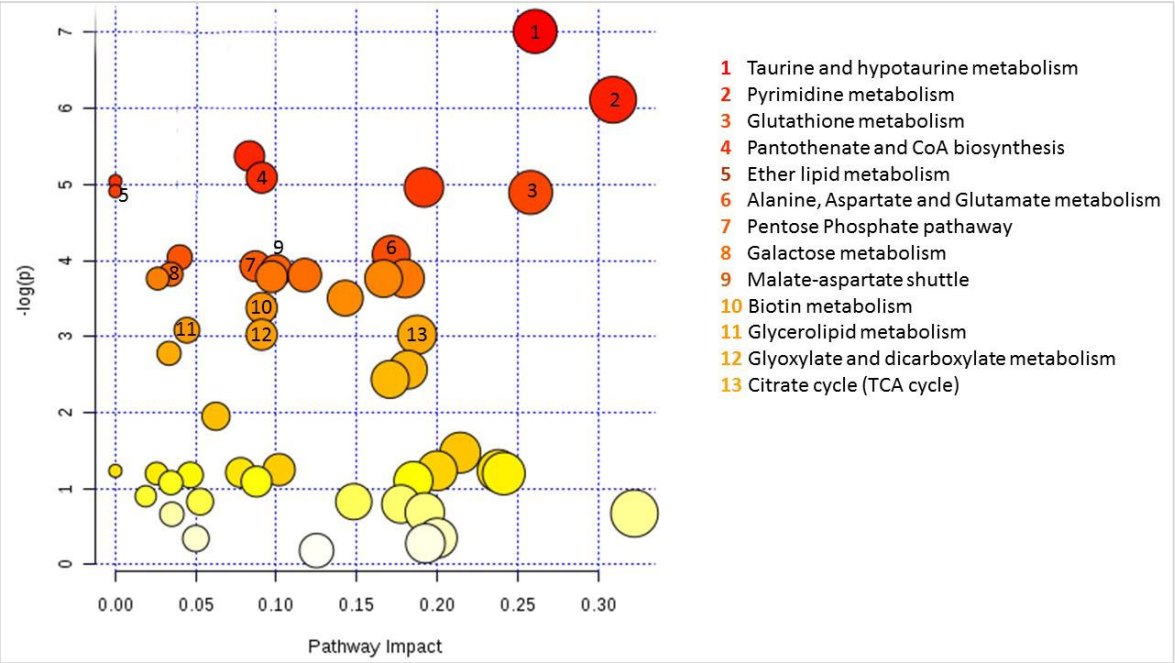

Figure 2.4. Metabolic Set Enrichment Analisys. We analyzed the MetPA plot using Metaboanalyst software. Color intensity, from yellow to red, reflects increasing statistical significance, while circle diameter covaries with pathway impact. The graph was obtained plotting on the y-axis the –log of p-values from pathway enrichment analysis and on the x-axis the pathway impact values derived from pathway topology analysis.

Under conditions of microgravity, the glycolysis pathway was moderately stimulated, since glucose-6-phosphate increased as well as other glycolytic precursors (Figure 2.5A). Interestingly, under microgravity conditions the amount of glycerone phosphate was reduced (Figure 2.5B), suggesting that the triose equilibrium was displaced in favour of glyceraldehyde-3-phosphate, thereby reducing the glycerol shuttle (Figure 2.5B). Further, under microgravity there was a decrease in acyl-carnitine, mirrored by an increase in acyl-CoA (Figure 2.5C), suggesting decreased free fatty acid transport into mitochondria and a reduction in the beta oxidation pathway, in agreement with a recent study (Adams et al., 2009).

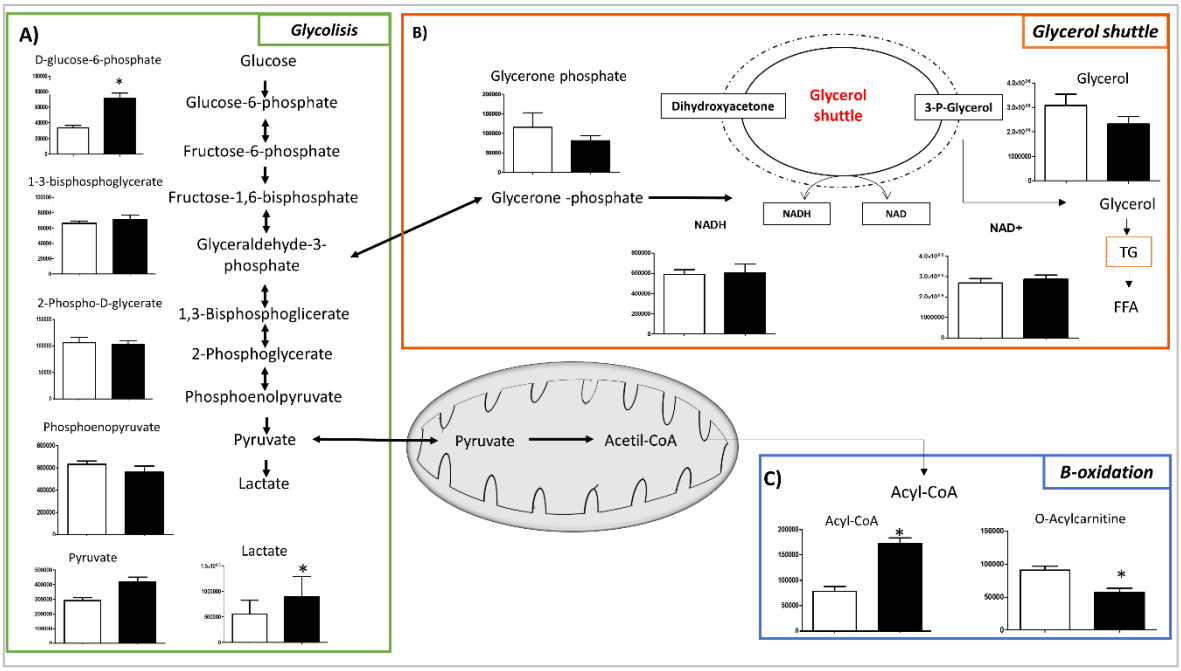

Figure 2.5. Metabolic cross-talk among glycolysis, glycerol shuttle and β-oxidation pathways. Variation in the levels of metabolic intermediates of: (**A**) glycolysis, (**B**) glycerol shuttle and (**C**) two intermediates of β-oxidation. Values represent mean ± SD (n = 9) of normogravity (white columns) and microgravity (black columns) metabolites. Statistical significance was indicated by *p < 0.05; **p < 0.01; ***p < 0.001.

PPP turned out to be particularly stimulated under microgravity, as demonstrated by both the proteomic analysis (up-regulation of glucose-6-phosphogluconate lactone dehydrogenase, connected to the first step reaction; shown in Table 2.1) and the metabolomic analysis, where the product of the first reaction step (D-glucono- 6-lactone) was more abundant (Figure 2.6A). Concurrently, this produced increased levels of oxidised glutathione (GSSG) intermediate (Figure 2.6B). These data, together with the up-regulation of glutathione peroxidases (Table 2.1), suggest that oxidative stress was induced by microgravity exposition. Interestingly, no accumulation of ribose-5-phosphate was recorded and, consequently nucleotide synthesis remained at a constant level (Figure 2.6C). Thus, in contrast to cancer and dedifferentiated cells (D'Alessandro et al., 2013), up-regulation of the glycolysis pathway under microgravity conditions did not stimulate cell replication. Under microgravity, the Kreb's cycle was activated, as indicated by acetyl-CoA accumulation.

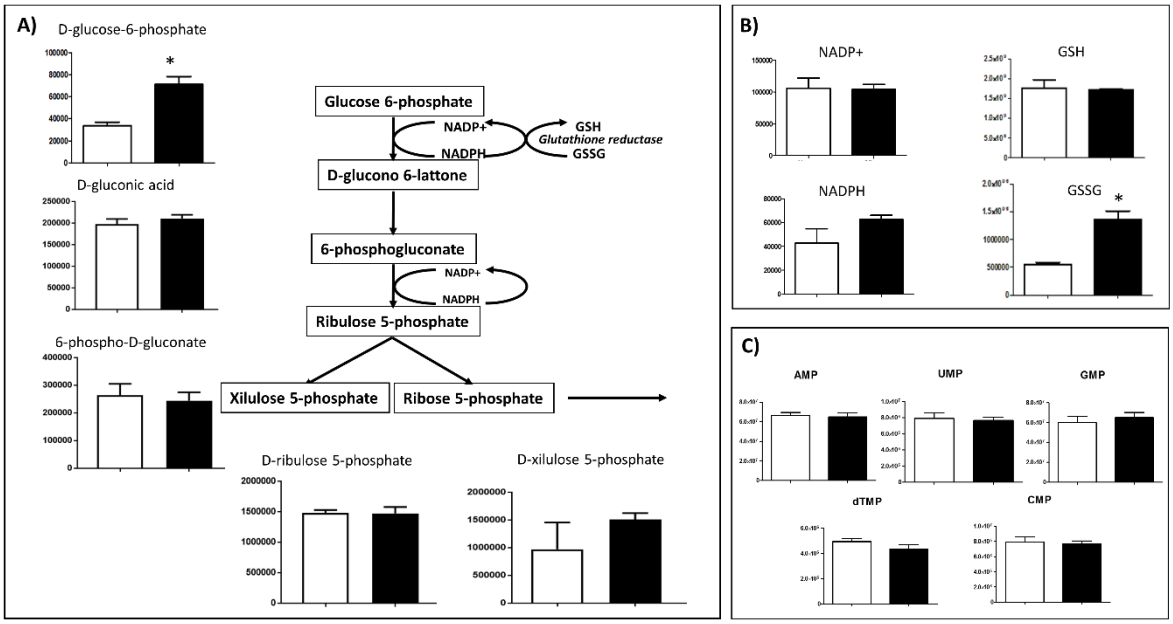

Figure 2.6. Intermediates of PPP pathway. Variation in the levels of metabolic intermediates in PPP cycle. Panel (**A**) represents NADP/ NADPH and GSH/GSSG. Panel (**B**) represents nucleotide monophosphate. Values are mean ± SD (n = 9) of normogravity (white columns) and microgravity (black columns) metabolites. Statistical significance was indicated by *p < 0.05; **p < 0.01; ***p < 0.001.

However, this stimulation only affected the first part of the cycle, showing an increase in products of the Krebs cycle, until succinate transformation into fumarate where the trend was reversed, with a consequent decrease in fumarate and malate (Figure 2.7). This result is consistent with down-regulation of both FUMH and MDHM enzymes reported in Table 2.1. Clearly, the decrease in malate production ultimately reversed the malate-aspartate shuttle (Figure 2.8), as well as cGMP concentration was decreased (Panel 2.8A) (see discussion). Finally, Figure 2.9 shows some interesting metabolites, such as FAD and FADH2, ATP and AMP, quinone 9 and 10, menaquinone and IP3, whose variations with exposure to microgravity will be discussed later. Interestingly, FADH2 increased with respect to FAD (Figure 2.9A), while, quinone 9 and 10 decreeased (by 40%; Figure 2.9B), as did, ATP (by >45%; Figure 2.9C).

With regard to amino acids, significative changes were observed for glutamic and aspartic acids which participate in the malate-aspartate shuttle, no additional significant changes were recorded, with the exception of serine (Figure 2.10).

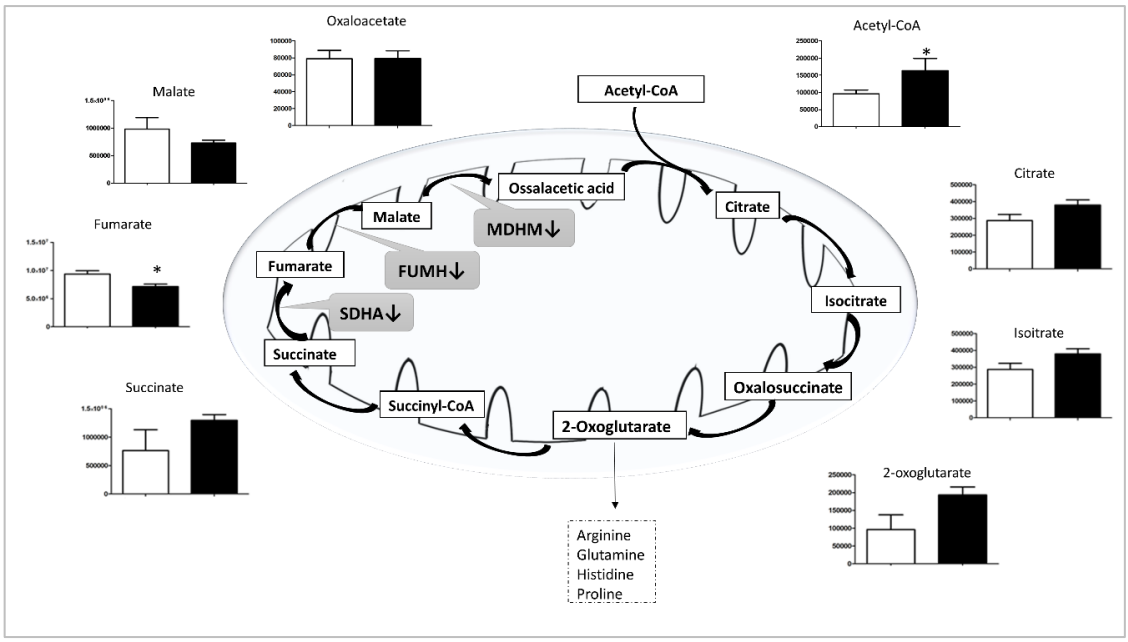

Figure 2.7. Intermediates of tricarboxylic acid pathway (TCA). Variation in the levels of metabolic intermediates in Kreb's cycle. It was interrupted at succinate production with a decrease in fumarate and malate levels, and down-regulation of FUMH, MDHM and succinate dehydrogenase enzymes (black arrow). Values are mean ± SD (n = 9) of normogravity (white columns) and microgravity (black columns) metabolites. Statistical significance was indicated by *p < 0.05; **p < 0.01; ***p < 0.001.

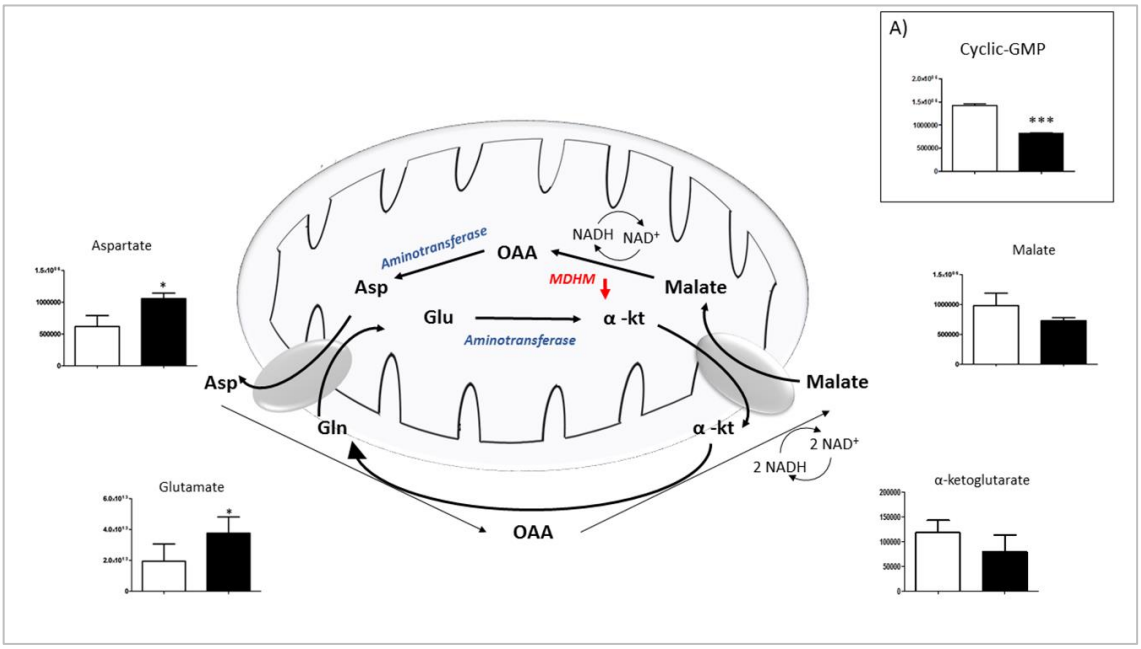

Figure 2.8. Intermediates of Malate-Aspartate Shuttle. Variation in the levels of metabolic intermediates of the malate-aspartate shuttle. Down-regulation of MDHM enzyme is represented by red arrow. Panel 6 (**A**) show the decrease of Cyclic-GMP. Values are mean ± SD (n = 9) of normogravity (white columns) and microgravity (black columns) metabolites. Statistical significance was indicated by *p < 0.05; **p < 0.01; ***p < 0.001. (OAA = Oxalacetate; Asp = Aspartate; Glu = Glutamate; α-kt = α-ketoglutarate).

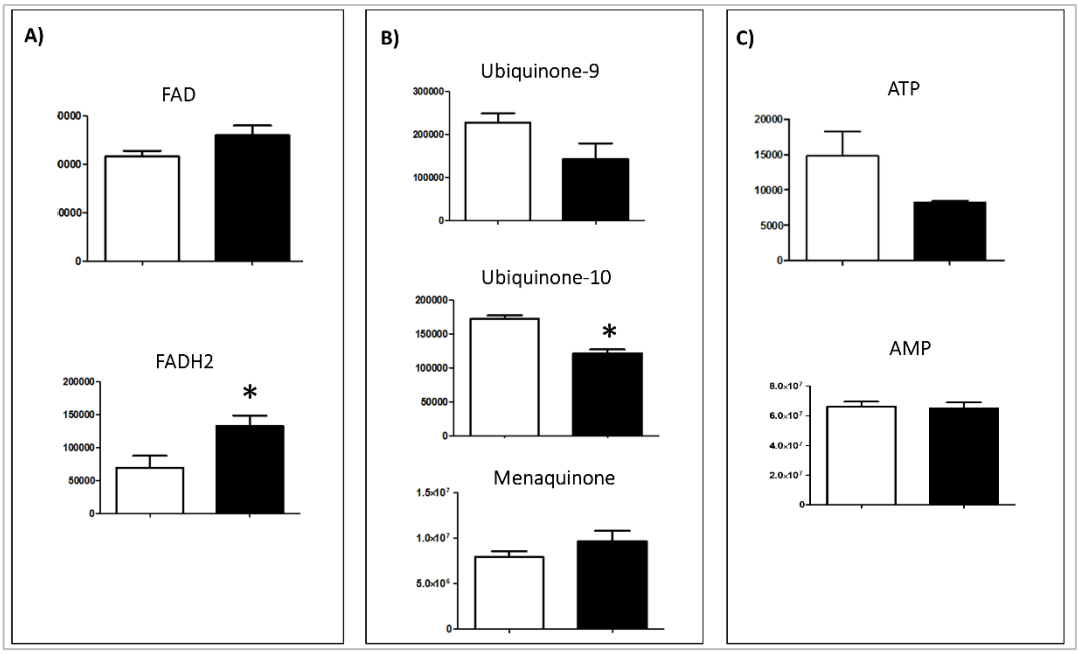

Figure 2.9. Cellular levels of FAD, Quinones, ATP. Variation in the levels of metabolic intermediates in (**A**) FAD/ FADH2, (**B**) ubiquinone 9, ubiquinone 10 and menachinone, (**C**) ATP and AMP. Values are mean ± SD (n = 9) of normogravity (white columns) and microgravity (black columns) metabolites. Statistical significance was indicated by *p < 0.05; **p < 0.01; ***p < 0.001.

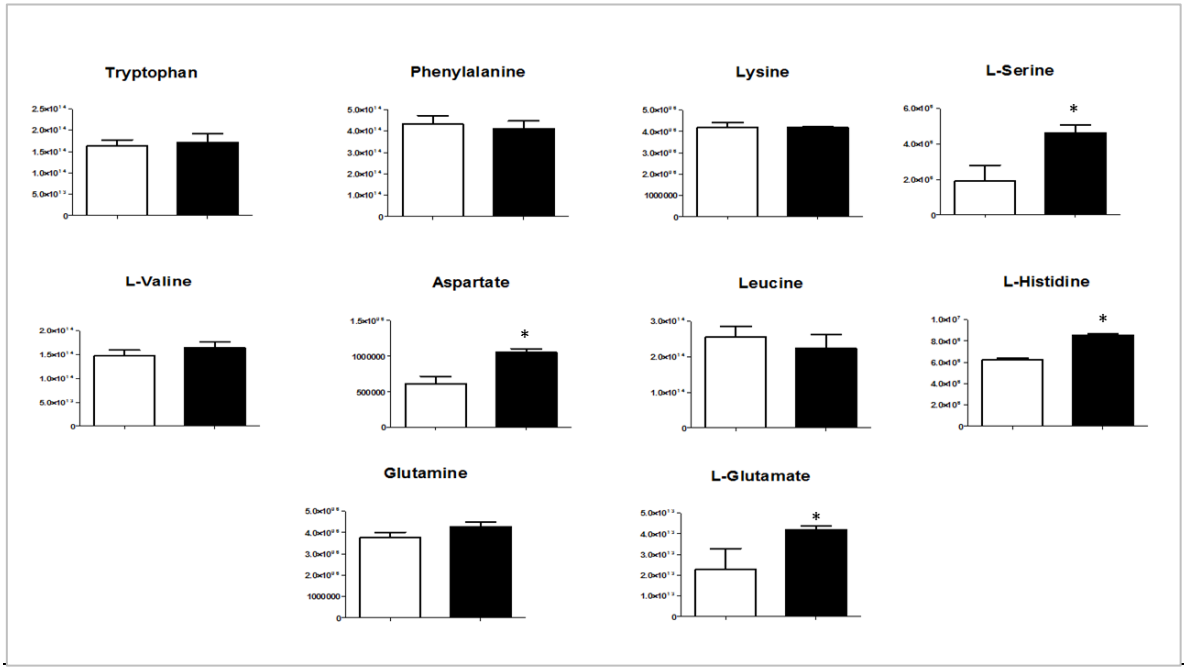

Figure 2.10. Amino acids. The columns white represented mean ± SD (n=9) of metabolite concentration in normogravity, the column in black represented mean ± SD (n=9) of metabolite concentration in microgravity. Statistical significance was indicated with *p < 0.05; **p < 0.01; ***p < 0.001.

Table 2.1. Spectral count-based quantitation of proteins identified between the human osteoblasts under normogtavity and microgravity. Protein content was estimated as percentage of normalized emPAI values, as reported in Shinoda et al. The table shows differentially regulated proteins in abundance with statistical significance. *p < 0.05; **p < 0.01; ***p < 0.001, and unique proteins in normogravity (UN) and microgravity (UM).

Molecular function enrichment item (FunRich)	**Uniprot Protein ID**	**Protein Name**	**EmPAI quantification**		**p-Value**	**Trend**
			mean_Normogravity	**mean_Microgravity**		
Glycolysis	TPI1	Triosephosphate isomerase	1,223948	0,641568	0,010695	DOWN (*)
	LDHA	L-lactate dehydrogenase A chain	0,399377	0,633762	0,000753	UP (***)
	G3P	Glyceraldehyde-3-phosphate dehydrogenase	0,9990652	0,0987282	0,000849	DOWN (***)
	ENOA	Enolase	1,15353047	0,70729455	0,020571	DOWN (*)
	PGAM1	Phosphoglycerate mutase 1	0,274401	0,329345	0,000607	UP (***)
Kreb's cycle	ODO2	2-oxoglutarate dehydrogenase, mitochondrial	0,01746131	0,00829692	0,047496	DOWN (*)
	SUCB1	Succinyl CoA Synthetase	0,015458	0,009332	0,003271	DOWN (**)
	FUMH	Fumarase	0,017809	0,008353	0,035839	DOWN (*)
	SDHA	Succinate dehydrogenase	0.01593	0.007965	3,836E-05	DOWN (***)
	MDHM	Malate dehydrogenase	0,156028	0,059646	0,000105	DOWN (***)
PPP	6PGD	6-phosphogluconate dehydrogenase	0,015458	0,036229	0,002285	UP (**)
	TKT	Transketolase	0,174453001	0,17323428	0,070788	DOWN

Ubiquinol-cytochrome-c reductase activity	UQCRC1	Cytochrome b-c1 complex subunit 1, mitochondrial	0,015736	0,02952	5,39E-05	UP (**)
	NQO1	NAD(P)H dehydrogenase [quinone] 1	0,051803	0,122297	5,39E-05	UP (***)
	UCRI	Cytochrome b-c1 complex subunit Rieske, mitochondrial	0,028819	0,016934	0,007927	DOWN (*)
	CYB5R3	NADH-cytochrome b5 reductase 3	0,099498	0,154874	0,001792	UP (*)
Cytochrome c oxidase activity	COX5A	Cytochrome c oxidase subunit 5A, mitochondrial	0,117605	0,065708	0,008712	DOWN (*)
	CYB5A	Cytochrome b5	0,051882	0,034082	0,000974	DOWN (***)
	COX6C	Cytochrome c oxidase subunit 6C	0,088148	0,060621	0,032165	DOWN (*)
Antioxydant activity	PRDX1	Peroxiredoxin-1	0,792314	0,718062	0,296566	DOWN
	PRDX2	Peroxiredoxin-2	0,387978	0,36369	0,085143	DOWN
	PRDX3	Thioredoxin-dependent peroxide reductase, mitochondrial	0,12877	0,1721	0,000297	DOWN (***)
	PRDX4	Peroxiredoxin-4	0,140379798	0,149817616	0,683571	UP
	PRDX5	Peroxiredoxin-5 mitochandrial	0,133505475	0,237667115	0,000334	UP (***)
	PRDX6	Peroxiredoxin-6	0,326313	0,417195	0.000055	UP (***)
	SODC	Superoxide dismutase	0,122147741	0,164447199	0,014818	UP (*)
	GPX7	Glutathione peroxidase 8	-	0,024664838	-	UM
	GPX8	Glutathione peroxidase 7	-	0,017486587	-	UM

2.4 DISCUSSION

Proteomic and metabolomic analyses performed on human primary osteoblasts exposed to simulated microgravity for five days enabled us to improve understanding of the responses of human osteoblasts to microgravity and to shed light on the risks associated with extended travel beyond Earth's orbit. The dominant effect of microgravity was disruption of osteoblast mitochondrial function, as previously observed in skeletal muscle tissue (Hoppeler et al., 2003), cardiomyocytes (Adams et al., 2009) and plants (Repp et al., 2004). These similar effects, although occurring in different species, suggest that mitochondrion changes could be an adaptative response to ensure sufficient cell energy for facing microgravity (Adams et al., 2009). Metabolomic analysis showed an "interruption" of the Krebs cycle at the fumarate production step, related to decreased expression of succinate dehydrogenase (Complex II of the mitochondrial respiratory chain), as confirmed by proteomic analysis (Table 2.1). This enzyme complex is involved in both the Kreb's cycle and the mitochondrial respiratory chain, catalysing succinate-fumarate transformation in the Kreb's cycle generating FADH2 from the prosthetic group FAD, which feeds electrons to Complex II. Interestingly, with microgravity exposure, osteoblasts showed a significant increase in menaquinone (Figure 2.9B), which is an essential component of FAD (Kroger et al., 1976) even though human electron transport chain does not metabolise it. Since, it is recognised that osteoporosis in astronauts can be prevented by menaquinone supplement (Cook et al., 2014; Mahdinia et al., 2017), we can speculate that a correlation might exist between effects of microgravity on the respiratory chain and effects on succinate dehydrogenase. It is interesting to underline that the accumulation of succinate is one of the metabolic mitochondrial responses to extreme environments, supporting a concerted down-regulation of Kreb's cycle and electron transport chain activity (O'Brien et al., 2015). For example, in the cellular response to ischemia, succinate accumulation showed a toxic effect, which has been directly linked to mitochondrial reactive oxygen species production from Complex I (Figure 2.11) (Chouchani et al., 2014). Thus, it is not surprising that mitochondrial Complex II deficiency is one of the rarest disorders of the oxidative phosphorylation system (OXPHOS) which could lead to clinical disturbances, accounting for 2–8% of cases of mitochondrial disease (Parfait et al., 2000; Ghezzi et al., 2009). Proteomic analysis also showed dysfunction of the mitochondrial membrane caused by impairment of the other mitochondrion respiratory chain components. Total Complex III were over-expressed (by more than 60%), related to the significant over-expression of its protein components, reported in Figure 2.8 and Table 2.1. Moreover, since the complete cycle between Complex II and III involves two electrons being transferred from ubiquinol to ubiquinone via two cytochrome c intermediates, it is unsurprising that microgravity resulted in decrease in the amount of

coenzymes Q9 and Q10, as well as in the proton gradient (Figure 2.9B). Primary coenzyme Q10 deficiency has been included among the mitochondrial respiratory chain disorders because of its central role as an electron carrier from Complex I and II to Complex III (Calco et al., 2015). More than 75% of the body's energy is a result of the role of coenzyme Q10 in mitochondrial production of ATP. Thus, people with low levels of this coenzyme may feel tired upon walking, or exhausted after just a few minutes of walking (Maes et al., 2009). It is tempting to speculate that the recorded decrease of ATP levels (Figure 2.9C), probably linked to the down-regulation of CoQ10 (Deichmann et al., 2010), and justifies the fatigue observed in astronauts (Scheuringa et al., 2007). Recently, an increase in Complex III in human embryonic kidney cells was reported to be related to increased mitochondrial membrane potentials and enhanced cell survival under conditions of oxidative stress (Etzler et al., 2017). This agrees with our proteomic and metabolomic analyses. In fact, during reactions between Complex III and IV, a small fraction of electrons leaves the electron transport chain, thus in the presence of oxygen the premature electron leakage generates superoxide species (O_2–). Since Complex III produces the membrane-permeable superoxide. $HOO^{\cdot}$ rather than the membrane-impermeable O_2– (Muller et al., 2004), this can be released into both he mitochondrial matrix and the intermembrane space, and thus can easily reach the cytosol (Muller et al., 2000). ROS are highly toxic and are thought to play a role in several pathologies, as well as in ageing (Muller et al., 2007), and mitochondrial ROS have been reported to increase under microgravity conditions, bringing about mitochondrial dysfunction in rat cerebral arteries (Zhang et al., 2014). Interestingly, metabolomics analysis reported an increased amount of GSSG, while with microgravity proteomics showed up-regulation of antioxidant enzymes, such as SODC, GPX7, GPX8, and PRDX 4, 5, and 6 (Table 2.1). Finally, cytocrome c oxidase (CytOx) activity (Complex IV) was reduced by 14%, as a consequence of a reduction in proteins belonging to Complex IV that were found to be significantly under-expressed (see Figure 2.11 and Table 2.1). As a final result, ATP synthesis coupled to proton transport and cytoskeleton proteins were down-regulated as well as ATP concentration (Figure 2.9C). Since the synthesis of ATP in healthy mitochondria is facilitated by the malate-aspartate shuttle system in order to restore the concentration of NADH in matrix, it is not surprising that under microgravity this shuttle system works in reverse (Figure 2.8). It is interesting to underline that reduction in CytOx by microgravity is tissue-specific, as previously reported for Complex II. Differences exist in the regulation of nuclear-encoded mitochondrial proteins in heart compared to skeletal muscle: in skeletal muscle CytOx was significantly reduced by 41%, while in cardiac muscle it remained unchanged (Connor et al., 1998). Finally, MetaboloAnalyst results showed interesting information: D-galactose (D-gal) metabolism is strongly altered by microgravity (Figure 2.4).

Recently, in rodents it was demonstrated that chronic administration of D-gal increased the activity of the respiratory chain Complex I in the prefrontal cortex and hippocampus.

Also, the activity of Complex II-III increased with oral D-gal treatment (Budni et al., 2017). In agreement with these findings, oral administration of D-gal appeared to induce alterations in the mitochondrial respiratory complexes observed in brain neurodegeneration (Long et al., 2007). Thus, with exposure to microgravity a relationship between D-galactose metabolism and respiratory chain proteins occurs. Consequently, to perturbation of mitochondrial chain reaction enzymes, induced adaptations of mitochondrial metabolisms. Glycolysis was stimulated in agreement with previous investigations, namely that during spaceflights microgravity increased glycolytic enzymes in rats (Fitts et al., 2013). This agrees with the significant increase of lactate (69%) reported here and its role in mitochondrial dysfunction. The impairment of succinate-fumarate reaction, catalysed by Complex II, as well as the down-regulation of MDHM enzyme (Table 2.1), reduced malate production and, as a result, the aspartate-malate shuttle was reversed (Figure 2.8). This contributed to, or is a consequence of, reduced ATP synthesis, since, after ATP synthesis, the concentration of NADH in the mitochondria (which cannot cross the mitochondrial membrane) needs to be restored in the matrix by the malate-aspartate shuttle. Thus, there is a strict correlation between ATP synthesis, MDHM activity, NADH and cGMP production. This was confirmed by treatment of ischemic cardiomyocytes (Gevi et al., 2017) with sildenafil: MDHM activity increases as well as the cGMP concentration and the malate-aspartate shuttle activity. Clearly, with microgravity this phenomenon is magnified by a reduced electron transport chain. With respect to lipid metabolism, microgravity exposure also increased lipid synthesis in the skeletal system, as observed in the fatigued muscle cells (Maes et al., 2009), which shifts from lipid toward glucose metabolism. The reduced glycerol shuttle, increased triglycerides production, shifting metabolism toward a higher reliance on lipids (Espinosa-Jeffrey et al., 2016). The increased lipid production was also paralleled by a reduction in beta oxidation of fatty acids inside the mitochondria, as indicated by a significant increase in acyl-CoA concentration and the concomitant decrease of acyl-carnitine (Figure 2.5), both of which are needed to activate or translocate fats into the mitochondria. This is in agreement with these results, Baldwin et al (Baldwin et al., 1985), where an increased reliance on glycolysis coupled with a reduced ability to oxidise fats contribute to fatigue of muscle cells (Debold et al., 2004; Debold et al., 2006; Knuth et al., 2006), with accumulation of lactic acid. Moreover, accumulation of lipids increases demineralization of bone, which, in addition to the increased oxidative stress (documented above), inhibits differentiation of osteoblasts and stops the mineralization process of bone. Overall, increased glycolysis and alterations in respiratory chain reactions, as well as changes in some metabolic pathways, are probably responsible for the subsequent microgravity-dependent effects (well documented in

literature), such as pro-apoptotic state and cell dedifferentiation (Nichols et al., 2006; Lescale et al., 2015), which will be discussed in a next manuscript. In this regard, it was recently found that alteration of mitochondrial cytochrome bc1, a component of the electron transport chain Complex III, leads to activation of tumor suppressor p53, followed by apoptosis induction (Khutornenko et al., 2014). Recently, it has also been observed that up-regulation of glycolytic genes and down-regulation of mitochondrial genes, as well as a marked increase in succinate, trigger the induction of IL-1β via HIF-1in macrophages (Tannahill et al., 2013). Clearly, all these aspects taken together are complex and merit further study which will be the subject of a subsequent report. However, taken together, our results indicate impairment in the physiological functions of mitochondria as well as impairment in osteoblast functionality as a specific effect of stress caused by exposure to microgravity.

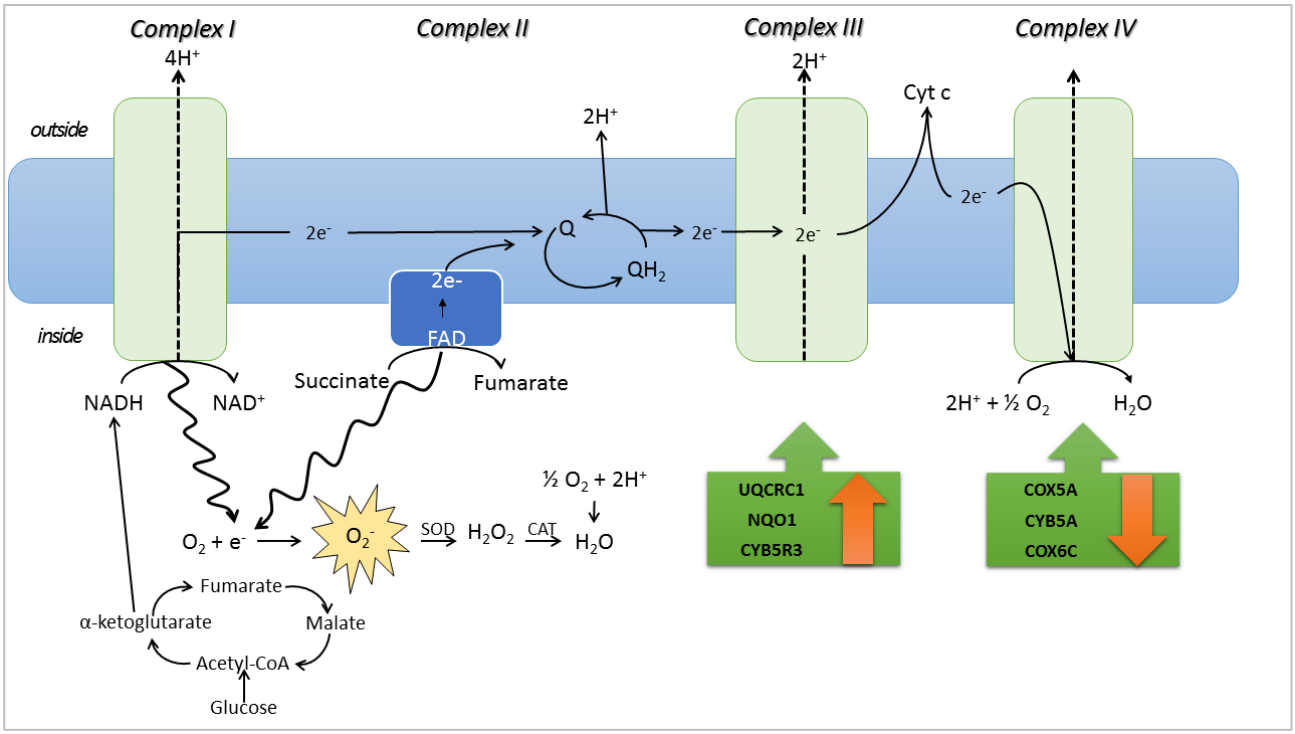

Figure 2.11. Crosstalk between TCA cycle and Mitochondrial electron transport chain in microgravity. Succinate accumulation shows toxic effect of reactive oxygen species from mitochondrial electron transport chain. An unbalanced proton pump could be associated with FADH2 accumulation. Green boxes show enzymes' trend (statistical significance is shown in Table 2.1).

3 SIMULATED MICROGRAVITY INDUCES A CELLULAR REGRESSION OF THE MATURE PHENOTYPE IN HUMAN PRIMARY OSTEOBLASTS

3.1 INTRODUCTION

Bone is a highly mechano-sensitive tissue, capable of undergoing rapid and robust rearrangement even in response to microscopic mechanical stimuli. Hence, cell mechano-transduction pathways are promising targets for new anabolic therapeutic strategies. So far, various biochemical factors are known to encourage osteoblast recruitment and osteogenesis (Fritton et al., 2012; Uchihashi et al., 2013; Brady et al., 2015; Andalib et al., 2013), whereas relatively little is known about how osteoblasts migrate/differentiate in response to mechanical signals. Studies on stem cell differentiation have defined the principles of mechanobiology; cells sense extracellular stiffness through contraction of the actomyosin cytoskeleton, regulating the suitable response through focal adhesion, rho-GTPase signaling, cytoskeletal contractility, and nuclear rearrangement processes (Yim et al-. 2012; Ivanovska et al., 2015). Empirical evidences report that mechanical unloading impairs osteoblasts differentiation of bone marrow mesenchymal stem cells, thus inhibiting osteogenesis (Engler et al., 2006; Zayzafoon et al., 2004). Differentiation process is tightly intertwined to cellular motility, since they both involve (i) a peculiar actin organization forming specific cell-protrusions (such as lamellipodia, filopodia, or blebs) (Alexandrova et al., 2014; Bear et al., 2014), (ii) a specific proteolytic set of enzymes (Bjørnland et al., 2005; Petrie et al., 2012; Wolf & Friedl, 2011), and (iii) adhesion proteins (e.g., cluster of differentiation proteins and integrins) (Bjørnland et al., 2005; Petrie et al., 2012; Wolf & Friedl, 2011; Nabavi et al., 2011; Zhu et al., 2006; Maleki et al., 2014). Although humans have limited regenerative capacity, inprinciple, a mechanical induction of dedifferentiation may be a logical strategy to promote regeneration in tissues that lack osteogenic ability (Jopling et al., 2011; Ozcivici et al., 2010). Unfortunately, neither mechano nor biochemical mechanisms of osteoblast dedifferentiation are comprehensively known. Apparently, cellular plasticity (i.e., cellular susceptibility to reprogramming) decreased during evolution processes. By contrast to what happens in fish biology (Geurtzen et al., 2014), in mammals mature osteoblasts do not contribute to bone repair (Park et al., 2012). However, some evidences are documented (in adult skull-cap-derived cells and pediatric osteosarcoma) (Lian et al., 1995; Pereira et al., 2009), suggesting that a dedifferentiation potential can still be conserved in mammalian mature osteoblasts.

Retinoic acid (RA), a metabolite of vitamin A, plays a central role in cellular dedifferentiation (Gudas et al., 2011), and it may also play a role in mechano-biology. Retinoids are considered promising leading compounds in differentiation therapy strategies (Nowak et al., 2009) as they are reported to inhibit osteoblast dedifferentiation at cellular and molecular levels (Blum et al., 2015; Sehring et al., 2016). Although on Earth osteoblasts have evolved and constantly behave in the presence of gravity, experiments performed in microgravity (either off planet or simulated) have shown how the gravitational force is a biological stressor of bone physiopathology (Nabavi et al., 2011; Jee et al., 1983; Schatten et al., 2011; Gupta et al., 2012; Manzey et al., 1999). In particular, investigations on human osteoblastic cell lines report that microgravity inhibits the osteogenesis across all differentiating morphological and molecular features (e.g., cell cytoskeletal organization and adhesion, bone phenotypic markers, alkaline phosphatase (ALP), hydroxyapatite (HA) crystals, matrix metalloproteinases) (Nabavi et al., 2011; Shi et al., 2017; Hu Z. et al., 2015 Hu L.F. et al., 2015; Ontiveros & Mccabe. 2003; Patel et al., 2007; Blaber et al., 2013). The present study has been carried out on human primary osteoblasts (hpOBs) from healthy donors with the aim of revealing effects of Sμg on cellular response. The investigation has been undertaken by ultra-structural, immune-cytochemistry, cell biochemistry, and quantitative mass spectrometry (MS) proteomic and metabolomic approaches to assess whether the Sμg-induced loosening of obsteoblast mature phenotype were correlated with hypo-functional cellular aspects. Overall, present data indicate that upon Sμg treatment hpOBs do not just lose the mature morphological phenotypebut they also become biochemically hypo-functional cells. Further, we report, for the first time, that under Sμg hpOBs display a reversal of mature-osteoblast differentiation features, which renders cells capable of healing a wound in vitro.

3.2 MATERIAL AND METHOD

3.2.1 SIMULATION OF MICROGRAVITY BY RPM

The desktop RPM system (Dutchspace, The Netherlands) was used for carrying out the investigation on the influence of the force of gravity on eukaryotic cells (Borst & Van Loon, 2009). All experiments were carefully planned according to procedures previously described (Wuest et al., 2015). Briefly, the rotating frame of the desktop RPM was placed inside an ordinary cell culture CO2 incubator. The software responsible for controlling the motion of RPM employed a tailored algorithm, which rotated with a random speed in such a way that the mean gravity vector reliably converged to zero over time, and it concurrently reduced fluid motion in the culture flask. In order to avoid artifacts

and to minimize centrifugal acceleration, the samples were compactly placed around the center of rotation. Cell samples were carefully processed for in vitro cultivation: the culturing media were accurately sealed with a transpiring membrane, which was pressed to completely remove air bubbles from the culture chamber. Control samples were cultured and processed in the same manner. Plates were placed beside the RPM machine so that all samples shared identical culture conditions. Since most of the ground-based microgravity research platforms are not vibration free, high-performance microscopy has not been applicable in Live Cell Imaging under RPM. Therefore, studies involving cell imaging have been carried out after chemical fixation of the cell. This approach implies a series of static shots, which reproduce dynamic events occurring in cells in response to Sμg exposure.

3.2.2 PATIENT CHARACTERISTICS

Patients selected for the study were screened to exclude any association with clinical or pathological variables (carefully grouped on the bases of BMD parameters obtained by dual-energy X-ray absorption T-score greater that −1). No patient showed any sign of bone or joint disease or autoimmune disorder. Informed consent was obtained from all patients. The biopsies were collected from high energy fractures of femoral head of healthy patients during hip replacement surgery. Biopsy samples were taken from selected patients to set up human primary cells cultures in vitro. All procedures were approved by the Institutional Review Board of Policlinico Tor Vergata Hospital, Rome, Italy (approval reference number #85/12). Since no effects of sex on adaptation to space had been previously observed (Ploutz-Snyder et al., 2014), we decided to analyze osteoblasts from both male and female patients in order to determine average effects.

Experiments were performed in accordance with relevant guidelines and regulations. hpOBs were isolated from 3 donors (2 males and 1 female, average age 53 years, namely, female 52 years, males 49 and 59 years) and used to perform separate experiments investigating the effects of Sμg *vs* normo-gravity conditions.

3.2.3 ISOLATION AND CULTURE OF PRIMARY HUMAN OB CELLS

Primary cultures of osteoblasts were isolated from the cancellous bone of healthy patients with high-energy femoral fracture. The bone tissue was minced, thoroughly washed to remove any remaining soft tissue, and placed in 6-well plates to initiate explant cultures. The culture medium consisted of DMEM/F12 (Biowest, Nuaillé, FR) supplemented with 15% FBS, 50 μg/ml gentamicin, and 0.08% Fungizone, penicillin streptomycin (Sigma Chemical Co., St. Louis, MO, USA), and

amphotericin B (biowest) and was changed twice per week. Cells were treated to select and isolate homogeneous populations of osteoblasts according to previously reported methods (Sggelkow et al., 1999). Briefly, after dissection, trabecular bone chips were repeatedly washed with PBS at 37°C for 2 h in shaking conditions. Then, two distinct enzymatic digestions were repeated and performed at 37°C. The first digestion employed 1mg/ml Trypsin from porcine pancreas ≥ 60 U/mg (SERVA Electrophoresis GmbH Heidelberg, DE) resuspended in PBS buffered at pH 7.2. After washing, trypsinized bone chips underwent to repeated digestions with a second type of protease employing 2.5 mg/ml Collagenase NB 4G Proved grade ≥ 0.18U/mg (SERVA Electrophoresis GmbH, Heidelberg, DE) in PBS buffer with Calcium and Magnesium. The supernatants from the 4th bone-chips digestion was collected and centrifuged at 310 RCF for 5'. The cell pellet was resuspended in DMEM with 15% FBS, thus cells were then grown in low calcium media, supplemented with fetal bovine serum (10%; Intergen, Purchase, NY, USA), penicillin (50 U/ml), and streptomycin *(50* pg/ml). When the cultures reached confluence in 3-5 weeks, the bone chips were removed, and the cellular outgrowths treated with trypsin (0.05%) and EDTA (0.02%) to prepare single cell suspensions. All cells were incubated at 37°C and 5% CO_2. Upon confluence, cells were detached from the plates by trypsinization, counted and subcultured at a density of 5 000 cells/cm^2 for three passages. Osteoblast proliferation was compared between different tissue sources at passage one. Third passage cells were used in all other experiments.

3.2.4 VALIDATION OF HPOBS

To assess the quality of each cell purification a fraction of the purified cells were inspected. Using immunochemistry analysis and morphological inspection the isolated primary cells were observed to be homogeneous and appropriate for osteoblasts, expressing BMP-2 RUNX2 and RANK L. Briefly, cells were seeded in a monolayer at 40 000 cells/cm^2 and cultured until the confluence was reached. Primary osteoblasts were cultured for two weeks in osteogenic medium (OGM) containing 10 mM biglycerol phosphate, 50 µM ascorbic acid, 25 ng/ml bone morphogenetic protein-2 (BMP-2; R&D Systems) in 10% serum containing alpha MEM. After two weeks of incubation, the cells were assessed for alkaline phosphatase activity as an indicator of differentiation. Morphological inspection was carried out to assess HA precipitated crystals. Osteoblast phenotype was characterised by immunohistochemistry as BMP-2, RUNX-2 and RANK-L. Osteoblast cell lysates were generated using standard lysis buffers. The total protein content in the cells was measured by BCA and Biuret assay. Whereas alkaline phosphatase activity was measured in normalized samples using p-

nitrophenyl phosphate (p-NPP; Pierce, Rockford, IL, USA) in a 1 M diethanolamine buffer at pH 9.8. Absorbance in control and treated cells was measured at 405 nm.

Cells were seeded in separate flasks, so that once cells reached the confluence, these could feasibly follow three different experimental steps. One subset of samples were devoted to cells inspection for the quality control (for providing cell baseline before treatment), a second subset was dedicated to the simulated microgravity treatment and the last one was employed for the nomogravity control conditions. Only the subset of samples that succeed this quality check they were employed to test the impact of gravity on hpOB differentiation.

3.2.5 IMMUNOSTAINING

Cell samples were washed with PBS and chemically fixed with 4% paraformaldehyde (PF, 4% in PBS). For immunocytostaining analysis, cells were treated, first for 30 min with EDTA citrate/tween 20, pH 7.8 at 95 °C, and then incubated with mouse monoclonal anti-RUNX2 antibody for 60 min (1 μg/ml, clone EPR14334, AbCam), rabbit monoclonal anti-RANKL for 60min (1 μg/ml, clone 12A668, AbCam), mouse monoclonal anti-BMP-2 antibody for 60 min (1 μg/ml, clone 65529.111, AbCam), rabbit monoclonal anti-CD44 for 60min (1 μg/ml, clone EPR1013Y, AbCam). Washings were performed with PBS/Tween20 pH 7.6 (UCS Diagnostic, Rome, Italy); reactions were revealed by using horseradish peroxidase—3,3′ diaminobenzidine (DAB) Detection Kit (UCS Diagnostic, Rome, Italy). To assess the background of immuno-staining, we included a negative control for each reaction by incubating the sections with secondary antibodies (HRP) and a detection system (DAB). The immuno-histochemical reaction was semiquantitatively evaluated by assigning a score from 1 to 3 according to the number of positive cells. Results were showed as percentage of positive cells.

3.2.6 TRANSMISSION ELECTRON MICROSCOPY

Cell samples were chemically fixed and processed for TEM to inspect the deposits of HA crystals. In detail, cells were fixed in 4% (v/v) p-formaldehyde and post-fixed in 2% osmium tetroxide. After washing with 0.1M phosphate buffer, the sample was dehydrated by a series of incubations in 30, 50, and 70% (v/v) ethanol. Dehydration was continued by incubation steps in 95% ethanol, absolute ethanol, and propylene oxide, after which samples were embedded in Epon (Agar Scientific, Stansted, Essex CM24 8GF, UK). Eighty micrometer ultra-thin sections were mounted on copper grids and examined with a transmission electron microscope (Model 7100FA, Hitachi,

Schaumburg, IL, USA). For EDX microanalysis, ultra-thin sections were mounted on copper grids. EDX spectra of HA crystal within osteoblasts were acquired with an EDX detector (Thermo Scientific, Waltham, MA, USA) at an acceleration voltage of 75 KeV and magnification of 12.000 Spectra were semi-quantitatively analyzed by the Noram System Six software (Thermo Scientific, Waltham, MA, USA) using the standardless Cliff–Lorimer k-factor method. Percentage of both osteoblasts and mesenchymal-like cells was evaluated by counting the number of them over a total of 100 cells.

3.2.7 ASSAYS TO EVALUATE THE EFFECT OF SIMULATED MICROGRAVITY ON CELL NUMBER

To determine the impact of Sμg on cell number we evaluate (i) the number of cells with intact membrane, (ii) the number of mitochondrial-active cells, and (iii) protein cell content as previously described by us (Michaletti et al., 2017). Briefly, the number of viable cells were assessed using the trypan blue dye exclusion procedure. When required, cells were detached by incubating plates with trypsin/versine solution for 10 minutes at 37°C. Cell solution was mixed 1:1 with trypan blue stain (Invitrogen) and cells with intact membranes (viable cells) were counted using a haemocytometer device under an optical microscope (Nikon Eclipse TE 2000-5). To determine the number of viable metabolically active cells (i.e. possessing active mitochondria), the cell titer 96 AQ cell colorimetric assay (Promega) was employed, following the manufacturers' instructions. After incubation for four hours, MTS formazan soluble product was measured at absorbance 490 nm with a Tecan Spark 10N spectrophotometer reader. Spectrophotometric determination of cell protein content was evaluated by the biuret colorimetric analysis of peptides and the bicinchoninic acid (BCA) method, with readings at wavelengths of 310 nm and 562 nm, respectively (Biuret reagent kit, Sigma-Aldrich; *BCA* Protein *Assay* Kit, The Thermo Scientific Pierce).

For all three assays, standard curve validated that the absorbance (at 490 nm, 310 nm or 562 nm, respectively) read were directly proportional to the number of living cells in culture. With all three methods, the effect of the treatment was reported in terms of percentages, as follows: the percentage calculation was based on the ratio of the mean value of Sμg-treated samples to the mean value of normo-gravity (control) samples. The statistical significance of data was determined using the Student's t-test (as reported by Michaletti et al., 2017).

3.2.8 SCRATCH WOUND HEALING ASSAY

The in vitro model of wound healing was employed for examining the ability of hpOBs to migrate under Sμg exposition. As referenced osteoblast cell line Sarcoma osteogenic Saos-2 (ATCC® HTB-85™) have been employed.

Cells were seeded on gelatin-coated glass slides and growth till confluence in regular medium. Cell monolayers were wounded by scratching monolayer with a sterile p200 pipette tip. Afterward, wounded monolayers were thoroughly washed with PBS, and the serum-free culture media were returned to the cells. Cell migration occurred in serum-free media guaranteed a growth arrest and to get read of proteases and other soluble factor which would interfere with cell mobility assay. Capture of the images during the cell migration close to the wound were taken employing Nikon reverse microscopy equipped with stacked IMX214 BSI sensor by Sony, upgraded type 1/3.06 imaging module and a wide f/2.0 aperture Shoot 50-megapixel photos with the Ultra-HD "multishot feature". To derive cell migration rate widths of the wound gaps were measured by an electronic micrometer scale, and the results were plotted on a graph (according the established method previously described) (Rodriguez et al., 2005). Migration of the cells into wounded areas of the monolayer by measuring the distance traveled toward the center of the wound area (percentage of overgrown area) over the time. To measure the distance between the leading edges of wounded region lacking cells a free software was employed, freely retrieved from website https://imagej. nih.gov/ij/.

3.2.9 MS SAMPLE PREPARATION

At day 5 Sμg-treated and control cells in three biological replicates were washed in phosphate saline buffer. Cellular suspensions were centrifuged at 1500 × g for 5 min. The supernatant was discarded and cell pellet was resuspended in lysis buffer (i.e., 7M urea, 2M thiourea, 4% w/v CHAPS, 40mM Tris-HCl, 0.1mM EDTA, 1mM DTT, 50mM NaF, 0.25mM Na_2VO_4). For an accurate determination of total protein concentration, 2D-Quant Kit (E Healthacare) was used. Aliquots of 150 μg for each sample were loaded per lane and separated through a 16–8% linear gradient polyacrylamide gel. Each lane was cut into 72 slices about 2mm thick and these were subjected to in-gel trypsin digestion (Shevchenko et al., 1996).

3.2.10 LC-MS/MS ANALYSIS

Peptide extracts were analyzed using a split-free nanoflow liquid chromatography system (EASY-nLC II, Proxeon, Odense, Denmark) coupled with a 3D-ion trap (model AmaZon ETD,

Bruker Daltonik, Germany) equipped with an online ESI nanosprayer (the spray capillary was a fused silica capillary, 0.090mm OD, 0.020 mm ID) in positive ion mode. For all experiments, a 15 µL sample volume was loaded by the autosampler onto a homemade 2 cm fused silica pre-column (100 µm I.D.; 375 µm O.D.; Reprosil C18-AQ, 5 µm, Dr. Maisch GmbH, Ammerbuch-Entringen, Germany). Sequential elution of peptides was accomplished using a flow rate of 300 nL/min and a linear gradient from Solution A (2% acetonitrile; 0.1% formic acid) to 50% of Solution B (98% acetonitrile; 0.1% formic acid) in 40 min over the pre-column online with a homemade 15 cm resolving column (75 µm I.D.; 375 µm O.D.; Reprosil C18-AQ, 3 µm, Dr. Maisch GmbH, Ammerbuch-Entringen, Germany). The acquisition parameters for the mass spectrometer were as follows:

- dry gas temperature, 220 °C; dry gas, 4.0 L/min;
- nebulizer gas, 10 psi;
- electrospray voltage, 4000 V;
- highvoltage end-plate offset, −200 V;
- capillary exit, 140 V;
- trap drive: 63.2;
- funnel 1 in 100 V out of 35 V and funnel 2 in 12 V out of 10 V;
- ICC target, 200,000, and maximum accumulation time, 50 ms.

The sample was measured with the Enhanced Resolution Mode at 8100m/z per second (which allows mono-isotopic resolution up to four charge stages), scan range from m/z 300 to 1500, 5 spectra averaged, and rolling average of 1. The “Smart Decomposition” was set to “auto”.

Label-free quantitative analyses were performed in biological triplicates by using the spectral counting method based on normalized emPAI as described by others (Shinoda et al., 2010). In detail, for each protein the percentage was calculated as follows:

$$\text{Protein content (\%)} = \text{emPAI}/\Sigma\text{emPAI} \times 100$$

Statistically significant differences were identified by unpaired t-Student's test.

3.2.11 MS DATA ANALYSIS

Compass DataAnalysis 4.0 software (Bruker Daltonics) was used for data processing. Generated mgf files were then merged per lane and used for database search (SwissProt, version 20150612) through the MASCOT Daemon application included in an in-house MASCOT server (version 2.5, Matrix Science, London, UK) with the following constraints:

- taxonomy = Homo sapiens (20,207 sequences);

- enzyme = trypsin; missed cleavage = 1;
- peptide and fragment mass tolerance = ± 0.3 Da;
- fixed modifications = Carbamidomethyl (Cys);
- variable modifications= Oxidation (Met).

Label-free quantitative analyses were performed in three biological triplicates by using the spectral counting method based on normalized emPAI as previously described (Shinoda et al., 2010). To obtain a comprehensive description of the overrepresented biological processes and functional-related groups of proteins within our data set, a Bioinformatic Gene Ontology analysis was performed by the online FunRich software 3.0 (www.funrich.org). As background, the default Homo sapiens genome was used.

3.2.12 METABOLOMIC EXTRACTION

1 × 106 cells from each treatment (three biological replicates × three technical replicates × two conditions; n= 18) were first subjected to three freeze-melt cycles (freezing in ice for 5 min, melting at 37 °C for 5 min; for five times). Next, 400 µl of freezing methanol and 600 µl of freezing chloroform were added to the cells. Samples were vortexed for 30 min at max speed at 4 °C. The next day, samples were centrifuged at 16,000 × g for 15 min at 4 °C, supernatants were evaporated to dryness using an SPD2010–230 SpeedVac Concentrator (Thermo Savant, Holbrook, USA). When samples were completely dried, 60 µl of 5% formic acid was added to the dried residue and vigorously vortex mixed.

3.2.13 UHPLC-HRMS

Twenty microliters of samples were injected into an ultra-high-performance liquid chromatography (UHPLC) system (Ultimate 3000, Thermo) and run on a positive mode: Samples were loaded onto a Reprosil C18 column (2.0mm× 150 mm, 2.5 µm—Dr. Maisch, Germany) for metabolite separation. Chromatographic separations were achieved at a column temperature of 30 °C and flow rate of 0.2 ml/min. For positive ion mode (+) MS analyses, a 0–100% linear gradient of solvent A (ddH2O, 0.1% formic acid) to B (acetonitrile, 0.1% formic acid) was employed over 20 min, returning to 100% A in 2 min and a 6-min post-time solvent A hold. Acetonitrile, formic acid, and HPLC-grade water and standards (≥98% chemical purity) were purchased from Sigma-Aldrich. The UHPLC system was coupled online with a mass spectrometer Q Exactive (Thermo) scanning in full MS mode (2 µscans) at 70,000 resolution in the 67–1000m/z range, target of 1106 ions and a

maximum ion injection time (IT) of 35 ms 3.8 kV spray voltage, 40 sheath gas, and 25 auxiliary gas, operated in positive ion mode. Source ionizatio parameters were: spray voltage, 3.8 kV; capillary temperature, 300 °C; and S-Lens level, 45. Calibration was performed before each analysis against positive or negative ion mode calibration mixes (Piercenet, Thermo Fisher, Rockford, IL) to ensure sub ppm error of the intact mass. Metabolite assignments were performed using computer software (Maven,18 Princeton, NJ), upon conversion of raw files into mzXML format through Mass- Matrix (Cleveland, OH).

3.2.14 DATA ELABORATION AND STATISTICAL ANALYSIS

Replicates were exported as mzXML files and processed through MAVEN.52; MS chromatograms were elaborated for peak alignment, matching and comparison of parent and fragment ions, and tentative metabolite identification (within a 2 ppm mass deviation range between observed and expected results against the imported KEGG database). Data are presented as mean ± SD. The difference between the two groups was compared with unpaired ttest, *$p < 0.05$ was considered significant. A one-way analysis of variance (ANOVA) was performed and followed by Tukey's honestly significant difference test. Asterisk represents data significantly different from the respective control. Statistics were calculated by GraphPad Prism software, version 5.0 (La Jolla, CA).

3.3 RESULTS

Simulated microgravity alters the morphological phenotype of mature hpOBs We employed random positioning machine (RPM) machine for reliably mimicking experimental cell culture conditions actually occurring in space (Paulsen et al., 2015). HpOBs from healthy donors were selected for monitoring the specific response to the weightless treatment. In our experimental set-up of simulated microgravity, osteoblasts retain cell viability, as variations in cell number (i.e., percentage of trypan-blue impermeable cells) and protein content (i.e., percentage of BCA absorbance) are not appreciable (Figure 3.1), whereas a dysfunction of the mithocondrion metabolism (reported by formazan 3-(4,5- dimethylthiazol-2-yl)-5-(3-carboxymethoxyphenyl)-2-(4-sulfophenyl)-2H-tetrazolium(MTS) formation) is detected, as also previously reported by metabolomic and proteomic approaches (Michaletti et al., 2017).

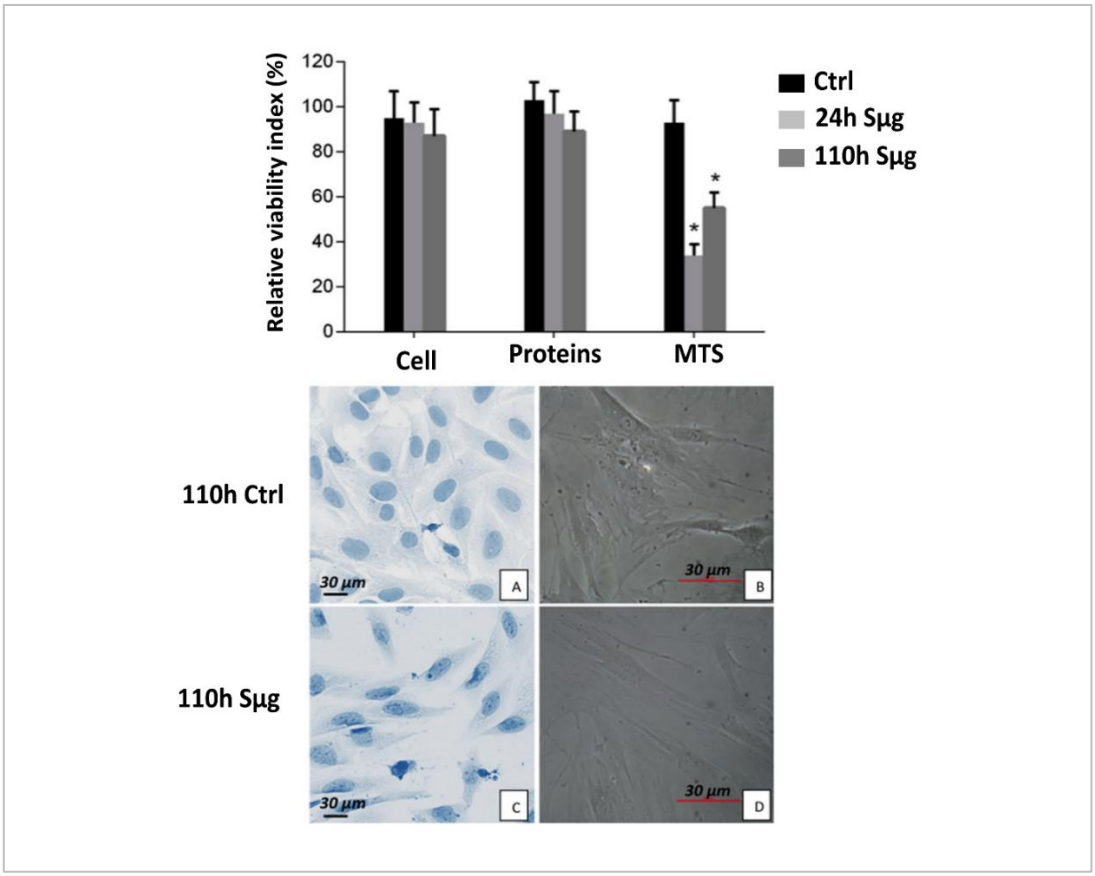

Figure 3.1. Effect of simulated microgravity on hpOP cells. Uppe panel: The relative effect of microgravity treatment on viability was expressed as relative cell viability index. The results were expressed as percentage of (i) number of cells with intact plasmamembrane (trypan blue impermeable cells), (ii) cell protein content (BCA absorbance), and (iii) metabolic active cells (MTS absorbance). Histograms represent mean ± SD (n = 6), black columns refer to control samples, light gray columns represent 24 h, and dark gray represent 110 h-Sμg-exposed cells. A one-way analysis of variance (ANOVA) was performed and followed by Tukey's honestly significant difference test (n = 6 for each experimental conditions). Significant decrease from respective controlvalues at $p < 0.05$ is denoted as *. Lower panel: Morphology of differentiated hpOB cells. a, b Toluidine blue staining pictures from inverted microscope (Leika) of cells under terrestrial gravity display a typical aspect of mature osteoblasts, respectively. c, d Pictures from up-right microscope (Nikon) of hpOBs exposed to 110 h Sμg. Image shows that Sμg hpOBs do not retain the mature phenotype of osteoblasts acquiring a spindle-shaped cell morphology.

Similarly to what reported for rat cells (Shi et al., 2017), our results show that also for hpOBs the in vitro differentiation is impaired by Sμg. Here we document a gravitational-sensitive response for human purified osteoblasts after a 110 h-treatment of Sμg. Consistently, cell inspection by inverted and up-right microscope revealed a morphological shift from flat-shape to spindleshape (Figure 3.1), clearly showing that the majority of cellpopulation treated with Sμg displays a spindle-shaped cell morphology (Figure 3.1 B,D) rather than the cuboidal cell shape typical of the mature osteoblast phenotype (Figure 3.1 A, C). A similar morphological cell shift occurs also after a shorter RPM treatment (i.e., 18 h).

Moreover, as expected, a decreased amount of HA crystals, which are laid down during the osteogenesis, is shown by the comparison of transmission electron microscopy (TEM) images between hpOBs cultured under Sμg and normo-gravity conditions (Figure 3.2 A,B respectively). Therefore, under Sμg cells produce less bone deposit material than control cells, confirming that the Sμg reduces the osteoblast differentiation rate (Hu et al., 2015 a,b; Ontiveros & Mccabe, 2003).

3.3.1 SIMULATED MICROGRAVITY ALTERS THE "BIOCHEMICAL PHENOTYPE" OF MATURE HPOBS

We investigated by analytic MS-proteomic alterations of cell functionality, comparing the proteome for molecular reporters of hpOB differentiation (i.e., biochemical phenotype) between cells exposed to Sμg and those left under normo-gravity for 110 h.

Exponentially modified protein abundance index (emPAI, a label-free relatively quantitative method) revealed that the decreased hpOB differentiation was accompanied by a reduction of some of key proteins involved in the skeletal mineralization process ($p < 0.01$) (Table in Figure 3.2). Table 3.1 resumes the trends of protein levels which were altered by Sμg, specifying the biological function of every single protein (according to the Gene ontology protein classification). Of particular note is the decrease of the osteogenic markers, such as alkaline phosphatase tissue-nonspecific isozyme (ALPL), and the tissue-specific proteins related to protein folding Crystallin Alpha B (CRYαB) (Graneli et al., 2014) (Table in Figure 3.2, for further information see next sections), indicating that upon Sμg hpOBs do not just lose the mature morphological phenotype but they also become biochemically hypofunctional cells.

3.3.1.1 Simulated microgravity-induced dedifferentiation

A deeper ultrastructural morphological inspection by TEM on cells exposed to Sμg confirmed an overall reversion of the differentiation determinants; in particular, a small but significant percentage of cells (about 4%) reverts back to a less-differentiated stage, displaying a mesenchymal cell-like phenotype (Figure 3.2 C).

No similar cell phenotype change was detected in cells cultured under normo-gravity conditions. These evidences suggest that the Sμg-induced cell hypo-functionality could stem from a dedifferentiation process rather than just a simple slowing down of the osteogenic process. An immune-cytochemistry approach was employed to characterize the dedifferentiation process looking at the osteogenic differentiative markers, such as the bone morphogenic protein-2 (BMP-2), runt-

related transcription factor 2 (RUNX-2), receptor activator of nuclear factor kappa-B ligand (RANK-L), and the pre-osteoblast state marker, named cluster of differentiation protein 44 (CD44) (Morath et al., 2016). Figure 3 indeed seems to support the occurrence of the dedifferentiation process, showing that the Sμg treatment induced: (i) the downregulation of BMP-2, RUNX-2, and RANK-L, and (ii) the upregulation of CD44 (Figure 3.3). Of note, a similar immune-cytochemistry trend was apparently observed even upon an incubation time shorter than 110 h. Thus, a semi-quantitative imaging analysis (according to HIC scoring), performed on specimens incubated for 18 h, proved that the differentiation markers (i.e., BMP-2, RUNX-2, and RANKL) decreased also upon a much shorter exposure (i.e., 18 h) (Table in Figure 3.3).

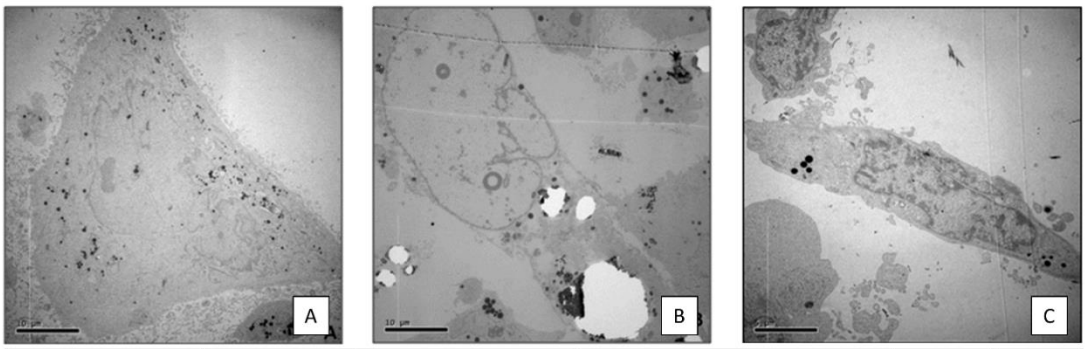

Molecular function enrichment item (FunRich)	Uniprot Protein ID	Protein Name	EmPAI quantification		P-Value	Trend
			mean_Normog	mean_Microg		
osteoblast differentiation	ALPL	alkaline phosphatase, tissue-nonspecific isozyme	0,044149309	0,009104496	0,000105	DOWN (***)
	CRYAB	alpha-crystallin B chain	0,790082982	0,427695416	0,007994	DOWN (**)
	TPM4	Tropomyosin alpha-4 chain	1,845236883	0,668106546	0,0053	DOWN (**)
	CLH1	Clathrin heavy chain 1	0,131334397	0,081128722	0,0073	DOWN (**)
	RRAS	Ras-related protein R-Ras2	0,126690834	0,071952878	0,0049	DOWN (**)
	FGFR2	Fibroblast growth factor receptor 2	0,017730002	0,01106954	0,0004	DOWN (***)

Figure 3.2. Loosening of osteoblast phenotype induced by Sμg. Upper panel: TEM micrographs of hpOBs. (**A)** Normo-gravity control mature hpOBs micrograph taken at 110 h time point. Ultrastructural image show osteoblast cell with intracellular granules of HA crystals (highlighted by arrows). (**B)** Mature osteoblasts exposed to 110 h Sμg. Image represent 90% of cells, which show large cells without both profuse endoplasmic reticulum and intracellular granules of HA crystals. (**C)** Representative TEM micrograph of 4% of cell after 110 h Sμg. Images display a "mesenchymal-like" cell induced from 110 h-Sμg treatment. Lower panel: Downregulation of pro-osteogenic proteins. The tables reports differential spectral-counts between normogravity and Sμg conditions. Protein content was estimated as normalized EmPAI values as percentage according to Shinoda et al. The table shows proteins differentially regulated in abundance with statistical significance. *$p < 0.05$; **$p < 0.01$; ***$p < 0.001$, and unique proteins in normo-gravity (UN) and microgravity (UM).

Table 3.1. Biological functions of the proteome which is differential regulated upon Sμg treatment. The table shows trends of osteoblast-differentiation proteins differentially regulated in abundance. ↓, indicates microgravity induced down regulation of proteins. ↑, indicates microgravity-induced up-regulation of protein. (UN), indicates Unique proteins in normo-gravity and (UM)refers to Unique proteins found Sμg proteome. For each protein its biological functions is specified.

Molecular function enrichment item (FunRich)	Protein subclass	Protein Name	Biological Function	Trend
osteoblast differentiation	mineralization proteins	Alkaline phosphatase, tissue-nonspecific isozyme	This isozyme may play a role in skeletal mineralization.	↓
		Alpha-crystallin B chain	Has chaperone-like activity, preventing aggregation of various proteins under a wide range of stress conditions. it is a novel osteogenic marker (Graneli et al 2014)	↓
	Tropomyosin alpha-4 chain		Binds to actin filaments in muscle and non-muscle cells. Plays a central role, in association with the troponin complex, in the calcium dependent regulation of vertebrate striated muscle contraction. Smooth muscle contraction is regulated by interaction with caldesmon. In non-muscle cells is implicated in stabilizing cytoskeleton actin filaments. Binds calcium	↓
	migration proteins	Clathrin heavy chain 1	Clathrin is the major protein of the polyhedral coat of coated pits and vesicles. Acts as component of the TACC3/ch-TOG/clathrin complex proposed to contribute to stabilization of kinetochore fibers of the mitotic spindle by acting as inter-microtubule bridge. The TACC3/ch-TOG/clathrin complex is required for the maintenance of kinetochore fiber tension. Plays a role in early autophagosome formation	↓
		Ras-related protein R-Ras2	It is a plasma membrane-associated GTP-binding protein with GTPase activity. It's important for osteoblast differentiation and cell migration	↓
		Fibroblast growth factor receptor 2	Tyrosine-protein kinase that acts as cell-surface receptor for fibroblast growth factors and plays an essential role in the regulation of cell proliferation, differentiation, migration and apoptosis. Plays an essential role in the regulation of osteoblast differentiation, proliferation and apoptosis, and is required for normal skeleton development.	↓
(i)Adhesion proteins		Talin	Probably involved in connections of major cytoskeletal structures to the plasma membrane. High molecular weight cytoskeletal protein concentrated at regions of cell-substratum contact and, in lymphocytes, at cell-cell contacts	↓

	Integrin binding proteins			
		Zyxin	Adhesion plaque protein. Binds alpha-actinin and the CRP protein. Important for targeting TES and ENA/VASP family members to focal adhesions and for the formation of actin-rich structures. May be a component of a signal transduction pathway that mediates adhesion-stimulated changes in gene expression	↓
	integrins	integrin beta 1	Involved in osteoblast compaction through the fibronectin fibrillogenesis cell-mediated matrix assembly process and the formation of mineralized bone nodules	↓
		Integrin alpha-3	It's a receptor for fibronectin, laminin, collagen, epiligrin, thrombospondin and CSPG4. Integrin alpha-3/beta-1 provides a docking site for FAP (seprase) at invadopodia plasma membranes in a collagen-dependent manner and hence may participate in the adhesion, formation of invadopodia and matrix degradation processes, promoting cell invasion	↓
	Arp2/3 complex proteins	Actin-related protein 2/3 complex subunit 1B (p41)	Subunits involved in regulation of actin polymerization and together with an activating nucleation-promoting factor (NPF) mediates the formation of branched actin networks	UN
		Actin-related protein 2/3 complex subunit 2 (ARPC2/p34)		↓
		Actin-related protein 2/3 complex subunit 3 (ARPC3/p21)		UM
		Actin-related protein 2/3 complex subunit 4 (p20)		↑
		Actin-related protein 2/3 complex subunit 5 (p16)		↑

(ii)Protrusion dynamic actin network		Actin-related protein 2 (ARP2)	Functions as ATP-binding component of the Arp2/3 complex which is involved in regulation of actin polymerization and together with an activating nucleation-promoting factor (NPF) mediates the formation of branched actin networks. Seems to contact the pointed end of the daughter actin filament.	UN
		Actin-related protein 3 (ARP3)		↓
	cytoskeletal organization proteins	ENAH Protein enabled homolog	Ena/VASP proteins are actin-associated proteins involved in a range of processes dependent on cytoskeleton remodeling and cell polarity such as axon guidance and lamellipodial and filopodial dynamics in migrating cells. ENAH induces the formation of F-actin rich outgrowths in fibroblasts. Acts synergistically with BAIAP2-alpha and downstream of NTN1 to promote filipodia formation	↓
		VASP Vasodilator-stimulated phosphoprotein	VASP promotes actin filament elongation. It protects the barbed end of growing actin filaments against capping and increases the rate of actin polymerization in the presence of capping protein. VASP stimulates actin filament elongation by promoting the transfer of profilin-bound actin monomers onto the barbed end of growing actin filaments. Plays a role in actin-based mobility of Listeria monocytogenes in host cells.	UM
		cofilin-1	Binds to F-actin and exhibits pH-sensitive F-actin depolymerizing activity. Regulates actin cytoskeleton dynamics. Important for normal progress through mitosis and normal cytokinesis. Plays a role in the regulation of cell morphology and cytoskeletal organization.	↓
		profilin	Binds to actin and affects the structure of the cytoskeleton. At high concentrations, profilin prevents the polymerization of actin, whereas it enhances it at low concentrations. By binding to PIP2, it inhibits the formation of IP3 and DG. Inhibits androgen receptor (AR) and HTT aggregation and binding of G-actin is essential for its inhibition of AR (Shao J. *et al*. Phosphorylation of profilin by ROCK1 regulates polyglutamine aggregation. *Mol Cell Biol*. 28(17):5196-208 (2008).)	↓
		fascin	Organizes filamentous actin into bundles. Plays a role in the organization of actin filament bundles and the formation of microspikes, membrane ruffles, and stress fibers. Important for the formation of a diverse set of cell protrusions, such as filopodia, and for cell motility and migration.	UM
		radixin	Probably plays a crucial role in the binding of the barbed end of actin filaments to the plasma membrane.	UM
		Myosin-10	Cellular myosin that appears to play a role in cytokinesis, cell shape, and specialized functions such as secretion and capping. During cell spreading, plays an important role in cytoskeleton reorganization, focal contacts formation (in the central part but not the margins of spreading cells), and lamellipodial extension; this function is mechanically antagonized by MYH9.	UN

(iii)RhoGTP signaling	**Rho GTPases**	RHOA transforming protein rhoA precursor	Regulates a signal transduction pathway linking plasma membrane receptors to the assembly of focal adhesions and actin stress fibers. Involved in a microtubule-dependent signal that is required for the myosin contractile ring formation during cell cycle cytokinesis. Plays an essential role in cleavage furrow formation. Required for the apical junction formation of keratinocyte cell-cell adhesion.	UM
		RHO G Rho related GTP-binding protein RhoG precursor	Required for the formation of membrane ruffles during macropinocytosis. Plays a role in cell migration and is required for the formation of cup-like structures during trans-endothelial migration of leukocytes.	UM
		RAC1 Ras-related C3 botulinum toxin substrate 1	Plasma membrane-associated small GTPase which cycles between active GTP-bound and inactive GDP-bound states. In its active state, binds to a variety of effector proteins to regulate cellular responses such as secretory processes, phagocytosis of apoptotic cells, epithelial cell polarization and growth-factor induced formation of membrane ruffles	UM
	negative regulators of GTPases	ARHGDIA Rho GDP-dissociation inhibitor 1	Controls Rho proteins homeostasis. Regulates the GDP/GTP exchange reaction of the Rho proteins by inhibiting the dissociation of GDP from them, and the subsequent binding of GTP to them.	↓
		ARHGDIB Rho GDP-dissociation inhibitor 2	Regulates the GDP/GTP exchange reaction of the Rho proteins by inhibiting the dissociation of GDP from them, and the subsequent binding of GTP to them (PubMed:8356058, PubMed:7512369). Regulates reorganization of the actin cytoskeleton mediated by Rho family members.	UN
		ARHGEF18 Rho guanine nucleotide exchange factor 18	Acts as guanine nucleotide exchange factor (GEF) for RhoA GTPases. Its activation induces formation of actin stress fibers.	UN
	activator of GTPase	RHG01 Rho GTPase-activating protein 1	GTPase activator for the Rho, Rac and Cdc42 proteins, converting them to the putatively inactive GDP-bound state. Cdc42 seems to be the preferred substrate.	UM
		ROCK2 Rho associate protein kinase 2	Protein kinase which is a key regulator of actin cytoskeleton and cell polarity. Involved in regulation of smooth muscle contraction, actin cytoskeleton organization, stress fiber and focal adhesion formation, neurite retraction, cell adhesion and motility	UN

vitamin A metabolism	**negative regulators of vit A metabolisms**	calreticulin	Calcium-binding chaperone that promotes folding, oligomeric assembly and quality control in the endoplasmic reticulum (ER) via the calreticulin/calnexin cycle. It can negatively regulate RAR function	↑
		HMGB1 High mobility group protein B1	Multifunctional redox sensitive protein with various roles in different cellular compartments. In the nucleus is one of the major chromatin-associated non-histone proteins and acts as a DNA chaperone involved in replication, transcription, chromatin remodeling, V(D)J recombination, DNA repair and genome stability. RA inhibits the release of HMB1 in TNFα activated endothelilal cells	↑
	positive regulators of vit A metabolisms	HMG A1 High mobility group protein HMG-I/HMG-Y	Interact selectively and non-covalently with retinoic acid receptor	↓
		ACTN4 Alpha-actinin-4	F-actin cross-linking protein which is thought to anchor actin to a variety of intracellular structures. ACTN4 modulates transcriptional activity of RA receptor (Khurana et al., 2012. Familial Focal Segmental Glomerulosclerosis (FSGS)-linked α-Actinin 4 (ACTN4) Protein Mutants Lose Ability to Activate Transcription by Nuclear Hormone Receptors)	↓
		Guanine nucleotide-binding protein GI/GS/GT subunit beta-1	Guanine nucleotide-binding proteins (G proteins) are involved as a modulator or transducer in various transmembrane signaling systems. The beta and gamma chains are required for the GTPase activity, for replacement of GDP by GTP, and for G protein-effector interaction. Rhodopsin mediated signaling pathway	↓

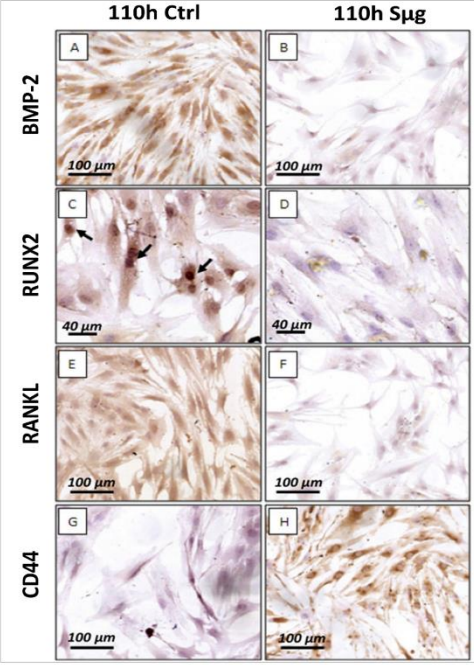

Differentiation marker	18h Ctrl	18Sμg
BMP-2	3	1
RUNX2	3	2
RANKL	3	1
CD44	1	3

Semi-quantification values for Immunochemistry staining.
A score (from 0 to 3) was assigned counting the number of positive cells over the total cell analyzed.
Score 0<5% positive cells; score:5<x<30%; score2: 30<x<60%; score 3: >60%

Figure 3.3. Sμg reduces hpOB differentiative potential. *Left panel*: Immuno-cyto-chemical staining of differentiation markers on hpOB cells. (**A**) Image shows numerous well-differentiated BMP-2-positive osteoblasts in normo-gravity condition. (**B**) After 24 h Sμg treatment, osteoblasts lose the expression of BMP-2. (**C**) Nuclear RUNX2 expression (arrows) in osteoblasts under terrestrial gravity. (**D**) After 24 h Sμg expostition, a decreases of RUNX2 nuclear expression is observed. (**E**) In normo-gravity condition more than 95% of osteoblast express RANKL. (**F**) After 24 h Sμg expostition, osteoblasts downregulate the expression of RANKL. (**G**) Image shows rare CD44-positive osteoblasts in normo-gravity. (**H**) 24 h Sμg treatment induces the expression of CD44 in osteoblasts. *Right panel*: Semi-quantitative analysis of the variation of osteoblast differentiation markers on hpOBs. The immuno-histochemical reaction was evaluated by assigning a score from 1 to 3 according to the number of positive cells. Semi-quantification values refer to the 18 h incubation time. Dashed lines highlight the place where the scratch occurred. Dotted lines indicate wound leading edges. Phase contrast images (microscopic magnification 4×).

3.3.2 CELL MIGRATION UNDER SIMULATED MICROGRAVITY INDUCES A REGENERATIVE RESPONSE IN HPOBS

Assuming that changes in cell locomotion were an indicator of a transition phase across the processes of osteogenic differentiation, we believed relevant to investigate how cell migration was affected by Sμg. Cell motility was examined by 2D wound healing assay which is an established method for assessing cancer aggression for osteosarcoma cells. Therefore, first we performed experiments on SAOS II osteosarcoma cells (osteoblastmodel cell line commonly used as reference). As also reported by others, (Bjørnland, et al., 2005) on Earth osteosarcoma cell migration was dependent on matrix metalloproteinase (MMP) activity (data not shown). By contrast, Figure 3.4 indicates that under Sμg conditions the malignant osteoblast migration to the site of injury occurred

even in the presence of 26 μM ilomastat (an irreversible broad-range inhibitor for MMPs). It indicates that the migration properties of osteosarcoma cells depend on the gravitational force, involving distinct proteolytic sets of enzymes.

Furthermore, a 24 hours-treatment of Sμg turned out to be an osteotropic agent which enhances SAOS-II cell-motility, as demonstrated by the difference of cell-migration rates between normo- (3.2±0.1 μm/h) and micro-gravity conditions (3.7±0.05 μm/h). Therefore, on the basis of the wound healing assay on SAOS-II cells we observe that Sμg *a*) increases the migration velocity by 15%, *b*) renders the cell migration process independent on MMPs proteolytic activities (Figure 3.4), *c*) induces a loosening of the confluence layer, motility becoming individual rather than collective (Figure 3.4 F-G). Since proteolytic and non-proteolytic cell motility involve distinct migration strategies, (Petrie et al., 2012; Wolf et al., 2011) these findings suggest that under Sμg conditions migration of osteosarcoma cell line occurs through a distinct migration strategy, which is sensitive to the gravitational force. Of note, Figure 3.4 clearly shows that under Sμg cell layers lose confluence (likely due to a decrease of cell-cell contacts) and the cell migration becomes individual (Figure 3.4 G). Similar procedures were applied to hpOBd.

The osteotropism effect of Sμg on hpOBs was examined by 24 h monitoring: thus, right after the wound was procured, the scratched hpOB monolayers were (or not) treated with Sμg. Figure 3.5 A shows fully differentiated hpOBs layer at the time of the wound (t0), Figure 3.5 B displays that after 24 h under normo-gravity the wound is not visible anymore as for cells detached and died. Thus, after the wound scratch, cell migration did not occur for the stationary normo-gravity cultured and almost all cells detached and died within the 24 h (Figure 3.5 B). On the other hand, when the scratched hpOB monolayer was exposed to Sμg for 24 h, an astonishing regenerative impulse was observed. Figure 3.5 C shows a complete coverage of the wounded area by loosely connected population of cells, suggesting that the Sμg treatment unveiled the hidden cellular plasticity (i.e., a cellular susceptibility to reprogramming) of hpOBs, which in Sμg conditions mimic migration of fibroblasts on Earth. In view of the reported anabolic effect of osteoblasts secretome as co-ordinator of bone formation, particularly in response to mechanical stimulation (Brady et al., 2015), we tested whether the Sμg-conditioned medium could recover the wound hpOBs monolayer left under normo-gravity conditions. However, cell-imaging analysis did not appreciate an meaningful improvement of the repair process under normo-gravity conditions in the presence of Sμg hpOB conditioned media (data not shown). It demonstrates that the anabolic Sμg response cannot be simply reproduced by a paracrine signal. A closer look at the wounded leading edges (Figure 3.5) indicates that (i) transition of cells induced the losening of the osteoblast phenotype and the acquisition of fibroblastlike features, (ii) cells display actin-based protrusions such as pseudopodia (similar to lamellipodia and filopodia

but not to blebs) (Figure 3.5 F, G), which mediate the migration of mesenchymal cells (Bear et al., 2014) (see Figure 3.4).

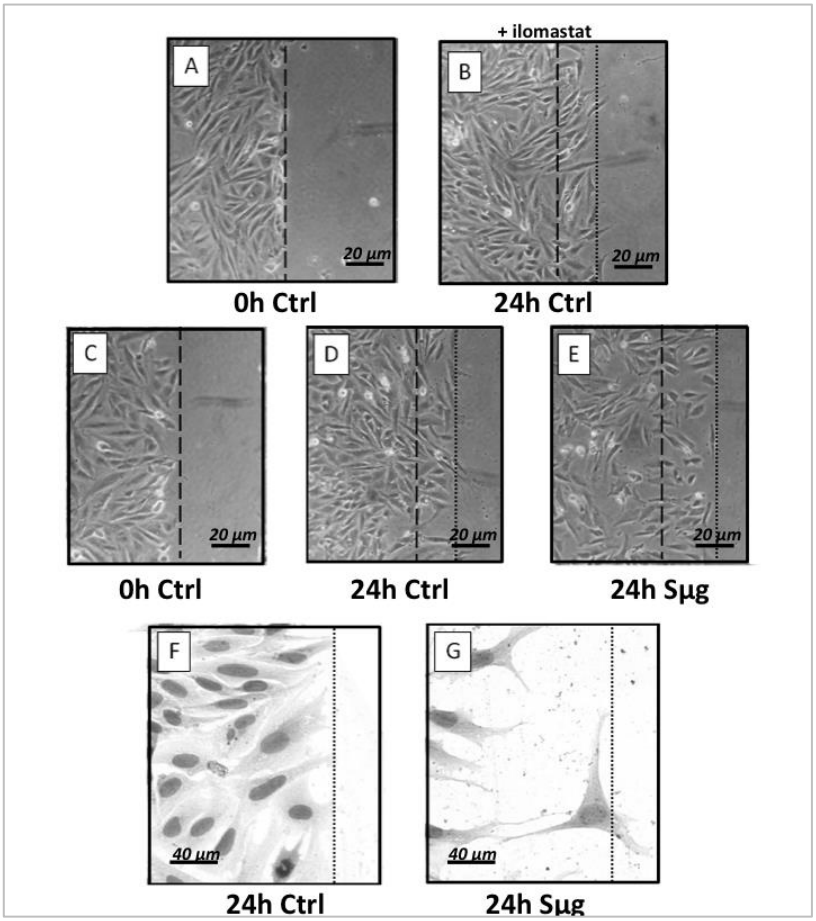

Figure 3.4 SAOS II cell migration under microgravity becomes. **I)** MMP independent**.** (A) Phase contrast image of cell monolayer recorded immediately after the scratch (t0).(B) The wound after 24h microgravity exposition in the presence of 26 µM ilomastat(MMP irreversible inhibitor). In microgravity environment cell motility occurs even in the presence of 26 µM ilomastat. **II)** faster (C) scratched cell monolayer at t0. (D) 24h post the wound under normo-gravity. (E) 24h post the wound under microgravity (microscopic magnification 4X). **III)** not-through sheet of cells (F) and (G): zoom on leading edges on BMP2 Immunostained cells 24h normo- and micro-gravity, respectively (magnification 40X).

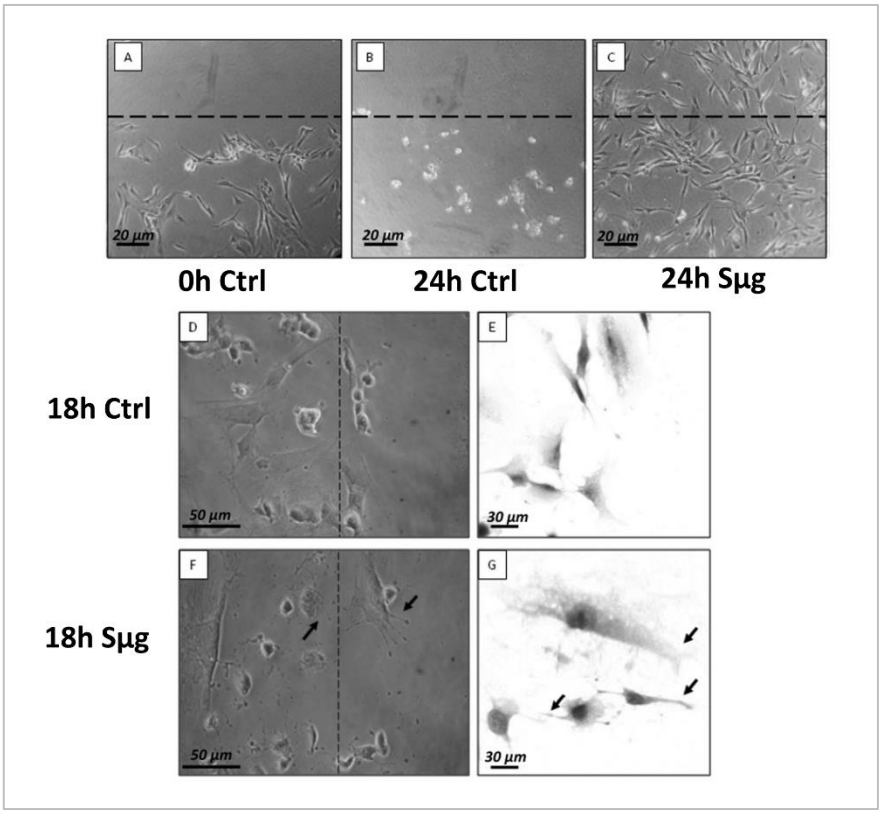

Figure 3.5. Effect of sµg on hpOb motility. *Upper panel*: Wound assay on hpOB cells normo-gravity vs. Sµg. (**A**) Scratched cell monolayer recorded at t0. (**B**) The wound after 24 h under normo-gravity. (**C**) The wound after 24 h Sµg exposition. Dashed lines highlight the place where the scratch occurred (microscopic magnification 4×). *Lower panel*: Cell migrating front: ZOOM of hpOBs at 18 h after the wound: normo-gravity vs. Sµg. (**D, E**) Micrograph of hpOBs close to leading edge under normo-gravity conditions from upright and inverted microscope, respectively. Images display no/rare cellular structures compatible with cell protrusions (filopodia or lamellipodia). (**F, G**) Images show osteoblasts next to leading edge after 18 h microgravity incubation from upright and inverted microscope, respectively. Arrows indicate the presence of several lamellipodia or filopodia-like protrusions. Tluidine blue staining in pictures from inverted microscope.

3.3.3 *SIMULATED MICROGRAVITY EFFECT ON THE "MOTILITY PROTEOME***"**

As reported above proteins concurrently involved in migration and differentiation were found downregulated in Sµg proteome (see Figure 3.2). To further investigate the gravitational impact on cell motility proteins the MSproteomic study was addressed to three classes of proteins, namely (i) adhesion proteins, (ii) protrusion dynamic networks, and (iii) rhoGTP signaling cascade, which are collectively reported to play important roles in migration and in biophysically induced cell response (Yim et al., 2012; Ridley, 2015). Within the "motility proteome" only proteins which displayed protein levels (emPAI) altered by Sµg were examined and classified according to Fun Rich (Platform 3.0). Spectral counts are reported in Table 3.2, whereas Table 3.1 resumes trends of protein levels after the

Sμg treatment, specifying the biological functions known for each protein. (i) Among the adhesion proteins we detected downregulation of two integrin subunits (i.e., integrin beta-1 (ITGB1 or CD29) and integrin alpha-3 (ITGA3 or CD49)), as well as of two integrin-binding proteins (i.e., tailin and zyxin) suggesting, as previously reported (Nabavi et al., 2011), that a suboptimal integrin-ligand level might reflect an inefficient cell adhesion (Table 3.1 and Table 3.2). (ii) Concerning the proteins involved in the formation of dynamic cell protrusions, the MS quantification revealed a Sμg dysregulation of proteins involved in the cytoskeletal dynamic formation of cell protrusions (i.e., lamellipodia and filopodia). In particular, these include actin-interacting regulatory proteins, such as the multifunctional organizer Arp2/3 complex, a conserved multi-protein complex that facilitates the formation of actin-based protrusions essential for cell motility. It must be outlined that the Arp2/3 complex is formed by seven members, three of which, namely, ARP2, ARP3, and p34/ARPC2, were reduced by Sμg, whereas other three, namely, p21/ARPC3, p20/ARPC4, and p16/ARPC5, displayed an upregulation. Similarly, a dysregulation was observed for another set of cytoskeletal organization proteins, such as Enah, cofilin, profilin1, fascin, radixin, myh10 (all of which were downregulated); conversely, vasodilator-stimulated phosphoprotein (Vasp) was upregulated (Table 3.1 and Table 3.2). Overall, these data indicate that the dynamic formation of distinct actin-dependent structures is sensible to the gravitational force, making it reasonable to speculate that under Sμg conditions the peculiar assembly/disassembly coordination could influence the kinetics of cell migration. (iii) With regard to rhoGTP signaling cascade, Sμg favors Rho GTPase activities, as these enzymes (namely, RHOA, RHO G, and RAC1) were uniquely found in the Sμg proteome, whereas a concurrent downregulation (or the complete absence) of their negative regulators (namely, Rho GDP Dissociation Inhibitor Alpha (ARHGDIA), Rho GDP Dissociation Inhibitor Beta (ARHGDIB), and Rho/ RAC GTP exchange factor (ARHGEF18)) were detected (Table 3.2). However, ROCK, one of the downstream target of rhoA, was downregulated, suggesting that ROCK may not be essential for migration under Sμg conditions (Table 3.1 and Table 3.2).

3.3.4 EFFECT OF SIMULATED MICROGRAVITY ON PROTEINS AND METABOLITES OF THE VITAMIN A METABOLISM

Since RA is known to be one of the major small molecular regulators of osteoblast dedifferentiation (Sehring et al., 2016), we have examined the vitamin A pathway. In order to detect any Sμg-induced perturbation on vitamin A metabolism, a quantitative metabolomic comparison was carried out between active and inactive metabolites of vit A (whose steps are sketched in Figure 3.6 left upper panel). The comparative analysis showed that after an exposure of 110 h to Sμg both

precursors and the active forms of vitamin A (i.e., retinol and RA) were decreased (see Figure 3.6 A,B), without affecting the cellular levels of vitamin A inactive forms (Figure 3.6 C,D). Searching for proteins directly related to the vitamin A pathway within the hpOB proteome, none of the peak lists could be assigned to direct enzymes nor to receptors involved in vitamin A metabolism, likely because these proteins are opaque to the employed experimental MS approach. However, proteins indirectly related to this metabolism (according to Funrich annotation) were identified by Mascot search. Interestingly, among these proteins, only those negatively affecting the vitamin A metabolism were upregulated (namely, calreticulin (CALR), which negatively regulates RAR function, and High Mobility Group Box 1 (HMGB1), whose release is inhibited by RA). Consistently, High Mobility Group Box 1 (HMGA1) and GBB1 guanidine were downregulated, as expected for a dampened vitamin A metabolism (see Figure 3.6 lower panel).

Table 3.2. Protein content was estimated as normalized emPAI values express as percentage according to Shinoda et al. The table shows proteins differentially regulated in abundance with statistical significance *p < 0.05; **p < 0.01; ***p < 0.001, and unique proteins in normo-gravity (UN) and microgravity (UM).

Molecular function enrichment item (FunRich)		**Uniprot Protein ID**	**Protein Name**	**EmPAI quantification**		**P-Value**	**Trend**
				mean_Normo	**mean_Micro**		
(i)Adhesion proteins		TLN1	Talin	0,188123068	0.070200944	**2,11E-06**	DOWN (***)
		ITGB1	integrine beta 1	0,06516658	0,044034984	**0,0507549**	DOWN
		ITGA3	Integrin alpha-3	0,006907204	0,004317346	**0,0155**	DOWN (*)
		ZYX	Zyxin	0,131873677	0,068814834	**0,039799**	DOWN (*)
(ii)Protrusion active network	**Arp2/3 complex**	ACTR2	Actin-related protein 2	0,051803205	-	-	UN
		ACTR3	Actin-related protein 3	0,049531658	0,033574567	**0,012523**	DOWN (*)
		ARPC1B	Actin-related protein 2/3 complex subunit 1B	0,022004409	-	-	UN
		ARPC2	Actin-related protein 2/3 complex subunit 2	0,167532621	0,065708433	**0,000261**	DOWN (***)
		ARPC3	Actin-related protein 2/3 complex subunit 3	-	0120347326	**-**	UM
		ARPC4	Actin-related protein 2/3 complex subunit 4	0,040176784	0,172100443	**6,68E-08**	UP (***)
		ARPC5	Actin-related protein 2/3 complex subunit 5	0,074171194	0,162733776	**0,046479**	UP (*)

	cytoskeletal organization proteins	ENAH	Protein enabled homolog	0,011537141	0,007866219	**0,022371**	DOWN (*)
		VASP	Vasodilator-stimulated phosphoprotein	-	0,014752477	-	UM
		CFL1	cofilin-1	0,742005965	0,304803386	**0,024149**	DOWN (*)
		PFN1	profilin	2,096222416	1,400267715	**0,044221**	DOWN (*)
		FSCN1	fascin	-	0,027958567	-	UM
		RDX	radixin		0,074884277	-	UM
		MYH10	Myosin-10	0,052986425	-	-	UN
(iii)RhoGTP signaling		RHOA	transforming protein rhoA precursor	-	0,109655994	-	UM
		RHOG	Rho related GTP-binding protein RhoG precursor	-	0,019540636	-	UM
		RAC1	Ras-related C3 boyulinum toxin substrate 1	-	0,04918568	-	UM
		ARHGDIA	Rho GDP-dissociation inhibitor 1	0,063887075	0,044089322	**0,04036**	DOWN (*)
		ARHGDIB	Rho GDP-dissociation inhibitor 2	0,035981062	-	-	UN
		ARHGEF18	Rho guanine nucleotide exchange factor 18	0,0087225	-	-	UN
		RHG01	Rho GTPase-activating protein 1	-	0,00929341	-	UM
		ROCK2	Rho associate protein kinase 2	0,010915361	-	-	UN

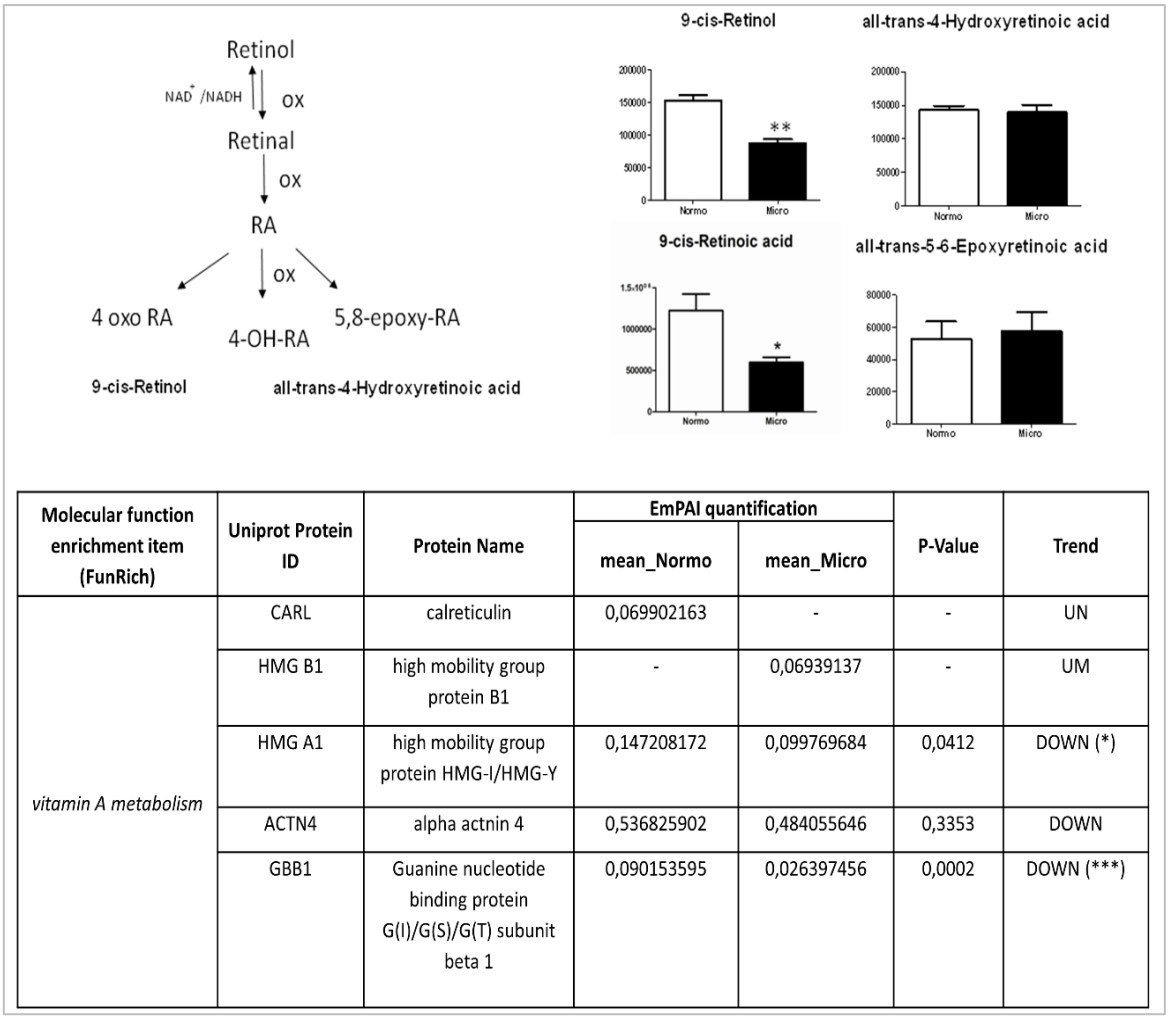

Molecular function enrichment item (FunRich)	Uniprot Protein ID	Protein Name	EmPAI quantification		P-Value	Trend
			mean_Normo	mean_Micro		
vitamin A metabolism	CARL	calreticulin	0,069902163	-	-	UN
	HMG B1	high mobility group protein B1	-	0,06939137	-	UM
	HMG A1	high mobility group protein HMG-I/HMG-Y	0,147208172	0,099769684	0,0412	DOWN (*)
	ACTN4	alpha actnin 4	0,536825902	0,484055646	0,3353	DOWN
	GBB1	Guanine nucleotide binding protein G(I)/G(S)/G(T) subunit beta 1	0,090153595	0,026397456	0,0002	DOWN (***)

Figure 3.6. Simulateded microgravity treatment hampers vitamin A metabolism on hpOB cells. Left upper panel: A sketch of metabolism of vitamin A (retinol): Physiological RA, the most bioactive form of the vitamin A, is biosynthesized from dietary retinol (vitamin A) through two oxidation steps and it is catabolized by additional oxidizing steps that generate several inactive species (i.e., 4-OH-RA, 4-oxo-RA, and 5,8 epoxy RA). Right upper panel: Variation in the levels of metabolic intermediates in Vitamin A metabolism. Values are mean ± SD (n = 9) of normo-gravity (white columns) and microgravity (black columns) metabolites. *p < 0.05; **p < 0.01; ***p < 0.001. Lower panel: Spectral count-relative abundance for "vitamin A proteome" on hpOBs between under normo-gravity and Sμg conditions. Protein content was estimated as normalized emPAI values as percentage according to Shinoda et al. The table shows proteins differentially regulated in abundance with statistical significance. *p < 0.05; **p < 0.01; ***p < 0.001, and unique proteins in normo-gravity (UN) and microgravity (UM).

3.4 DISCUSSION

The absence of gravity is a biological stressor whose impact on biological systems is far from being defined; its role in determining cellular functions can be cheaply investigated on earth with Sμg. Bone is a highly mechanosensitive tissue, so that even a healthy bone can rapidly develop an osteoporotic-like phenotype upon prolonged exposure to unloading conditions, as it is experienced by astronauts during space-flights or by patients forced t bed rest. Although a hypo-function of the osteoblasts isr eported to be involved in the progression of unloadinginduced osteoporosis, the gravitational stress response of human not-genetically-transformed cells remains largely unknown. Previously on hpOBs, we reported that Sμg changes cell metabolism, as revealed by an increased glycolysis pathways and by a severe impairment of the Krebs cycle pathway associated to a decrease of the malateaspartate shuttle (Michaletti et al., 2017). This was related to a significant alteration of chain electron transport of respiratory proteins, mainly affecting complex III (Michaletti et al., 2017). Thereby suggesting that Sμg suppresses bone cell functions through a prominent dysregulation of mitochondria, which impairs the energy state and antioxidant capacity of hpOB cells. Here we examined the effect of weightless conditions on osteogenesis, comparing cellular morphology, proteome profiling, metabolism, and cell motility between hpOBs exposed to Sμg vs. those kept under normo-gravity conditions. Our data show that upon Sμg treatment hpOBs (i) assume a spindle-shape morphology, characteristic of a less differentiated phenotype, (ii) decrease the production of HA crystals (laid down during the ossification process) (Figure 3.2 A,B), and (iii) reduce osteogenic differentiation markers (e.g., ALPL, CRYα-B, Runx-2, Rank-L, and BMP-2) (Figure 3.3). A similar behavior was also reported by others through different experimental approaches (Shi et al., 2017; Hu et al., 2015 a,b; Ontiveros et al., 2003; Patel et al., 2007), confirming that Sμg significantly impairs osteoblastic differentiation. Our findings show that the Sμg affects the hpOBs not just slowing down their differentiation process, but also inducing a phenotypic regression (accompanied to a loosening of pro-osteogenic specialized functions). Here we report for the first time that under Sμg condition hpOBs display a transition process toward a mesenchymal-like phenotype, in which a mature osteoblast cell loses levels of adhesive proteins (see Table 3.1 and Table 3.2), enhancing mesenchymal-like components (Figure 3.2C, 3.3 G,H), which allows it to acquire motility properties. Although this phenotype conversion can be reversible and often incomplete (Nieto & Fernando, 2015; Harada & Rodan, 2003), its occurrence is certainly a demonstration of a cellular regenerative potential.

This observation is of particular interest, since under normo-gravity conditions mature-osteoblasts, though conserving a dedifferentiation potential (Lian & Stein, 1995; Pereira et al., 2009), do not participate to bone-healing neither in vitro nor in bone fracture repair processes in vivo (Figure 3.5) (Park et al., 2012; Harada & Rodan, 2003). Conversely, under Sμg conditions, hpOB cells show an unusual degree of plasticity as all of them revert to a prior developmental stage, and 4% of them switch to a mesenchymal-like phenotype. Therefore, we can reasonably assess that hpOB receive an impulse to dedifferentiate by gravitational unloading, probably as a consequence of a metabolic/mitochondrial perturbation (Figure 3.6) (Michaletti et al., 2017). The Sμg dedifferentiation impulse is also consistent with the overall metabolic profile observed in hpOB exposed to Sμg (Michaletti et al., 2017). Similarly to what reported for the metabolism of dedifferentiated cells (Feger et al., 2016; D'Alessandro et al., 2013), we previously reported for osteoblasts under Sμg an enhanced glycolysis associated to an increased production of lipids and nucleotides, which are followed by a reduction of the Krebs cycle (Michaletti et al., 2017). Interestingly, in Sμg conditions the reduced differentiation phenotype was not accompanied by a proliferative state (Michaletti et al., 2017), supporting that the metabolic changes are compatible with a dedifferentiation switch. Nevertheless, a closely related developmental regression to a less differentiated cell phenotype was also reported for tumors and may contribute to metastasis (Alexandrova, 2014; Nieto & Cano 2012; Fernando et al., 2015), indicating that the Sμg-induced dedifferentiation process deserves further studies studies to understand more accurately the mechanism underlying these complex changes for developing effectively novel biomechanical strategies in medicine. In addition, the analysis of metabolites and protein profiling on the metabolism of vitamin A (i.e., retinol and RA), one of the major small molecular suppressors of osteoblast dedifferentiation (Geurtzen et al., 2014; Blum & Begeman, 2015), revealed that RA metabolism is dampened under Sμg conditions (see Figure 3.6).

Thereby, in view of the inhibitory effect of RA on the osteoblast dedifferentiation (Blum & Begeman 2015; Sehring et al., 2016), a realistic hypothesis can be that the Sμg-induced dedifferentiation is triggered by low levels of bioactive vitamin A, even though we cannot rule out the possibility of additional factors (e.g., NFkB and BMPs). Additional results which support that the dedifferentiation can be triggered by a Sμg exposure come from the alteration of cell migrating ability induced by Sμg treatment. During osteoblast differentiation, cells pass through several stages where cell morphology and biochemical phenotype change remarkably, overall influencing cell migration abilities. As a result, at the

end of the differentiation process osteoblasts stop to migrate turning into the mature phenotype (Uchihashi et al., 2013). However, the exposure to Sμg induces a reversion of mature cell phenotype with pregulation of CD44, allowing hpOBs to acquire a resistance to death and motility properties that make wound healing possible in vitro (Figure 3.5). Since it is recognized that the gravitational force influences movement kinematics, it is not surprising that under Sμg cell motility was affected by a decrease of adhesive proteins and an increase of the numbers of cell protrusions with respect to normo-gravity control counterpart. In particular, the Sμg suboptimal integrin level of ITGB1 and ITGA3 (Table 3.2) might reflect an inefficient cell adhesion, as also reported by others (Nabavi et al., 2011). Macroscopically, migration under Sμg conditions takes place through isolated rather than clustered cells, and it occurs through morphological protrusions which explore their surroundings by polymerization of the structural protein actin into filaments (i.e., protrusions dynamic networks), being morphologically compatible with filopodia and/or lamellipodia, but not with blebs (Figure 3.5). Moreover, according to the Schafer's model for the growing ends of actin filaments (Schafer, 2004), the unique presence of the promoters of actin filament elongations (i.e., Vasp, fascin, and radixin; Table 3.1 and Table 3.2) in the Sμg proteome suggests that in these conditions filaments are filopodium-like. Thus, our findings indicate that Sμg triggers an osteotropic effect on human primary cells hpOBs, which induces a "survival impulse" avoiding cells from detaching (Figure 3.5). This was also supported by the increased number of morphological protrusions (most likely filopodia) (Figure 3.5) and by the dysregulation of levels of proteins related to protrusion dynamic networks and upregulation of GTPases activities (Table 3.2), which collectively play important roles in the biophysically induced cell response and migration (Ivanovska et al., 2015; Ridley, 2015; Eleniste et al., 2014). Notably, although the hpOBs secretome on Earth, particularly in response to mechanical stimulation, is reported to provide anabolic effects (Brady et al., 2015), the conditioned medium from hpOBs exposed to Sμg could not rescue the repair process after wound scratch in hpOBs kept under normogravity conditions, thus indicating that the benefic effect of Sμg cannot be simply reproduced by a paracrine signal. Overall, this investigation gives a functional and morphological overview of how hpOBs receive an impulse to dedifferentiate by gravitational unloading. Present findings suggest that Sμg could be employed to promote cell dedifferentiation and potentially be addressed to transdifferentiate to alternative cell types (Figure 3.7). Clearly, the complexity of dedifferentiation processes deserves further studies to understand more accurately how they work and eventually to harness them for use in regenerative medicine. On the other hand, ex

vivo, screening of unloading treatments on hpOBs from osteodegenerative patients could be of help for developing a rational new therapeutically biomechanical strategies for the treatment of skeletal disorders on Earth and to assure safe and effective aerospace missions.

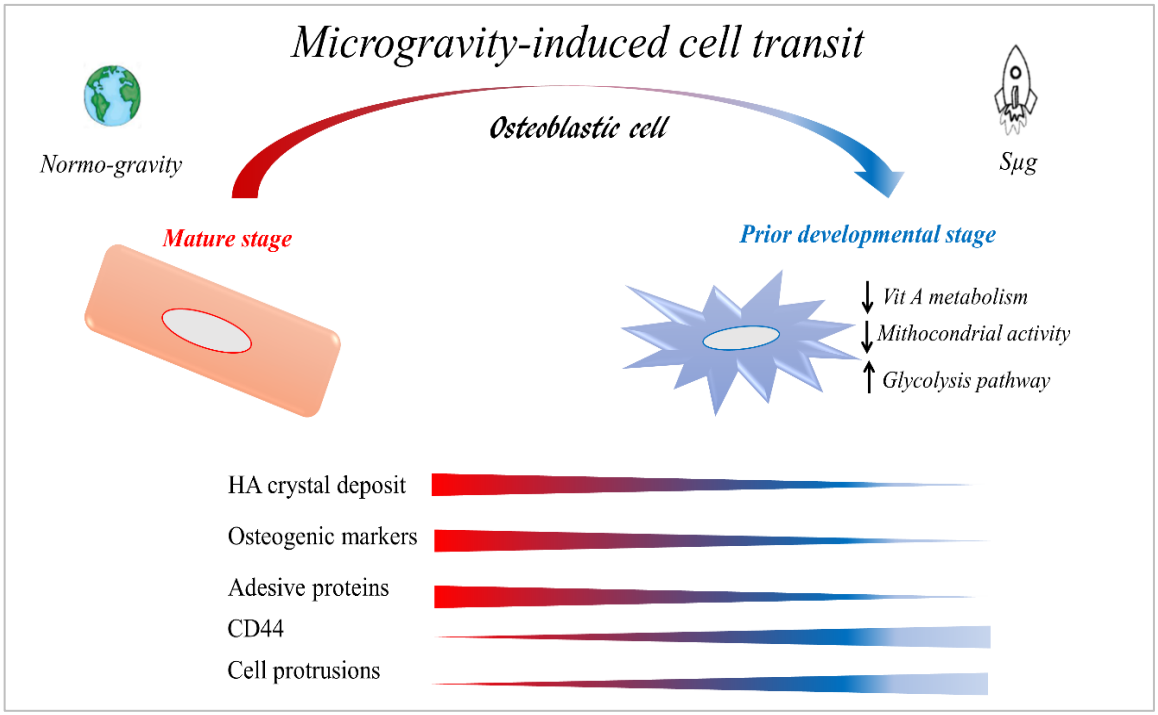

Figure 3.7. Graphical sketch of the effect of Sμg treatment on hpOBs. Microgravity uncovers a developmental state transition on human osteoblasts. Upon simulated microgravity exposition human primary osteoblasts assume spindle-shape morphology reverting the mature phenotype and their specialized functions. A mature osteoblast cell loses levels of bone crystal deposit, osteogenic markers, and adhesive proteins, enhancing prior developmental state features (glycolysis, pre-osteoblast state marker, and cell protrusions), which in turn allows it to acquire motility properties.

4. CONCLUSION

The absence of gravity, or more precisely microgravity, produces profound changes in the musculoskeletal system, with a consequent decrease in bone density, similar to that found in pathological conditions such as osteoporosis. This has been attributed to the abnormal activity of the cells specialized in bone mineralization, that are osteoblasts. Hence the interest of investigating, from a molecular point of view, the effects of microgravity on these cell cultures, in an attempt to understand which biological processes, cellular components and molecular functions are most affected by the absence of gravity. First at all, for this thesis work it was performed a preliminary analysis to investigate any difference in cellular viability between osteoblastic cells grown under micro- and normogravity, using three different colorimetric assays (Trypan blue, BCA and Formazzano test). This study showed that treatment in microgravity conditions does not alter cell proliferation or protein concentration, but strongly affects mitochondrial activity. This effect has been further investigated, using two different "omics" approaches in order to evaluate changes at both the proteomic and the metabolomic levels. These analyses showed that the absence of gravity induces a general alteration of both mitochondrial proteins and the metabolic pathways connected to oxidative phosphorylation, such as the Krebs cycle and the electron transport chain, confirming what was seen by previous analyses. In particular, a disfunction of malate-aspartate shuttle, connected with Krebs cycle, could explain the reduced production of ATP and the alterations of the protein components of mitochondrial complexes, observed in microgravity conditions. In addition, proteomic and metabolomic analyses showed an up-regulation of antioxidant enzymes and a greater quantity of GS-SG in cells subjected to the absence of gravity, indicating, in agreement with the literature, a strong cellular oxidative stress.

Overall, our results indicate an alteration of the physiological functions of mitochondria, which could be one of the causes of reduced osteoblastic function.

Furthermore, the data obtained from the omic analyses were integrated with those obtained through histochemical and ultrastructural approaches, with the aim of studying the effects of gravitational discharge on the biology of human bone cells. From these ex vivo studies it was found that simulated microgravity can trigger a transition to a mesenchymal-like phenotype, triggering a de-differentiation process. In particular, there is an alteration of pro-osteogenesis determinants (i.e. cell morphology and hydroxyapatite crystal deposition),

accompanied by a down-regulation of adhesive proteins and markers of bone differentiation that compromise osteogenesis. For the first time, it was also observed, , that Sμg can trigger the transition to the mesenchymal-like phenotype, through a probable blockage of the vitamin A metabolism, loss of adhesion molecules, acquisition of mesenchymal components and increase of GTPase activity. All of these features, in turn, allow osteoblastic cells to acquire migration properties, typical of pre-differentiation stage cells.

Although this phenotypic conversion is not complete and may be reversible, one might think of using the Sμg environment as an ex vivo impulse to promote the de-differentiation of hpOBs. These findings could, in the future, open the doors to innovative therapeutic strategies for the treatment of certain osteo-degenerative pathologies.

5. REFERENCES

1. Adams S. H. *et al*. Plasma acylcarnitine profiles suggest incomplete long-chain fatty acid beta-oxidation and altered tricarboxylic acid cycle activity in type 2 diabetic African-American women. *J Nutr.* **139**(6), 1073–1081 (2009).
2. Aleshcheva *G. et al*. Moderate alterations of the cytoskeleton in human chondrocytes after short-term microgravity produced by parabolic flight maneuvers could be prevented by up-regulation of BMP-2 and SOX-9. *FASEB J.* **29**(6):2303-14 (2015).
3. Alexandrova A. Y. Plasticity of tumor cell migration: acquisition of newproperties or return to the past? *Biochemistry* **79**: 947–963 (2014).
4. Amaldi U. La fisica per i licei scientifici. Quarta edizione. Zanichelli, 1998.
5. Andalib M. N., Lee J. S., Ha L., Dzenis Y. & Lim, J. Y. The role of RhoA kinase(ROCK) in cell alignment on nanofibers. *Acta Biomater*. **9**: 7737–7745 (2013).
6. Arana-Chavez V.E., Soares A.M. & Katchburian E. Junctions between early developing osteoblasts of rat calvaria as revealed by freeze-fracture and ultrathin section electron microscopy. *Arch Histol Cytol.* **58**(3):285-292 (1995).
7. Arfat W.Z., *et al*. Physiological Effects of Microgravity on Bone Cells. *Calcif Tissue Int.* **94**(6):569-79 (2014).
8. Aslam B., Basit M., Nisar M.A., Khurshid M., Rasool M.H. Proteomics: Technologies and Their Applications. *J Chromatogr Sci.* **55**(2): 182–196 (2017).
9. Atencia R., Asumendi A., García-Sanz M. Role of cytoskeleton in apoptosis. *Vitam Horm.***58**:267-97 (2000).
10. Aubin J.E., Lian J.B. & Stein G.S. Bone formation: maturation and functional activities of osteoblast lineage cells. In: Primer on the metabolic bone diseases and disorders of mineral metabolism, ed. by Favus M.J., American society for Bone and Mineral Research, Washington, pp20-29 (2006). Book
11. Balaji R.H.R. *et al*. A Comparative Study on In Vitro Osteogenic Priming Potential of Electron Spun Scaffold PLLA/HA/Col, PLLA/HA, and PLLA/Col for Tissue Engineering Application. *Plos One*. **9**(8): e104389 (2014).
12. Baldwin K., Herrick R. E. & McCue S. A. Substrate oxidation capacity in rodent skeletal muscle: effects of exposure to zero gravity. J Appl Physiol 75, 2466–2470 (1993). (1985).

13. Baron R. & Kneissel M. WNT signaling in bone homeostasis and disease: from human mutations to treatments. *Nat. Med*. **19**: 179–192 (2013)
14. Battista N., *et al*. 5-Lipoxygenase-dependent apoptosis of human lymphocytes in the International Space Station: data from the ROALD experiment. *Fed Am Soc Exp Biol J*. **26:** 1791-1798 (2012).
15. Bauer T.W. & Muschler G.F. Bone graft materials: an overview of the basic science. *Clin Orthop Relat*. **371**:10-27 (2000).
16. Bear J. E. & Haugh J. M. Directed migration of mesenchymal cells: wheresignaling and the cytoskeleton meet. *Curr Opin Cell Biol*. **30**: 74–82 (2014).
17. Bianco P., Riminucci M., Gronthos S., Robey P.G. Bone marrow stromal stem cells: nature, biology, and potential applications. *Stem Cells*.**19**:180–192 (2001).
18. Bjørnland K. et al. Matrix metalloproteinases participate in osteosarcoma invasion. *J Surg Res*. **127:** 151–156 (2005).
19. Blaber E. A. et al. Microgravity induces pelvic bone loss through osteoclasticactivity, osteocytic osteolysis, and osteoblastic cell cycle inhibition by CDKN1a/p21. *PLoS ONE* **8**: e61372 (2013).
20. Blaber E.A., Pecaut M.J., Jonscher K.R. Spaceflight Activates Autophagy Programs and the Proteasome in Mouse Liver. Int J Mol Sci. **18**(10): E2062 (2017).
21. Blum N. & Begemann G. Osteoblast de- and redifferentiation are controlled by a dynamic response to retinoic acid during zebrafish fin regeneration. *Development* **142**: 2894–2903 (2015).
22. Boja E.S, Kinsinger C.R., Rodriguez H., Srinivas P. Integration of omics sciences to advanced biology and medicine. *Clinical Proteomics* **11**(1):45 (2014)
23. Borst A. G. & van Loon J. J. W. A. Technology and developments for the Random Positioning machine, RPM. *Microgravity Sci. Technol*. **21**: 287–292 (2009).
24. Brady R. T., O'Brien F. J. & Hoey D. A. Mechanically stimulated bone cells secrete paracrine factors that regulate osteoprogenitor recruitment, proliferation, and differentiation. *Biochem. Biophys Res Commun.* **459:** 118–123 (2015).
25. Bremer J. Carnitine: metabolism and functions. *Physiol Rev*. **63**(4):1420-.480 (1983).
26. Buckwalter J.A., Glimcher M.J., Cooper R.R. &Recker R. Bone biology. I: structure, blood supply, cells, matrix, and mineralization. *Instr Course Lect*. **45**:371– 386 (1996).

27. Budni J. *et al*. The oral administration of D-galactose induces abnormalities within the mitochondrial respiratory chain in the brain of rats. *Metab Brain Dis.* **32**(3), 811–817 (2017).
28. Bungo M. W., Goldwater D. J., Popp R. L. & Sandler H. Echocardiographic evaluation of space shuttle crewmembers. *J Appl Physiol.* **62**, 278–283 (1987).
29. Caiozzo V.J., *et al*. Microgravity-induced transformation of myosin isoforms and contractile properties of skeletal muscle. J Appl Physiol. **81**:123–132 (1996).
30. Calvo G. B. *et al*. COQ4 Mutations Cause a Broad Spectrum of Mitochondrial Disorders Associated with CoQ10 Deficiency. *Am J Hum Genet.* **96**(2), 309–317 (2015).
31. Campione M., Ausoni S., Guezennec C.Y., Schiaffino S. Myosin and troponin changes in rat soleus muscle after hindlimb suspension. *J Appl. Physiol*. **74**: 1156-1160(1993).
32. Capulli M., Paone R., & Rucci N. Osteoblast and osteocyte: games without frontiers. *Arch Biochem Biophys*. **561**:3-12 (2014).
33. Carraro S., Giordano G., Reniero F., Perilongo G., Baraldi E. Metabolomics: a new frontier for research in pediatrics. *J Pediatr*. **154**: 638-644 (2009).
34. Chang T.T., *et al*. The Rel/NF-κB pathway and transcription of immediate early genes in T cell activation are inhibited by microgravity. *J Leukoc Biol*., **92:** pp. 1133-1145 (2012).
35. Chatani, M. *et al*. Microgravity promotes osteoclast activity in medaka fish reared at the international space station. *Sci Rep.* **21**(5), 14172 (2015).
36. Chen D., *et al.* Bone morphogenetic protein 2 (BMP-2) enhances BMP-3, BMP-4, and bone cell differentiation marker gene expression during the induction of mineralized bone matrix formation in cultures of fetal rat calvarial osteoblasts. *Calcif Tissue Int*. **60**(3): 283–90 (1997).
37. Chen P., *et al*. Human metabolic responses to microgravity simulated in a 45-day 6° head-down tilt bed rest (HDBR) experiment. Analytical methods **8**(22) (2016).
38. Chouchani E. T. *et al*. Ischaemic accumulation of succinate controls reperfusion injury through mitochondrial ROS. *Nature*. **515**(7527), 431–435 (2014).
39. Ciftçioglu N., Haddad R.S., Golden D.C., Morrison D.R., McKay D.S. A potential cause for kidney stone formation during space flights: enhanced growth of nanobacteria in microgravity. *Kidney Int.* **67**(2):483-91 (2005).

40. Ciofani G. *et al*. Hypergravity effects on myoblast proliferation and differentiation. *J. Biosci. Bioeng.* **113**, 258–261 (2012).
41. Collet P. *et al*. Effects of 1- and 6-month spaceflight on bone mass and biochemistry in two humans. *Bone.* **20**, 547–551 (1997).
42. Connor M.K. & Hood, D.A. Effect of microgravity on the expression of mitochondrial enzymes in rat cardiac and skeletal muscles. *J Appl Physiol*. 1985. **8**4(2), 593–8 (1998).
43. Convertino V.A. Mechanisms of microgravity induced orthostatic intolerance: implications for effective countermeasures. *J Gravit Physiol.* **9**(2):1-13 (2002).
44. Cook G. M., Greening C., Hards K. & Berney M. Energetics of pathogenic bacteria and opportunities for drug development. *Adv Microb Physiol.* **65**, 1–62 (2014).
45. Cox J. & Mann M. Is proteomics the new genomics?; *Cell*. **130** (3): 395–398(2007).
46. Crockett J.C., Mellis D.J., Scott D.I. & Helfrich, M.H. New knowledge on critical osteoclast formation and activation pathways from study of rare genetic diseases of osteoclasts: Focus on the RANK/RANKL axis. *Osteoporos Int*. **22**(1):1-20 (2011).
47. D'alessandro A. & Zolla L. Proteomics and metabolomics in cancer drug development. *Expert Rev Proteomics.* **10**(5), 473–88 (2013).
48. Dai Z., *et al*. Actin microfilament mediates osteoblast Cbfa1 responsivenessto BMP2 under simulated microgravity. *PLoS One*. **8**(5): e63661 (2013).
49. Dallas S.L., Bonewald, LF. Dynamics of the transition from osteoblast to osteocyte. *Ann N Y Acad Sci.* **1192**:437-43 (2010).
50. Dallas S.L., Prideaux M. & Bonewald L.F. The osteocyte: an endocrine cell ... and more. *Endocr Rev*. **34**(5):658-90 (2013).
51. Debold E. P. et al. Fiber type and temperature dependence of inorganic phosphate: implications for fatigue. *Am J Physiol Cell Physiol*. **287**, C673–C681 (2004).
52. Debold E. P., Dave, H. & Fitts, R. H. The depressive effect of Pi on the force-pCa relationship in skinned single muscle fibers is temperature dependent. *Am J Physiol Cell Physiol*. **290**, C1041–C1050 (2006).
53. Deichmann R., Lavie, C. & Andrews, S. Coenzyme Q10 and Statin-Induced Mitochondrial dysfunction. *Ochsner J.* **10**(1), 16–2 (2010).
54. Del Signore A. *et al*. Hippocampal gene expression is modulated by hypergravity. *Eur. J. Neurosci.* **19**, 667–677 (2004).
55. Dettmer K, Aronov PA, Bruce D. Hammock BD. Mass spectrometry based metabolomics; *Mass Spectrom Rev*. **26**(1): 51–78 (2007).

56. Di Benedetto A. *et al*. N-cadherin and cadherin 11 modulate postnatal bone growth and osteoblast differentiation by distinct mechanisms. *J Cell Sci*. **123**:2640–2648 (2010).
57. Di Prampero P.E. & Narici M.V. Muscles in microgravity: from fibres to human motion. *J Biomech*. **36(**3): 403-412 (2003).
58. Di S.M., et al. Graviresponses of osteocytes under altered gravity. *Adv Space Res.* **48**:1161–1166 (2011)
59. Domon B.& Aebersold R.; Mass spectrometry and protein analysis; *Science* (New York, NY), **312**(5771): 212–217(2006).
60. Downey P.A & Siegel M. I. Bone biology and the clinical implications for osteoporosis. *Phys Ther*. **86**(1):77-91 (2006).
61. Ducy P, Schinke T, Karsenty G. The osteoblast: a sophisticated fibroblast under central surveillance. *Science.* **289**: 1501-1504 (2000*)*.
62. Ducy P., Zhang R., Geoffroy V., Ridall A.L, & Karsenty G. Osf2/Cbfa1: a transcriptional activator of osteoblast differentiation. *Cell*. **89**(5):747–754 (1997).
63. Dunham I., *et al*. The DNA sequence of human chromosome 22. *Nature* **402**:489–495 (1999).
64. Ebnerasuly F., Hajebrahimi Z., Tabaie S.M., Darbouy M. Effect of Simulated Microgravity Conditions on Differentiation of Adipose Derived Stem Cells towards Fibroblasts Using Connective Tissue Growth Factor. *Iran J Biotechnol*. **15(**4): 241–251 (2017).
65. Eden P., Go E.P. Database Resources in Metabolomics: An Overview; *J Neuroimmune Pharmacol* **5**:18–30 (2010).
66. Eleniste P. P., Huang S., Wayakanon K., Largura H. W. & Bruzzaniti, A. Osteoblast differentiation and migration are regulated by dynamin GTPase activity. *Int J Biochem Cell Biol.* **46**, 9–18 (2014).
67. Ellis D. I., Dunn, W. B., Griffin, J. L., Allwood, J. W. & Goodacre, R. Metabolic fingerprinting as a diagnostic tool. *Pharmacogenomics* **8**, 1243-1266 (2007).
68. Engler A. J., Sen S., Sweeney H. L. & Discher D. E. Matrix elasticity directs stemcell lineage specification. *Cell* **126**: 677–689 (2006).
69. Espinosa-Jeffrey, A. et al. Simulated microgravity enhances oligodendrocyte mitochondrial function and lipid metabolism. J Neurosci Res. 94(12), 1434–1450 (2016).

70. Etzler J. C. *et al*. Cyclophilin D over-expression increases mitochondrial complex III activity and accelerates supercomplex formation. *Arch Biochem Biophys.* **613**, 61–68 (2017).
71. Feger B. J. et al. Microgravity induces proteomics changes involved in endoplasmic reticulum stress and mitochondrial protection. *Sci Rep*. **6:** 34091 (2016).
72. Feng L., *et al*. LC/MS-based metabolomics strategy to assess the amelioration effects of ginseng total saponins on memory deficiency induced by simulated microgravity. J Pharm Biomed Anal. **125**:329-38 (2016).
73. Fernando J. et al. A mesenchymal-like phenotype and expression of CD44 predict lack of apoptotic response to sorafenib in liver tumor cells. *Int J Cancer* **136**, E161–E172 (2015).
74. Fitts R.H. et al. Effects of prolonged space flight on human skeletal muscle enzyme and substrate profiles. *J Appl Physiol* (1985). **115**(5), 667–79 (2013).
75. Fitts R.H., Riley D.R. & Widrick J.J. Functional and structural adaptations ofskeletal muscle to microgravity. *J Exp Biol.* **204**(18):3201-8 (2001).
76. Fitts R.H., Riley D.R. & Widrick J.J. Physiology of a microgravity environmentinvited review: microgravity and skeletal muscle. *J Appl Physiol.* **89**(2):823-39 (1985).
77. Fletcher D.A., & Mullins R.D. Cell mechanics and the cytoskeleton. *Nature*. **463**(7280): 485–492 (2010).
78. Florencio-Silva R., *et al*. Biology of Bone Tissue: Structure, Function, and Factors That Influence Bone Cells. *BioMed Res Int*. **17** (2015).
79. Fonseca J.E. Rebalancing bone turnover in favour of formation with strontium ranelate: implications for bone strength. *Rheumatology (Oxford*). **47**(4): iv17–iv19 (2008).
80. Forgacs G., Yook S.H., Janmey P.A., Jeong H., Burd C.G. Role of the cytoskeleton in signaling networks. *J. Cell Sci* **117**: 2769-2775 (2004).
81. Franz-Odendaal T.A, Hall B.K. & Witten P.E. Buried alive: how osteoblastsbecome osteocytes. *Dev Dyn.* **235**(1):176-90 (2006).
82. Friedman M.S., Long M.W. & Hankenson K.D. Osteogenic differentiation of human mesenchymal stem cells is regulated by bone morphogenetic protein-6. *J Cell Biochem*. **98**:538–554 (2006).
83. Fritton K. et al. Exogenous MC3T3 preosteoblasts migrate systemically and mitigate the adverse effects of wear particles. *Tissue Eng. Part A* **18:** 2559–2567 (2012).

84. Fulda S., Gorman A.M., Hori O., Samali A. Cellular Stress responses: Cell Survival and Cell Death. *Int J Cell Biol*. 214074 (2010).
85. Genchi G. G. *et al*. Hypergravity stimulation enhances PC12 neuron-like cell differentiation. *Biomed Res Int.* **2015**, 748121 (2015).
86. Geurtzen K. et al. Mature osteoblasts dedifferentiate in response to traumatic bone injury in the zebrafish fin and skull. *Development* **141:** 2225–2234 (2014).
87. Gevi F., Campolo, F., Naro, F. & Zolla, L. The cardioprotective effect of sildenafil is mediated by the activation of malate dehydrogenase and an increase in the malate-aspartate shuttle in cardiomyocytes. Biochem. Pharmacol. 127, 60–70 (2017).
88. Ghezzi D. *et al*. SDHAF1, encoding a LYR complex-II specific assembly factor, is mutated in SDH-defective infantile leukoencephalopathy. *Nature Genetics.* **41**, 654–656 (2009).
89. Gomase V.S., Changbhale S.S., Patil S.A., Kale K.V. Metabolomics; *Current Drug Metabolism***, 9:** 89-98 (2008) .
90. Görg A., Weiss, W., Dunn, M.J. (2004) Current two-dimensional electrophoresis technology for proteomics. Proteomics. **4**: 3665-3685.
91. Granéli C. et al. Novel markers of osteogenic and adipogenic differentiation of human bone marrow stromal cells identified using a quantitative proteomics approach. Stem Cell Res. **12**, 153–165 (2014).
92. Gravallese E.M. Bone destruction in arthritis. *Ann Rheum Dis*. **61**(2): ii84-6 (2002).
93. Gridley D.S., *et al*. Spaceflight effects on T lymphocyte distribution, function and gene expression. *J Appl Physiol* **106**:194–202 (2009)
94. Griffin J.L. Metabolic profiles to define the genome: can we hear the phenotypes? *Philos Trans R Soc Lond B Biol Sci* **359**: 857 (2004).
95. Grigoriev A.I., *et al*. Clinical and physiological evaluation of bone changes among astronauts after long-term space flights. Aviakosm Ekolog Med. **32**(1):21–25 (1998).
96. Grimm D., Wise P., Lebert M., Richter P. & Baatout, S. How and why does the proteome respond to microgravity? *Expert Rev Proteomics* **8**, 13–27 (2011).
97. Grosse J. *et al.* Short-term weightlessness produced by parabolic flight maneuvers altered gene expression patterns in human endothelial cells. *FASEB J* **26**, 639–655 (2012).
98. Grossmann J., Walther K., Artinger M., Kiessling S., Schölmerich J. Apoptotic signaling during initiation of detachment-induced apoptosis ("anoikis") of primary human intestinal epithelial cells. *Cell Growth Differ.* **12**(3):147-55 (2001).

99. Gudas L. J. & Wagner, J. A. Retinoids regulate stem cell differentiation. *J Cell Physio*. **226:** 322–330 (2011).

100. Gueguinou N. *et al*. Stress response and humoral immune system alterations related to chronic hypergravity in mice. *Psychoneuroendocrinology*. **37**, 137–147 (2012).

101. Gupta S., Vijayaraghavan S., Uzer G. & Judex S. Multiple exposures to unloading decrease bone's responsivity but compound skeletal losses in C57BL/6 mice. *Am J Physiol Regul Integr Comp Physiol.* **303**: R159–R167(2012).

102. Hammond T.G., Hammond J.M. Optimized suspension culture: the rotating-wall vessel. *Am J Physiol Renal Physiol* **281**:F12–F25 (2001).

103. Harada S. & Rodan G. A. Control of osteoblast function and regulation of bone mass. *Nature* **423**, 349–355 (2003).

104. Heppener M. Spaceward ho! The future of humans in space. *EMBO Rep*.**9**(1):S4-12 (2008).

105. Hill T.P., Spater D., Taketo M.M., Birchmeier W., Hartmann C. Canonical Wnt/beta-catenin signaling prevents osteoblasts from differentiating into chondrocytes. *Dev Cell.* **8**(5):727-738 (2005).

106. Hollinger J.O. & Kleinschmidt J.C. The critical size defect as an experimental model to test bone repair materials. *J Craniofac Surg*. **1**: 60-68 (1990).

107. Hollywood K., Brison D.R., Goodacre R. Metabolomics: current technologies and future trends. *Proteomics*. **6**: 4716-4723 (2006).

108. Holtrop M E. Light and electron microscopic structure of boneformingm cells. In: Hall BK, ed. The Osteoblast and Osteocyte. Caldwell, NJ: Telford Press Inc: *Bone*. **1**: 1–39 (1990).

109. Hoppel C. The role of carnitine in normal and altered fatty acid metabolism. *Am J Kidney Dis*. **41** (4 Suppl. 4): S4-12 (2003).

110. Hoppeler H. & Fluck, M. Plasticity of skeletal muscle mitochondria: structure and function. *Med Sci Sports Exerc.* **35**(1), 95–104 (2003).

111. Hori O., *et al.* Deletion of SERP1/RAMP4, a component of the endoplasmic reticulum (ER) translocation sites, leads to ER stress. *Mol Cell Biol*. **26**(11): 4257–4267 (2006).

112. Hu L. F., Li J. B., Qian A. R., Wang F. & Shang P. Mineralization initiation of MC3T3-E1 preosteoblast is suppressed undersimulated microgravity condition. *Cell Biol Int*. **39**_ 364–372 (2015).

113. Hu, Z. *et al*. miRNA-132-3p inhibits osteoblast differentiation by targeting Ep300 in simulated microgravity. *Sci Rep.* **21**(5), 18655 (2015).

114. Huang Y., *et al*. Gravity, a regulation factor in the differentiation of rat bone marrow mesenchymal stem cells. *J Biomed Sci* **16**:87 (2009)

115. Hughes-Fulford M. Physiological effects of microgravity on osteoblast morphology and cell biology. *Adv Space Biol Med*. **8**:129-57 (2002).

116. Ikawa T. *et al*. Hypergravity suppresses bone resorption in ovariectomized rats. *Adv Space Res.* **47**, 1214–1224 (2011).

117. Ivanovska I. L., Shin J. W., Swift J. & Discher D. E. Stem cell mechanobiology: diverse lessons from bone marrow. *Trends Cell Biol*. **25:** 523–532 (2015).

118. Jee W. S., Wronski T. J., Morey E. R. & Kimmel D. B. Effects of spaceflight on trabecular bone in rats. *Am J Physiol Regul Integr Comp Physiol* **244**, 310–314 (1983).

119. Jensen E.D., Gopalakrishnan R., Westendorf J.J. Regulation of gene expression in osteoblasts. *Biofactor.* **36**(1): 25–32 (2010).

120. Jopling C., Boue S. & Izpisua Belmonte J. C. De-differentiation, transdifferentiation and reprogramming: three routes to regeneration. *Nat Rev Mol Cell Biol*. **12**: 79–89 (2011).

121. Katagiri T., *et al*. Bone morphogenetic protein-2 converts the differentiationpathway of C2C12 myoblasts into the osteoblast lineage. *JCell Biol* **127**(6):1755-1766 (1994).

122. Kawaguchi J., *et al.* Targeted disruption of cadherin-11 leads to a reduction in bone density in calvaria and long bone metaphyses. *J Bone Miner Res.* **16**(7):1265-1271 (2001).

123. Khosla S. Oursler M.J. & Monroe D.G. Estrogen and the skeleton. *Trends Endocrinol Metab.* **23**(11): 576–581 (2012).

124. Khutornenko A., Dalina A. A., Chernyak B. V., Chumakov P. M. & Evstafieva, A. G. The Role of Dihydroorotate Dehydrogenase in Apoptosis Induction in Response to Inhibition of the Mitochondrial Respiratory Chain Complex III. Acta Naturae. 6(1), 69–75 (2014).

125. Knuth S. T., Dave H., Peters J. R. & Fitts R. H. Low cell pH depresses peak power in rat skeletal muscle fibres at both 30 °C and 15 °C: implications for muscle fatigue. J Physiol. 575, 887–899 (2006).

126. Komori T., *et al*. Targeted disruption of Cbfa1 results in a complete lack of bone formation owing to maturational arrest of osteoblasts. *Cell*. **89**(5): 755–64 (1997).

127. Kononikhin A.S., et al. Spaceflight induced changes in the human proteome. *Expert Rev Proteomics*. **14**(1):15-29 (2017).

128. Kopp S., *et al*. The role of NFκB in spheroid formation of human breast cancer cells cultured on the Random Positioning Machine. *Sci Rep*. **8** (1): 92, (2018).

129. Krane S.M. Identifying genes that regulate bone remodeling as potential therapeutic targets. *J Exp Med*. **201**: 841-843 (2005).

130. Krishna R.G. & Wold F. Post-translational modification of proteins; InAdvances in Enzymology and Related Areas of Molecular Biology.Wiley-Blackwell, Hoboken, NJ, USA, (1993), pp. 265–298.

131. Kroger A. & Innerhofer A. The Function of Menaquinone, Covalently Bound FAD and Iron-Sulfur Protein in the Electron Transport from Formate to Fumarate of Vibrio succinogenes. *Eur. J. Biochem.* **69**(2), 487–495 (1976).

132. Krüger M., Bauer J., Grimm D. Cancer Research in Space, Biotechnology in Space, Biotechnology in Space. 87-106 (2017).

133. Kuo J.C. Mechanotransduction at focal adhesions: integrating cytoskeletal mechanics in migrating cells. *J Cell Mol Med*. **17**(6): 704–712 (2013).

134. LeBlanc A., *et al*. Bone mineral and lean tissue loss after long duration space flight. *J Musculoskelet Neuronal Interact* **1**:157–160 (2000).

135. Lee S.B. & Kang K.Y. The effects of isokinetic eccentric resistance exercise for the hip joint on functional gait of stroke patients. *J Phys Ther Sci*. **25**(9):1177-9 (2013).

136. Lee S.G. *et al*. A load of mice to hypergravity causes AMPKα repression with liver injury, which is overcome by preconditioning loads via Nrf2. *Sci Rep.* **5**, 15643 (2015).

137. Leivo I., Kauhanen S. & Michelsson J.E. Abnormal mitochondria and sarcoplasmic changes in rabbit skeletal muscle induced by immobilization. *Michelsson APMIS*. **106** :1113-1123 (1998).

138. Lescale, C. *et al*. Hind limb unloading, a model of spaceflight conditions, leads to decreased B lymphopoiesis similar to aging. *FASEBJ*. **29**, 455–463 (2015).

139. Lian J. B. & Stein G. S. Development of the osteoblast phenotype: molecular mechanisms mediating osteoblast growth and differentiation. *Iowa Orthop J*. **15**: 118–140 (1995).

140. Lian J.B., Stein G.S., Canalis E., Robey P.G., Boskey A.L. Bone formation: osteoblast lineage cells, growth factors, matrix proteins and the mineralization process. In: Primer on the metabolic bone diseases and disorders of mineral metabolism, ed. by Favus M.J., Lippincott Williams & Wilkins, Philadelphia, pp14-29 (1999). Book

141. Long F. Building strong bones: Molecular regulation of the osteoblast lineage. *Nat Rev Mol Cell Biol*. **13**(1): 27–38 (2012)

142. Long J. *et al*. D-galactose toxicity in mice is associated with mitochondrial dysfunction: protecting effects of mitochondrial nutrient R-alpha-lipoic acid. *Biogerontology*. **8**(3), 373–81 (2007).

143. Ma X. et al. *Differential gene expression profile and altered cytokine secretion of thyroid cancer cells in space*. *FASEB J* **28**, 813–835 (2014).

144. Mackie E.J. Osteoblasts: novel roles in orchestration of skeletal architecture. *Int J Biochem Cell Biol*. **35**: 1301-1305 (2003).

145. Madsen R., Lundstedt, T. & Trygg, J. Chemometrics in metabolomics—A review in human disease diagnosis. *Anal. Chim. Acta.* **659**: 23-33 (2010).

146. Maes M. *et al*. Coenzyme Q10 deficiency in myalgic encephalomyelitis/chronic fatigue syndrome (ME/CFS) is related to fatigue, autonomic and neurocognitive symptoms and is another risk factor explaining the early mortality in ME/CFS due to cardiovascular disorder. *Neuro Endocrinol. Lett.* **30**(4), 470–476 (2009).

147. Mahdinia E., Demirci A. & Berenjian A. Production and application of menaquinone-7 (vitamin K2): a new perspective. *World J Microbiol Biotechnol.* **33**(1), 2 (2017).

148. Maleki M., Ghanbarvand F., Reza Behvarz M., Ejtemaei M. & Ghadirkhomi, E. Comparison of mesenchymal stem cell markers in multiple human adult stem cells. *Int J Stem Cells* **7**: 118–126 (2014).

149. Mamas M., Dunn W.B., Neyses L., Goodacre R. The role of metabolites and metabolomics in clinically applicable biomarkers of disease. *Arch Toxicol*; **85**: 5 (2011).

150. Mangala L.S., *et al*. Story, et al. Effects of simulated microgravity on expression profile of microRNA in human lymphoblastoid cells. *J Biol Chem*. **286:** 32483-32490 (2011).

151. Manolagas S.C. Cellular and molecular mechanisms of osteoporosis. *Aging (Milano*), **10**(3):182-90 (1998).

152. Manzey D. & Lorenz B. Human performance during spaceflight. *Hum Perf Extrem Environ*. **4**: 8–13 (1999).

153. Marks S.C. & Hermey D.C. The structure and development of bone. In: Bilezikian J.P., Raisz L.G., Rodan G.A., eds. Principles of Bone Biology. San Diego, Calif: Academic Press. 3–14 (1996).

154. Marks S.C. Jr. & Popoff S.N. Bone cell biology: the regulation of development, structure, and function in the skeleton. *Am J Anat*. **183**(1):1-44 (1988).

155. Matic I., *et al*. Quiescent Bone Lining Cells Are a Major Source of Osteoblasts During Adulthood. *Stem Cells*. **34**(12): 2930–2942 (2016).

156. Matsuo K. & Irie N. Osteoclast-osteoblast communication. *Arch Biochem Biophys*. **473**(2), 201-209 (2008).

157. McCarthy I.D. Fluid shifts due to microgravity and their effects on bone: a review of current knowledge. *Ann Biomed Eng***. 33**:95–103 (2005).

158. McGovern J.A., Griffin M. & Hutmacher D.M. Animal models for bone tissue engineering and modelling disease. *Dis Model Mech*. **11**(4) (2018)

159. Meng R., *et al*. Human mesenchymal stem cells are sensitive to abnormal gravity and exhibit classic apoptotic features. *Acta Biochim Biophys Sin* **43**:133–142 (2011)

160. Meshkov D. & Rykova M. The natural cytotoxicity in cosmonauts on board space stations. *Acta Astronaut* **36**: 719–726(1995)

161. Meyers V.E., *et al*. Modeled microgravity disrupts collagen I/integrin signaling during osteoblastic differentiation of human mesenchymal stem cells. *J Cell Biochem.* **93**(4):697-707 (2004).

162. Michaletti A., Gioia M., Tarantino U. & Zolla, L. Effects of microgravity on osteoblast mitochondria: a proteomic and metabolomic profile. *Sci Rep*. **7**(1), 15376 (2017).

163. Mohamed A.M. An Overview of Bone Cells and their Regulating Factors of Differentiation. *Malays J Med Sci*. **15**(1): 4–12 (2008).

164. Morath I., Hartmann T. N. & Orian-Rousseau V. CD44: more than a mere stem cell marker. *Int J Biochem Cell Biol*. **81**, 166–173 (2016).

165. Morimoto R. I., Kroeger P. E., & Cotto J. J. The transcriptional regulation of heat shock genes: a plethora of heat shock factors and regulatory conditions. *EXS*. **77:** 139–163 (1996).

166. Muller F. L., Liu, Y. & Van Remmen H. Complex III releases superoxide to both sides of the inner mitochondrial membrane. *J. Biol. Chem.* **279**(47), 49064–73 (2004).

167. Muller F. L., Lustgarten M. S., Jang Y., Richardson, A. & Van Remmen H. Trends in oxidative aging theories. *Free Radic. Biol. Med.* **43**(4), 477–503 (2007).

168. Muller F.L. The nature and mechanism of superoxide production by the electron transport chain: Its relevance to aging. *AGE*. **23**(4), 227–253 (2000).

169. Nabavi N., Khandani A., Camirand A., Harrison R.E. Effects of microgravityon osteoclast bone resorption and osteoblast cytoskeletal organization and adhesion. *Bone*. **49**(5):965-74 (2011).

170. Nagele E., Vollmer M., Horth P., Vad C. (2004) 2D-LC/MS techniques for the identification of proteins in highly complex mixtures. Expert Rev Proteomics. **1**: 37-46. Review.

171. Nakamura H. Morphology, Function, and Differentiation of Bone Cells. *J hard tissue biol.* **16**(1):15-22 (2007).

172. Nakayama T. *et al*. Polarization of osteoclasts on dental implant materials is similar to that observed on bone. *J Oral Biosci*. **56:**136–142 (2014).

173. Ndozangue-Touriguine O., Hamelin J., Breard J. Cytoskeleton and apoptosis. *Biochem Pharmacol* **76**:11–18(2008)

174. Nichols H. L., Zhang N. & Wen X. Proteomics and genomics of microgravity. *Physiol Genomics.* **26**, 163–171 (2006).

175. Nicholson J. K., Connelly J., Lindon J. C. & Holmes, E. Metabonomics: a platform for studying drug toxicity and gene function. *Nat. Rev. Drug Discov*. **1**: 153-161 (2002).

176. Nicholson J.K., Lindon J.C. Systems biology: Metabonomics. *Nature.* **455**: 1054 (2008).

177. Nieto M. A. & Cano A. The epithelial-mesenchymal transition under control: global programs to regulate epithelial plasticity. *Semin Cancer Biol*. **22**, 361–368 (2012).

178. Nishimura R. *et al.* Regulation of bone and cartilage development by network between BMP signalling and transcription factors. *J Biochem.* **151**(3): 247–54 (2012).

179. Norsk P. Cardiovascular and fluid volume control in humans in space. *Curr Pharm Biotechnol* **6:** 325–330 (2005).

180. Nowak D., Stewart D. & Koeffler H. P. Differentiation therapy of leukemia: 3 decades of development. *Blood* **113**: 3655–3665 (2009).

181. O'Brien K. A., Griffin J. L. & Murray, A. J. & Edwards, L.M.4. Mitochondrial responses to extreme environments: insights from metabolomics. *Extrem Physiol Med.* **4**, 7 (2015).

182. Ohira Y., *et al*. Rat soleus muscle fiber responses to 14 days of spaceflight and hindlimb suspension. *J Appl Physiol*. **73**: 51S-57S (1992).

183. Ontiveros C. & Mccabe L. R. Simulated microgravity suppresses osteoblast phenotype, Runx2 levels and AP-1 transactivation. *J Cell Biochem*. **88**: 427–437 (2003).

184. Orsini S.S., Lewis A.M., Rice K.C. Investigation of simulated microgravity effects on Streptococcus mutans physiology and global gene expression. npj Microgravity. **3**(4) (2017).

185. Oshima M., Oshima, H. & Taketo, M. M. Hypergravity induces expression of cyclooxygenase-2 in the heart vessels. *Biochem. Biophys. Res. Commun.* **330**, 928–933 (2005).

186. Ozcivici E. et al. Mechanical signals as anabolic agents in bone. *Nat Rev Rheumatol*. **6:** 50–59 (2010).

187. Papachron, K. K., Karatzas D. N., Papavassiliou K. A., Basdra, E. K. & Papavassiliou, A. G. Mechanotransduction in osteoblast regulation and bone disease. *Trends Mol Med*. **15**: 208–216 (2009).

188. Parfait, B. *et al*. Compound heterozygous mutations in the flavoprotein gene of the respiratory chain complex II in a patient with Leigh syndrome. *Hum Genet.* **106** (2), 236–43 (2000).

189. Parfitt A.M Bone-forming cells in clinical conditions In Bone. Volume 1: theosteoblast and osteocyte. B.K. Hall, editor. Telford Press and CRC Press. 1990 Boca Raton, FL. 351–429.

190. Park D. et al. Endogenous bone marrow MSCs are dynamic, fate-restricted participants in bone maintenance and regeneration. *Cell Stem Cell* **10:** 259–272 (2012).

191. Patel M. J. et al. Identification of mechanosensitive genes in osteoblasts bycomparative microarray studies using the rotating wall vessel and the random positioning machine. *J Cell Biochem*. **101**: 587–599 (2007).

192. Paulsen K. et al. Regulation of ICAM-1 in cells of the monocyte/macrophage system in microgravity. *Biomed. Res Int*. **2015**, 538786 (2015).

193. Paulsen K., *et al.* Microgravity-induced alterations in signal transduction in cells of the immune system. *Acta Astronaut*., **67**:1116-1125 (2010).

194. Pereda-Loth V., *et al*. An innovative in vitro device providing continuous low doses of γ-rays mimicking exposure to the space environment: A dosimetric study. Life Sci Space Res (Amst). **16**:38-46 (2018).

195. Pereira B. P. et al. Runx2, p53, and pRB status as diagnostic parameters forderegulation of osteoblast growth and differentiation in a new prechemotherapeutic osteosarcoma cell line (OS1). *J Cell Physiol*. **221:** 778–788 (2009).

196. Petrie R. J. & Yamada K. M. At the leading edge of three-dimensional cell migration. *J Cell Sci*. **125**: 5917–5926 (2012).

197. Phan T.C.A., Xu J. & Zheng M.H. Interaction between osteoblast and osteoclast: Impact in bone disease. *Histol Histopathol*. **19**(4):1325-44 (2004).

198. Pino A.M., Rosen C.J., Rodríguez J.P. In osteoporosis, differentiation of mesenchymal stem cells (MSCs) improves bone marrow adipogenesis. *Biol Res*. **45**(3):279-87 (2012).

199. Pittenger M.F, *et al.* Multilineage potential of adult human mesenchymal stem cells. *Science*. **284**(5411):143-7 (1999).

200. Ploutz-Snyder, L. et al. Effects of Sex and Gender on Adaptation to Space: Musculoskeletal Health. *J. womens health*. **23**(11), 963–966 (2014).

201. Poole RA. The growth plate: cellular physiology, cartilage assembly and mineralization. In: Hall BK, Newman S, eds: Cartilage: Molecular Aspects. Boca Raton, Fla: CRC Press; 179–210 (1991).

202. Porazinski S. *et al*. YAP is essential for tissue tension to ensure vertebrate 3D body shape. *Nature*. **521**, 217–221 (2015).

203. Prakash S. Bisen, Mousumi Debnath, Dr. G. Prasad. In book: Molecular Diagnostics: Promises and PossibilitiesEdition: FirstChapter: Omics TechnologyPublisher: Dordrech Heidelberg London, Springer, 2010 pp 11-31.

204. Provenzano P.P. & Keely P.J. Mechanical signaling through the cytoskeleton regulates cell proliferation by coordinated focal adhesion and Rho GTPase signaling. *J Cell Sci*. **124**(8): 1195–1205 (2011).

205. Qian A., et al. Development of a ground-based simulated experimental platform for gravitational biology. *IEEE Trans Appl Supercond.* **19**:42–46 (2009).

206. Rea G., *et al*. Imbriani M, Visai L, Rizzo AM. Microgravity-driven remodeling of the proteome reveals insights into molecular mechanisms and signal networks involved in response to the space flight environment. *J Proteomics*. **137**(30):3-18 (2016).

207. Reinders J, Lewandrowski U, Moebius J, Wagner Y, Sickmann A. (2004) Challenges in mass spectrometry-based proteomics. Proteomics. **4**: 3686- 3703.

208. Repp A., Mikami K., Mittmann F. & Hartmann E. Phosphoinositide-specific phospholipase C is involved in cytokinin and gravity responses in the moss Physcomitrella patens. *The Plant Journal.* **40**, 250–259 (2004).

209. Ridley A. J. Rho GTPase signalling in cell migration. *Curr Opin Cell Biol*. **36**,103–112 (2015).

210. Riwaldt S., *et al.* Preparation of A Spaceflight: Apoptosis Search in Sutured Wound Healing Models. Int J Mol Sci. **18**(12): E2604 (2017).

211. Robling AG & Turner CH. Mechanical Signaling for Bone Modeling and Remodeling. *Crit Rev Eukaryot Gene Expr*. **19**(4): 319–338 (2009).

212. Rodriguez L. G., Wu X. & Guan J. L. Wound-healing assay. *Methods Mol Biol*. **294**, 23–29 (2005).

213. Roodman G.D. Biology of osteoclast activation in cancer. *J Clin Oncol.* **19**(15):3562-71 (2001).

214. Sahana J, et al. Decreased E-Cadherin in MCF7 Human Breast Cancer Cells Forming Multicellular Spheroids Exposed to Simulated Microgravity, PROTEOMICS, **18**, 13, (2018).

215. Saidak Z., *et al*. Wnt/β-catenin signaling mediates osteoblast differentiation triggered by peptide-induced α5β1 integrin priming in mesenchymal skeletal cells. *J Biol Chem*. **290**(11):6903-12 (2015).

216. Sandonà D., *et al*. Adaptation of Mouse Skeletal Muscle to Long-Term Microgravity in the MDS Mission. *PLoS One*. **7**(3): e33232 (2012).

217. Sarkar P., *et al*. Proteomic Analysis of Mice Hippocampus in Simulated Microgravity Environment. J Proteome Res. **5** (3): 548–553 (2006)

218. Saxena R., Pan G., McDonald J.M., Ann N.Y. Osteoblast and osteoclast differentiation in modeled microgravity. *Acad Sci*. **1116**:494-8 (2007).

219. Schafer D. A. Cell biology: barbed ends rule. *Nature* **430**, 734–735 (2004).

220. Schatten H., Lewis M. L. & Chakrabarti A. Spaceflight and clinorotation cause cytoskeleton and mitochondria changes and increases in apoptosis in cultured cells. *Acta Astronaut.* **49**, 399–418 (2001).

221. Scheuringa R. A. *et al*. The Apollo Medical Operations Project: Recommendations to improve crew health and performance for future exploration missions and lunar surface operations. *Acta Astronautica.* **63**, 980–987 (2007).

222. Sehring I. M., Jahn C. & Weidinger G. Zebrafish fin and heart: what's special about regeneration? *Curr Opin Genet Dev* **40:** 48–56 (2016).

223. Shevchenko A., Wilm M., Vorm O. & Mann M. Mass spectrometric sequencing of proteins silver-stained polyacrylamide gels. Anal. Biochem. 68, 850–858 (1996).

224. Shevchenko A., Wilm M., Vorm O. & Mann M. Mass spectrometric sequencing of proteins silver-stained polyacrylamide gels. *Anal Biochem*. **68**, 850–858 (1996).

225. Shi W. et al. Microgravity induces inhibition of osteoblastic differentiation and mineralization through abrogating primary cilia. *Sci Rep*. **7**: 1866 (2017).

226. Shinoda K., Tomita M. & Ishihama Y. emPAI Calc–for the estimation of protein abundance from large-scale identification data by liquid chromatography-tandem mass spectrometry. *Bioinformatics*. **26**: 576–577 (2010).

227. Siggelkow H. et al. Development of the osteoblast phenotype in primary human osteoblasts in culture: comparison with rat calvarial cells in osteoblast differentiation. J Cell Biochem. **75**(1): 22–35 (1999).

228. Siggelkow H. et al. Development of the osteoblast phenotype in primary human osteoblasts in culture: comparison with rat calvarial cells in osteoblast differentiation. *J Cell Biochem.* **75**, 22–35 (1999).

229. Sims N.A. & Gooi J.H. Bone remodeling: Multiple cellular interactions required for coupling of bone formation and resorption. *Semin Cell Dev Biol*. **19**(5):444-51 (2008).

230. Singh K.P., Kumari R., Dumond J.W. Simulated microgravity-induced epigenetic changes in human lymphocytes. *J Cell Biochem*. **111**: 123-129(2010)

231. Smith S.M. & Heer M. Calcium and bone metabolism during space flight. *Nutrition.* **18**:849–852 (2002).

232. Sobacchi C., Schulz A., Coxon F.P., Villa A. & Helfrich M.H. Osteopetrosis: genetics, treatment and new insights into osteoclast function. *Nat Rev End*. **9**(9):522–536 (2013).

233. Son S.M., *et al*. Influence of Isokinetic Strength Training of Unilateral Ankle on Ipsilateral One-legged Standing Balance of Adults. *Phys Ther Sci*. **25**(10):1313-5 (2013).

234. Stains J.P. & Civitelli R. Genomic approaches to identifying transcriptional regulators of osteoblast differentiation. *Genome Biol.* **4**: 222 (2003)

235. Starr D.A. Communication between the cytoskeleton and the nuclear envelope to position the nucleus. *Mol Biosyst.* **3**(9): 583–589 (2007).

236. Stein G.S., *et al.* Runx2 control of organization, assembly and activity of the regulatory machinery for skeletal gene expression. *Oncogene*. **23**(24): 4315–29 (2004).

237. Tamma R., *et al*. Microgravity during spaceflight directly affects in vitro osteoclastogenesis and bone resorption. *FASEB J.* **23**(8):2549-54 (2009).

238. Tang D.D. & Gerlach B.D. The roles and regulation of the actin cytoskeleton, intermediate filaments and microtubules in smooth muscle cell migration. *Respir Res*. **18**: 54 (2017).

239. Tannahill, G. M. et al. Succinate is a danger signal that induces IL-1β via HIF-1α. Nature. 496, 238–242 (2013).

240. Terpos E, Dimopoulos, MA. Myeloma bone disease: pathophysiology and management. *Ann Oncol*. **16**(8):1223-31 (2005).

241. Thiel C.S, *et al*. Rapid alterations of cell cycle control proteins in human T lymphocytes in microgravity. *Cell Commun. Signal*. **10**(1):1 (2012).

242. Trotter B., *et al*. The influence of simulated microgravity on the proteome of Daphnia magna Benjamin. Nj Microgravity. **1**: 15016 (2015)

243. Tsao Y.T. *et al*. Osteocalcin Mediates biomineralization during Osteogenic Maturation in Human Mesenchymal Stromal Cells. *Int J Mol Sci*. **18**(1): 159 (2017).

244. Tsukita S. *et al*. Specific proto-oncogenic tyrosine kinases of src family are enriched in cell-to-cell adherens junctions where the level of tyrosine phosphorylation is elevated. *J Cell Biol* **113**(4):867-879 (1991).

245. Uchihashi K., Aoki S., Matsunob, A. & Toda S. Osteoblast migration into type I collagen gel and differentiation to osteocyte-like cells within a self-produced mineralized matrix: a novel system for analyzing differentiation from osteoblast to osteocyte. *Bone* **52:** 102–110 (2013).

246. Ulbrich C. *et al.* Differential gene regulation under altered gravity conditions in follicular thyroid cancer cells: relationship between the extracellular matrix and the cytoskeleton. *Cell Physiol Biochem* **28**, 185–198 (2011).

247. Valentijn A.J., Zouq N., Gilmore A.P. Anoikis. *Biochem Soc Trans*. **32**(3):421-5 (2004).

248. Van der Greef J., Stroobant P., Van der Heijden R. The role of analytical sciences in medical systems biology. *Curr Opin Chem Biol.* **8**: 559 (2004).

249. Van Loon J.J.W.A. Some history and use of the random positioning machine, RPM, in gravity related research. *Adv Space Res.* **39**:1161–1165 (2007).

250. Vico L., *et al*. Effects of long-term microgravity exposure on cancellous and cortical weight-bearing bones of cosmonauts. *The Lancet*. **355(**9215):1607–1611 (2000).

251. Wang JH, Byun J, Pennathur S. Analytical Approaches to Metabolomics and Applications to Systems Biology; *Semin Nephrol*, **30**(5): 500–511 (2010).

252. Westermarck J., Ivaska J., Corthals G.L. dentification of Protein Interactions Involved in Cellular Signaling. *Mol Cell Proteomics*. **12**(7): 1752–1763 (2013).

253. Wilke A., *et al*. Bioinformatics support for high-throughput proteomics. *J Biotechnol* **106(**2–3): 147-156 (2003).

254. Wilkins M.R., *et al*. Progress with proteome projects: why all proteins expressed by a genome should be identified and how to do it. *Biotec Genet Eng Rev,* **13**(1): 19–50 (1996).

255. Williams, D. *et al*. Acclimation during space flight: effects on human physiology. *CMAJ*. **180**, 1317–1323 (2009).

256. Wittmann-Liebold B., Graack H. R., Pohl T. (2006) Two-dimensional gel electrophoresis as tool for proteomics studies in combination with protein identification by mass spectrometry. Proteomics. **6**: 4688-4703.

257. Wolf K. & Friedl P. Extracellular matrix determinants of proteolytic and nonproteolytic cell migration. *Trends Cell Biol*. **21**: 736–744 (2011).

258. Wuest S. L., Richard S., Kopp, S., Grimm D. & Egli M. Simulated microgravity: critical review on the use of random positioning machines for mammalian cell culture. *Biomed Res Int*. **2015**, 971474 (2015).

259. Xue J. H. *et al*. Differential regulation and recovery of intracellular Ca2 + in cerebral and small mesenteric arterial smooth muscle cells of simulated microgravity rat. *PloS one.* **6**(5), e19775 (2011).

260. Yavropoulou M.P. & Yovos J.G. The role of the wnt signaling pathway in osteoblast commitment and differentiation. *HORMONES.* **6**(4):279-294 (2007).

261. Yim E. K. & Sheetz M. P. Force-dependent cell signaling in stem cell differentiation. *Stem Cell Res Ther*. **3**, 41 (2012).

262. Yudoh K., *et al*. Decreased cellular activity and replicative capacity of osteoblastic cellsisolated from the periarticular bone of rheumatoid arthritis patients comparedwith osteoarthritis patients. *Arthritis Rheum.* **43**(10):2178-88 (2000).

263. Zayzafoon M., Gathings W. E. & McDonald J. M. Modeled microgravity inhibit sosteogenic differentiation of human mesenchymal stem cells and increasesadipogenesis. *Endocrinology*, **145:**2421–2432 (2004).

264. Zhang C., *et al*. Space microgravity drives transdifferentiation of human bone marrow–derived mesenchymal stem cells from osteogenesis to adipogenesis. *FASEB J*. **32**(8):4444-4458 (2018).

265. Zhang R. *et al*. Simulated microgravity-induced mitochondrial dysfunction in rat cerebral arteries. *FASEB J.* **28**, 2715–2724 (2014).

266. Zhang Y., Wang H., Lai C., Wang L., Deng. Comparative proteomic analysis of human SH-SY5Y neuroblastoma cells under simulated microgravity. Astrobiology. **13**(2):143-50 (2013).

267. Zhu H. et al. The role of the hyaluronan receptor CD44 in mesenchymal stem cell migration in the extracellular matrix. *Stem Cells* **24**: 928–935 (2006).

6. AKNOWLEDGEMENTS

Firstly, I would like to express my sincere gratitude of Prof. Lello Zolla for giving me the chance to work on this scientific field and to give access to the laboratory and research facilities.

I'm extremely grateful to Prof.ssa Anna Maria Timperio and Prof.ssa Sara Rinalducci for the continuous support of my PhD study and related research, for their patience, motivation, and immense knowledge. Thanks from scientifically and non-point of view; thanks for all useful discussions, never-ending encouragement and motivation throughout this journey.

My sincere thanks also goes to Prof. Massimo Coletta and Dott.ssa Magda Gioia, with whom I had the pleasure of collaborating, for the realization of the thesis project and for the drafting of scientific articles.

I would like to thank Prof. Roberta Cimmaruta for her guidance and for carefully coordinating the XXXI PhD course.

I thank my fellow labmates in for the stimulating discussions, and for all the fun we have had in the last years. Thanks to Federica, Antonio, Giuseppina, Veronica..thank you guys for your companionship and friendship…thanks for all laughs and for all crying that you shared with me.

My sincere gratitude goes to my friends..my ladies, my sisters, my second family. Thanks for everything..thanks for always been there. Thanks my gentlmen (and not so) for the evenings spent together, for the bad movies that you show me, for the long chats in the car, for all the glasses of wine that we drank together and for all my songs out of tune.

Last but not the least, I would like to thank my **big** family for supporting me in each moment of my life. Thank you because you still endure me ...

Anna